THE GENERAL CIRCULATION OF THE TROPICS

by

JOHN WINTON KIDSON

B. Sc., University of New Zealand
(1961)

M. Sc., University of Canterbury
(1963)

SUBMITTED IN PARTIAL FULFILLMENT
OF THE REQUIREMENTS FOR THE
DEGREE OF DOCTOR OF
SCIENCE
at the
MASSACHUSETTS INSTITUTE OF TECHNOLOGY

September, 1968

Signature of Author.....
Department of Meteorology, August 18, 1968

Certified by.....
Thesis Supervisor

Accepted by.....
Chairman, Departmental Committee
on Graduate Students

THE GENERAL CIRCULATION OF THE TROPICS

by

John W. Kidson

Submitted to the Department of Meteorology on August 19, 1968 in partial fulfillment of the requirement for the degree of Doctor of Science.

ABSTRACT

Data from 303 radiosonde and radar wind reporting stations between 45°N and 30°S have been analysed for the overall period July 1957 to December 1964 giving for the first time a comprehensive picture of the general circulation of the Tropics. The tropospheric statistics presented were obtained from objective analyses of the long term station means for four seasons while in the stratosphere latitude band means were used because of the reduction in data coverage.

The object of the study was firstly to define the average state of the tropical circulation and its seasonal variation and secondly to look for year to year changes in the tropospheric circulation which might be related to the biennial oscillation of the stratosphere.

The seasonal variation of the zonal means of temperature, meridional and zonal wind components is presented together with the momentum and energy fluxes and associated terms in the atmospheric energy cycle.

The pattern emerges of a dominating Hadley circulation which acts to generate the momentum and energy fluxes transported poleward by eddy processes at higher latitudes. The centre of the rising motion varies with the season, and is found at 5 - 10° latitude in the summer hemisphere. The winter hemisphere cell is the most important and generates more angular momentum than is dissipated by the surface westerlies in the winter hemisphere. The balance is transferred across the equator and represents an appreciable fraction of the peak poleward flux in the summer hemisphere.

An area of equatorward flux of sensible heat by transient eddies has been found in the Southern Hemisphere Tropics similar to that previously observed in the Northern Hemisphere. These areas of equatorward flux are associated with a pattern of divergence away from the adiabatic heating in the descending branch of the Hadley circulation and convergence into its ascending branch. Because of the small temperature gradients in the Tropics the energy conversions associated with these counter gradient fluxes are small, and in general the conversions involving momentum fluxes are more important. The largest conversion of all, however, is the generation of zonal kinetic energy from zonal available potential energy by the Hadley circulation.

Although the amplitude of biennial fluctuations in the troposphere is small in comparison to seasonal changes some evidence has been found for a modulation in the intensity of the Hadley circulation.

Thesis Supervisor: Reginald E. Newell

Title: Associate Professor of Meteorology

ACKNOWLEDGEMENTS

The writer is particularly grateful to his advisor, Prof. R. E. Newell for his advice and encouragement throughout the course of this study. It has been made possible through the award of a fellowship by the New Zealand Government and has been supported by the U. S. Atomic Energy Commission under contract AT (30-1) 2241.

Since the tropical studies under this contract began here in 1963, many people have contributed to the immense task of data processing and aided in the interpretation and presentation of the results. Professor V. P. Starr graciously provided access to the Northern Hemisphere data collected for his five year study under National Science Foundation Grants GP 820 and 3657, and has continually encouraged our efforts. J. M. Wallace processed much of the stratospheric data and reference has been made to his results throughout the text. Although space does not permit the mention of all who contributed, the writer would particularly like to thank his colleague Mr. D. G. Vincent for his assistance and Prof. Amos Eddy who supplied the original objective analysis program.

Finally, thanks are due to Miss Isabel Kole for drawing the figures and to Mrs. Cynthia Webster for her patience in typing the manuscript.

TABLE OF CONTENTS

LIST OF FIGURES

LIST OF TABLES

CHAPTER 1.

INTRODUCTION

It is generally recognized that the tropics play a major role in the atmospheric circulation. As a consequence of the small value of the Coriolis parameter and the weak meridional temperature gradient, they tend to be dominated by a zonally symmetric Hadley circulation in contrast to the Rossby regime prevailing at higher latitudes. The easterly surface winds in the lower branch of the Hadley cell lead to the generation of westerly angular momentum which is transferred poleward through the atmosphere into the sink region of mean surface westerlies at higher latitudes and maintains the kinetic energy of the subtropical jet streams. The tropics are also an energy source for higher latitudes since the greater amount of solar radiation received is only partially offset by the increase in outgoing longwave radiation. The net energy surplus is transferred poleward by the atmosphere and oceans to maintain approximate temperature equilibrium. The Hadley circulation, which is primarily driven by the release of latent heat in its ascending branch, is in the direct or energy-producing sense and the conversion by it of available potential energy to zonal kinetic energy is a major item in the global budget.

A good quantitative description of these features has so far been lacking and estimates of the global energy cycle are usually

based on conditions poleward of about 20° N (eg. Oort 1964). These are not necessarily typical of hemispheric conditions as a whole since the tropics cover an appreciable part of the hemisphere and are dominated by a different type of circulation. At the same time, the relative contributions of the mean cell and the eddy fluxes to transport processes within the tropics are in need of further evaluation together with their role in interhemispheric exchange. As Bjerknes (1966, 1968) has shown, relatively small changes in sea surface temperature can significantly influence the Hadley circulation and in turn the strength of the westerlies at midlatitudes. A greater understanding therefore of the tropical circulation may in turn lead to a better understanding of the climatic changes of higher latitudes, as well as such problems as the prediction of monsoon rainfall.

Despite the importance of the tropics to the atmospheric circulation as a whole, no good quantitative description of all the basic parameters is currently available. The main reason for this has undoubtedly been the lack of sufficient observational data on a global scale. In the past, most studies have been made for limited areas or in association with specific projects such as the International Indian Ocean Expedition. It has not been until fairly recently that sufficient data have been available to undertake a general circulation study of the type previously made at higher latitudes. As Riehl (1966) has pointed out, the total number of aerological stations within 25° of the

equator has approximately doubled since 1955 when the total was 79 and the number is increasing at a rate of about six per year. While the coverage is still not as complete as would be desired and large gaps remain over ocean areas, the data are now sufficient for a detailed evaluation of the tropical circulation. Another factor which has helped has been the more widespread use of electronic data processing facilities by countries with observing stations in the tropics. In this way it has been possible to obtain aerological data already on punched cards in most cases so that a minimum of hand processing has been required. There is unfortunately no central agency responsible for the world wide collection of research data although the National Weather Records Center at Asheville, N. C. is a valuable source for the Northern Hemisphere and uses a limited number of different data formats.

The research presented in this thesis grew out of a desire to gain a better understanding of the dynamics and the source of the biennial oscillation which is most pronounced in the tropical lower stratosphere. Despite the considerable interest it has aroused since its discovery nearly ten years ago (Reed 1960) no completely satisfactory theory yet exists for its downward propagation and its ultimate source is still unknown. As Newell (1964) has pointed out, the oscillation occurs in a region whose driving energy comes from the troposphere and may therefore be due to changes in the dynamical

forcing from below. As a first step in testing this hypothesis, the momentum transports by transient eddy processes in the stratosphere were computed and a biennial modulation found with the maximum occurring in the winters whose January fell in an even year (Wallace and Newell 1966). The eddy transports were apparently accompanied by mean meridional circulations which also were an integral part of the momentum budget (Wallace 1967). Subsequent studies have been directed towards a search for the biennial oscillation in the troposphere and attempts to relate it to the stratospheric oscillation. A direct measurement of the energy flux from the troposphere to the stratosphere is of course too difficult for meaningful results to be obtained. It is encouraging to note that there is evidence for a widespread oscillation in the troposphere (Landsberg 1962; Landsberg et al. 1963; Wright 1968) and, as for the stratospheric oscillation, it appears to be locked in phase to the annual cycle and to be largely due to changes in the intensity of the winter circulation from year to year.

In view of the importance of the tropical circulation to the global circulation as a whole and its direct influence on the mid latitude circulation, the present investigation was aimed towards producing a comprehensive picture of the dynamics of the tropical circulation as well as a search for year to year modulations in its intensity which could provide a clue to the source of the biennial oscillation.

The study has been mainly directed towards finding seasonal mean conditions and no attempt has been made to study daily weather patterns although the day to day variations are of course represented statistically by the eddy flux quantities. The relatively low station density and the long averaging periods have meant that only the large scale features which remain relatively fixed from year to year appear in the analyses and that the smaller scale features are lost. In particular, such features as the double ITC structure over the Eastern Pacific shown clearly in satellite pictures and reproduced in the model of Charney (1968) can not be represented in the analyses. In all cases the statistics have been presented as zonal means which do not show the variations in the parameters along latitude circles. In cases of particular interest maps have also been presented to show the longitudinal variation but because of the fair degree of zonal symmetry prevailing in the tropics the cross sections are a better representation of conditions at individual meridians than would be the case at higher latitudes.

The methods used are essentially those which have been applied to studies of higher latitude circulations in the past and the present investigation is complementary to a major study of the Northern Hemisphere circulation by the writer's colleagues under the direction of Professor V. P. Starr. The exchange of basic data between the two projects has improved the mid latitude coverage of the

present study and the tropical coverage of the five year Northern Hemisphere study. It is anticipated that the combined results of the two will lead to the best understanding yet obtained of the atmospheric circulation as a whole.

The results of this study are presented in two parts. The first, which includes Chapters 2-8, describes the data sources and analysis techniques and presents the long term mean statistics obtained for the four seasons. The results are reviewed in Chapter 8. The second part opens with a review of the present status of the biennial oscillation with particular emphasis on current theories of its dynamics and its possible source, together with possible linkages between the tropospheric and stratospheric oscillations. The final chapter contains the results of a pilot study of year to year changes in the tropospheric circulation. Some evidence has been found for a biennial modulation of the intensity of the tropical circulation although the results are difficult to obtain because of the small amplitude of the tropospheric oscillation.

CHAPTER 2.

DATA SOURCES AND PROCESSING

2.1 THE OBSERVATIONAL NETWORK

The results presented in this thesis have been based on the data from 303 radiosonde and radar wind stations within the overall period July 1957 to December 1964. Virtually all stations available between latitudes 35° N and 30° S were included together with a sufficient number of regularly reporting stations to extend the area covered to 45° N. Stations making pilot balloon observations alone were not included since their coverage is poor at higher levels in the troposphere and their statistics tend to be biased in favour of light winds and fair weather. The quality and quantity of the data varied considerably between stations. Many did not report regularly throughout the entire period and 15 stations had fewer than twelve months of observations. The principle reporting time was 0000 GMT but where necessary data at 0600 and 1200 GMT were included to improve the coverage. Fig. 2.1 shows the complete set of stations used and their report type. In general the data coverage was not good above 100 mb and faded out below this over China as can be seen from the maps presented in the following chapters.

Daily data for most of the Northern Hemisphere stations were supplied by the National Weather Records Center at Asheville, North

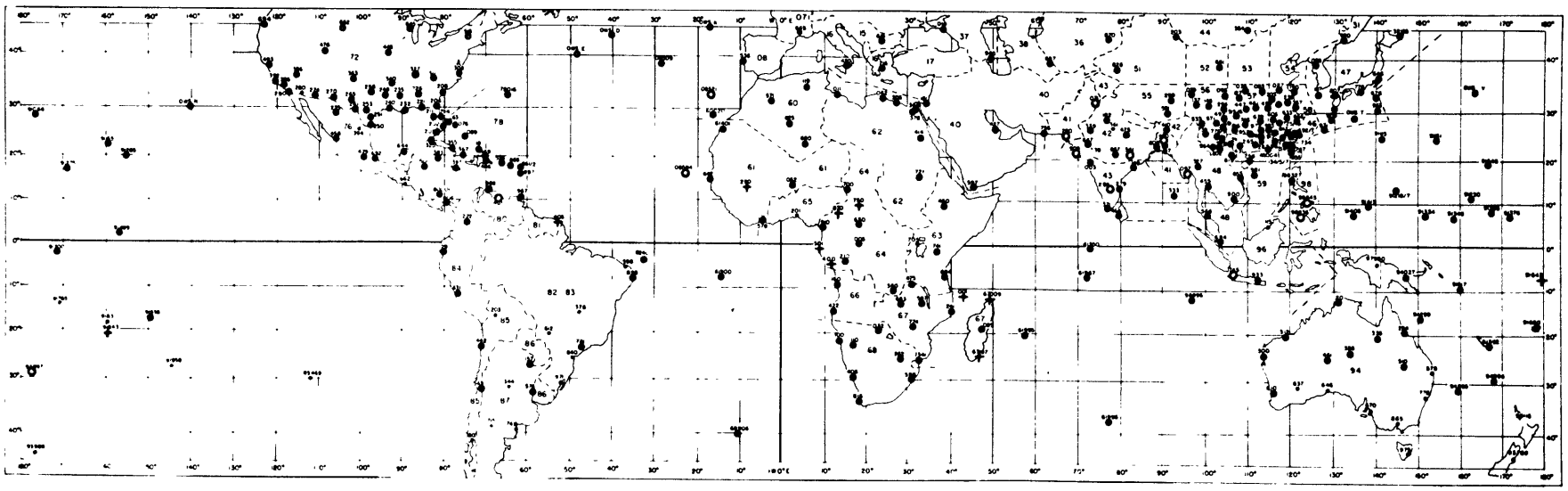

Fig. 2.1: Stations used in the study. Those reporting winds only are indicated by a cross and those with radiosonde data only by an open circle.

Carolina on card decks used for the Northern Hemisphere Data Tabulations. For 212 of these stations the data for levels up to 100 mb were obtained indirectly from tapes prepared by the Travellers Research Center (TRC) for the five year study mentioned previously through the courtesy of Prof. V. P. Starr. For one third of these, the data were augmented by cards obtained directly from Asheville to improve the coverage and to extend the period of study at each end of the five year period May 1958 - April 1963. Data for levels above 100 mb had previously been obtained for 250 Northern Hemisphere stations from the same sources and 120 of these were included in the present study. They had already been processed by J. M. Wallace as described in his thesis (Wallace 1966) and his monthly mean statistics were used instead of the original daily values.

In the Southern Hemisphere approximately one third of the stations were again supplied by Asheville, but most were obtained on card decks from the Australian, British, French, New Zealand and South African Meteorological Services. To fill some of the gaps, cards were punched from Portugese and Mauritian tabulations and from the IGY-IGC microcards. A complete station list will be found in Appendix A together with a more detailed description of the data sources which are summarized for convenience in Table 2.1.

Table 2.1

Data Sources

SUMMARY

	N. Hemisphere	S. Hemisphere	Total:
TRC	142	0	142
TRC + ASH	69	1	70
ASH	12	14	26
MCDS + ASH	5	3	8
MCDS	6	6	12
FOREIGN	5	34	39
FRN TABS	0	6	6
TOTALS:	239	64	303

2.2 BASIC PROCESSING

The daily data for each station were first used to compute monthly mean statistics at all available levels from the surface to 7 mb. The following quantities $\overline{u}$, $\overline{v}$, $\overline{T}$, $\overline{Z}$, σu, σv, σT, σZ, $\overline{u'v'}$, $\overline{u'T'}$, $\overline{v'T'}$, $\overline{u'Z'}$ and $\overline{v'Z'}$ were computed, where the bar denotes a time average and a prime deviations from it. At the same time the mean specific humidities and water vapour transports were computed and the results supplied to Dr. E. G. Rasmusson of ESSA for analysis.

The standard deviations of temperature, T, and geopotential, Z were used as a check for gross errors in the data and when these

values were excessive the reason could usually be traced to perhaps one or two observations with obvious coding or punching errors. Initially these were removed by hand and the monthly statistics recomputed but with the changeover from the IBM 7094 to the IBM 360 the opportunity was taken to perform the data checking during execution of the program. The machine editing procedure was later made necessary by obtaining the data on tapes rather than on cards and was extended to cover the wind components u and v. At each level the standard deviations were first computed and if any were found to be above a reasonable upper limit a checking procedure was initiated. This rejected observations differing from the mean by more than two standard deviations or by a fixed amount if the standard deviations were particularly large. All terms were then computed for the checked data. Although at first sight a cut-off value of two standard deviations appears rather small the checking procedure was only executed in cases where the standard deviation was unusually large at the level in question. In most cases this could be attributed to large deviations resulting from coding or punching errors which produce an artificially high standard deviation.

The IBM 360 programs were also adapted to be more flexible and contained common data checking and output subroutines. Assembler language subroutines were used to decode the varying card for-

mats and store the observations by level and day in standard units of m/sec, ^{o}C, g.p.m. and g/kg. For the Australian and Indian data the winds were interpolated between the reporting levels at 5000 ft. intervals to the constant pressure surface, using the reported height of the surface, or a climatological height if it was missing.

The output from the covariance programs was printed and also punched on cards in a standard format. The punched output from all stations was sorted and then written on magnetic tape in order of a station index, KN, within each month. (The KN index appears in the first column of the station list in Appendix A.) To minimize the amount of tape required for storage and the time required to read it, records were omitted where stations did not report at all in a given month and the data were written in a packed format using an assembler language subroutine. This format is described in Appendix B and may be read without much difficulty on any computer with 7 track tape facilities. Programs for tape handling are available for both the IBM 360 and IBM 7094. A total of approximately 17000 records was written on two tapes, each record containing the covariance data for a particular station and month. A certain amount of editing was carried out during the preparation of these tapes but this was mostly confined to eliminating terms involving Z and T where they had large standard deviations. The packed record on the tape contained the 13

terms listed earlier in this section, together with the numbers of observations, at all levels from the surface to 7 mb although in practice only the main synoptic reporting levels had sufficient data for analysis. Since the covariances computed earlier by Wallace comprised the bulk of the data at 100 mb and above and did not include $\overline{u'T'}$ or the terms involving Z, these terms were not included on the tape above 100 mb.

2.3 COMPUTATION OF LONG TERM MEAN VALUES

In order to facilitate the computation of long term values three tapes were prepared from the covariance tapes described in Section 2.2. These three tapes contain the monthly sums required for the computation of $\bar{u}$, $\bar{v}$, σu, σv, $\overline{u'v'}$; $\bar{T}$, σT, $\overline{v'T'}$ and Z, σZ, $\overline{v'Z'}$ respectively. The values for the covariances $\overline{v'T'}$ and $\overline{v'Z'}$ are not strictly correct since in most cases the numbers of observations of v and T or Z differ. The expressions used, for example, to generate the sums on the temperature tape are as follows:

$$\sum T = NT \times \bar{T} \qquad 2.1$$

$$\sum T^2 = NT \times \left((\sigma T)^2 + \bar{T}^2\right) \qquad 2.2$$

$$\sum vT = NVT \times \left(\overline{v'T'} + \bar{v}\,\bar{T}\right) \qquad 2.3$$

$$\sum v_T = NVT \times \bar{v} \qquad 2.4$$

$$\sum T_v = NVT \times \bar{T} \qquad 2.5$$

where NT is the number of temperature observations and NVT is the number of observations used in forming the covariance. Strictly, the values of $\bar{v}$ and $\bar{T}$ in 2.3 - 2.5 should be only those of the observations used in forming the monthly covariance but these were not included in the output from the covariance program. It should be pointed out that reversing this procedure according to the equations

$$\bar{T} = \sum T / NT$$

$$\sigma T = \sqrt{\sum T^2/NT - \bar{T}^2}$$

$$\overline{v'T'} = \sum vT/NVT - \sum v_T \sum T_v/(NVT)^2$$

leads to a correct value of $\overline{v'T'}$ for any individual month although the results obtained from a combination of a number of months could possibly show some bias. Some possible causes for a differing number of wind and temperature observations are

(i) Balloon lost during tracking

(ii) Observations rejected during computation of the covariances

(iii) Restricting radiosonde releases to every 2nd or 3rd day

while wind observations are made every day.

While Case (iii) should not introduce any bias in the long term means it is generally recognised (eg. Priestley and Troup 1964) that Case (i) occurs during stronger wind conditions and may cause a significant reduction in the mean winds and flux quantities. The effect of rejecting observations during the calculation of the monthly means is somewhat uncertain. If the errors are randomly distributed then no bias is introduced in the long run but it is conceivable that large values might be selectively eliminated with an effect similar to (i).

The three sum tapes were used to obtain long term means for each station of the quantities listed above at the main synoptic levels. Four seasons were chosen,December-February, March-May, June-August and September-November, and the wind and temperature statistics were obtained for the entire period and for even year and odd year combinations in order to examine possible changes related to the biennial oscillation. The odd year and even year combinations were not obtained for the geopotential terms as the $\overline{v'Z'}$ flux was small in comparison to other terms in the energy budget and the changes in $\overline{Z}$ are directly related to those in $\overline{T}$.

CHAPTER 3.

ANALYSIS TECHNIQUES

The long term mean statistics presented in the following chapters were obtained in two principle ways. In the troposphere up to the 100 mb level where data coverage is satisfactory the zonal means were obtained from grid point values resulting from objective analysis of station means. Above the 100 mb level the data were no longer adequate for machine analysis and instead the cross sections were obtained by grouping stations into 10^{o} latitude bands centred on the equator. In order to reduce the bias associated with denser observing networks over the continents a weighting scheme was employed which weighted each station according to the distance from its neighbors. Since machine analyses could not be attempted for individual months, the latitude band means for the troposphere were used to examine the year to year variation of selected parameters.

A more detailed description of the analysis techniques will be presented in the following sections.

3.1 THE OBJECTIVE ANALYSIS TECHNIQUE

The objective analysis technique used was based on the screening regression approach of Eddy (1967a, b), whose method is appropriate for the case of isotropic, stationary scalar fields. The main steps

in this analysis procedure are:

(1) Data checking and trend removal:

Data are grouped into latitude bands and within each band the mean and standard deviation are found. Stations differing from the mean by more than a prescribed number of standard deviations are eliminated. Following this a mean latitudinal trend is computed by filtering the zonal means or by fitting a polynomial to them. The trend thus computed becomes the first approximation to the analysis and is removed from each of the station values.

(2) Computation of the autocorrelation function:

The lag correlation is now computed for the residues at each station as a function of the separation between stations. Averaging is carried out over all possible pairs of points.

(3) Smoothing of the autocorrelation:

The autocorrelation computed from the raw data is now extrapolated back to small lags and where necessary missing values are interpolated. The Fourier transform is now taken to determine the contribution of all scales to the total variance. On the assumption that observational errors will contribute most to the power in the shorter wavelengths, the spectrum is truncated at a suitably determined upper frequency limit. Applying the inverse Fourier transform to the truncated spectrum leads to the final smoothed autocorrelation function which is taken to be zero at every point beyond the first posi-

tive lobe.

(4) Regression analysis:

Finally a screening regression analysis is carried out at each grid point where the predictand is located. As predictors, a limited number of stations closest to the grid point are selected. Their correlations with each other and with the predictand are determined solely by the separation distance which is used to index the table of smoothed correlation coefficients formed in step (3). With the correlation (or covariance) matrix formed in this way, the screening procedure is followed as described by Efroymson (1962). The predictors which give the largest reduction in the predictand variance are selected in turn until no further significant reduction is obtained. The predictand value is obtained by multiplying the station residues by the regression coefficients and is added to the latitudinal trend. The reduction in predictand variance is retained to indicate the reliability of the analysis. Typically it ranges from zero in isolated areas to about 90% where data coverage is good.

Although rather complex and time-consuming the regression technique does have two main advantages over simpler schemes such as that of Cressman (1959) which take an average of all station values around the grid point using a weighting function dependent on their distance from it:

(i) Since the correlation between adjacent stations is relatively high, selection of one station from an area of high station density tends to prevent the selection of others and the analyzed value is based on a more uniform distribution of stations about the grid point. Consequently better analyses are obtained where field gradients are sharper.

(ii) The sum of the regression coefficients or weights is not usually equal to one, and may be greater. For this reason high and low values may be built up in areas surrounded by anomalies of the same sign. In the simpler schemes the analyzed value has to lie between the highest and lowest values of the nearby stations.

At first it was hoped that the Eddy scheme could be used without modification and early results for temperature fields were encouraging. However, for quantities such as the momentum flux, which are very susceptible to observational error and show less continuity between adjacent stations, the results were far from satisfactory. This could be traced to a small zero lag correlation and a relatively short influence radius. The resulting analyses were lacking in continuity and gave a poor fit to apparently well defined maxima and minima. From a statistical viewpoint the Eddy scheme represents the ultimate analysis and the low autocorrelations are simply a reflection of the uncertainty in the observations. Examination of the plot-

ted maps, however, showed that although hand analysis was difficult in places quite reasonable results could be obtained if some averaging of neighboring values was carried out by eye. With the belief that the hand analyses came closer to representing the true situation, various modifications of the Eddy scheme were tried with the intention of reproducing the hand analyses as closely as possible. One approach was to use the good autocorrelation curve from the temperature field to analyze the wind component fields. The reasoning behind this is somewhat tenuous but similar to that used in setting up the equivalent barotropic model for numerical weather prediction. With the temperature field (and hence the thickness field) showing a similar pattern to the geopotential field, the geostrophic relation implies similar scales of variation in the wind and temperature fields. Not much can be inferred about the scales of variation of covariance fields such as the momentum and heat fluxes although the plotted maps suggest that the largest scales are similar to those of the wind and temperature fields.

With a view also to reducing the computer time per map experiments were made in which steps 2 and 3 of the Eddy scheme were eliminated entirely and a purely artificial smoothed autocorrelation function was employed. The function chosen was

$$r(d) = 0.9 \times \frac{D^2 - d^2}{D^2 + d^2} \qquad 3.1$$

where d is the separation distance and D the influence radius beyond which the correlation is taken as zero. The form of this function is identical to that frequently used for a weighting function in the simple Cressman-type schemes. The zero lag value of 0.9 was based on typical values for temperature fields which show good continuity and are most suited to the Eddy approach. A suitable value for the influence radius D was obtained by experimenting with different parameters and levels. In general shorter influence radii gave a better fit to station values while longer radii afforded better continuity in regions of fewer observations. The difference in the analyses however was not very great even when D was changed by a factor of two and this was taken as an indication that the analysis was not too sensitive to the form of the autocorrelation curve. The initial set of analyses presented in Kidson, Vincent and Newell (1969) were made with D = 1900 nm at the equator while the more recent analyses used a D value of 1600 nm. The resulting zonal means and energy integrals showed only slight changes. The analyses were performed on a square grid on a mercator projection with the grid size being 10^{o} longitude. The latitudes corresponding to the nine rows of the grid are 41.0N, 33.0 N, 24.2 N, 14.8 N, 5.0 N, 5.0 S, 14.8 S, 24.2 S and 33.0 S. Zonal means were formed from the 36 grid point values at each of these latitudes without regard for surface elevation and this is the reason for the seemingly odd choice of latitudes occurring in the tables in

later chapters. The latitudinal trend removal and data checking were carried out using the original Eddy subroutine. A limit of three standard deviations was used to eliminate bad wind observations and four standard deviations for the temperature and heat flux. Stations were also rejected if fewer than 30 observations were available for means of single quantities and 90 observations for covariances. The trend was obtained by fitting a 6th degree polynomial to some 19 latitude band means with a spacing of 1/2 grid square. As well as converting the original Eddy program to work in grid coordinates instead of latitude and longitude,part of it was converted from FORTRAN to Assembler Language. The net result of all these changes was to reduce the execution time of the program from the order of a minute to 10 seconds. This made the analysis of a large number of maps economically feasible. Inclusion of steps 2 and 3 of the Eddy scheme would have raised the time to about 30 seconds.

The resulting analyses were printed out on the line printer using a contouring subroutine kindly provided by Mr. R. C. Gammill. This program fitted 3rd degree polynomials to the grid point values so that discontinuities were of 2nd and higher orders and a smoothly varying field was obtained.

Comparison of the printed analyses with the hand analyses showed their standard to be comparable. Differences occurred for the most part where some observations had been given less weight in

the hand analyses while they were assumed to be equally reliable in the machine analysis. The machine analysis scheme still retains the screening regression part of the Eddy scheme and with it the two principal advantages mentioned earlier. As a check on its performance one analysis was also made using the same weighting function and influence radius in the simple Cressman scheme. The results were seen to be clearly inferior in this case and the comparisons were not pursued any further.

3.2 LATITUDE BAND MEANS

In order to obtain mean cross sections on a monthly basis in the troposphere and long term means in the stratosphere, latitude band means were used. All stations were grouped into 10^{o} latitude bands centred at eight latitudes from 40^{o}N to 30^{o}S. In view of the dense network of stations over the continents, particularly the U.S. and China, it was decided to try and reduce any possible bias by giving each station a weight based on the distance to its nearest neighbors within the latitude band. Tests of different weighting schemes were carried out with the results compared against zonal means from analyzed maps. Some earlier runs were also available in which the station values has been weighted by the corresponding number of observations without regard to station location. Although the

means did not vary much between the different weighting schemes it appeared that the weighting by numbers of observations was least successful. The scheme finally adopted had weights computed as follows

$$w_i = \frac{MIN(\lambda_i - \lambda_{i-1}, \Delta) + MIN(\lambda_{i+1} - \lambda_i, \Delta)}{\Delta}$$

where λ_i is the longitude of station i and $\lambda_{i\pm1}$ are the longitudes of its nearest neighbors within the same band. Δ is twice the average arc length per station obtained by dividing 360^o by the number of stations in the band. MIN indicates the minimum of the two quantities in parentheses. It will be seen from the form of this function that the weight for isolated stations can not exceed 2 while if the stations were evenly distributed each would have a weight of 1. The minimum weight was set at 0.1 so that all stations could give some contribution. Summation of the station weights over 30^o longitude intervals showed the weighting to be reasonably uniform over most sections except those over the empty oceans. Although in principle the station weights could have been computed for each month and level on the basis of stations reporting it was decided simply to compute a single weight for each station and use this for all calculations.

Early runs showed the need for some data checking as some large and erroneous station values were responsible for errors which were particularly prominent in 12 month running mean values. For-

tunately the IBM 360/65 at the MIT Information Processing Services Center had sufficient memory size to store a complete month's observations for the 306 stations. After all station values for the month had been read in and sorted into latitude bands checking proceeded as in the first stage of the objective analysis scheme. The zonal means and standard deviations were formed and stations whose values differed from the mean by more than 3.5 standard deviations were excluded. The two parameters were computed again after each pass and the checking procedure was concluded when all stations were inside the current 3.5σ limit. If fewer than five stations reported no mean was computed for the band; each station was required to have a minimum of 3 observations for the month.

CHAPTER 4.

MEAN TEMPERATURE AND WIND FIELDS

The mean temperature and wind fields presented in this chapter were obtained from objective analyses of the long term station means up to 100 mb and from the latitude band means between 70 mb and 10 mb. The analysis techniques used have been described in Chapter 3. Since the biennial oscillation is most pronounced in the tropical stratosphere with an amplitude comparable to the seasonal changes the means for the stratosphere were computed giving equal weight to the data for odd and even years over the period July 1957 to June 1963. Three month seasons were chosen to reduce the irregularity in the flux quantities although the long term means for individual months appeared to be satisfactory for the determination of the mean zonal wind and temperature. The maps presented in this chapter have been based on the machine analyses used in the standing eddy computations and in most cases the analysis was not changed appreciably.

4.1 THE TEMPERATURE FIELD

While previous workers have been able to construct mean cross sections of the zonal wind using a variety of data sources (eg. Buch 1954, Mintz 1954, Obasi 1963a) the lack of data has made it dif-

ficult in the past to obtain accurate mean temperature cross sections. For the Northern Hemisphere the results of Peixoto (1960a) for the year 1950 are available but no studies on a comparable scale have yet been published for the tropical region and the Southern Hemisphere. Indeed the lack of reporting stations at mid latitudes in the Southern Hemisphere makes it unlikely that good representative cross sections will be obtained in the immediate future.

The mean temperature cross sections for the four seasons are presented in Tables 4.1 and 4.2. The main features are summarized briefly as follows:

(i) Temperatures decrease poleward on the average up to about the 200 mb level, above which the minimum occurs at the equatorial tropopause near 100 mb.

(ii) The minimum at the equator disappears above the 30 mb level, but it is difficult to draw any firm conclusions because of the limited amount of data, particularly near the equator and in the Southern Hemisphere. It appears that warmer temperatures are found in the summer hemisphere and that the colder temperatures in the Northern Hemisphere for the December-February period persist into the March-May season. The corresponding feature does not appear in the September-November season but few observations are available in the Southern Hemisphere.

(iii) Between 15^{o}N and 15^{o}S temperature gradients are small and seasonal changes are limited to a range of about 1.5^{o} over most of the troposphere. This is comparable to the errors in the analysis and few clear patterns of seasonal change emerge. Extreme values occur with comparable frequency through all seasons except September-November when they occur about one half as often. Outside this region the tropospheric changes follow those of higher latitudes with colder temperatures experienced in the winter hemisphere. These variations extend closer to the equator at the 1000 and 850 mb levels.

(iv) The tropospheric temperature maximum occurs in the vicinity of 5^{o}S in the December-February period although it is not sharply defined. In the June to August period it moves to about 20^{o}N and it occupies intermediate positions in the other seasons. This asymmetry between the two hemispheres is apparently due to stronger heating over the continents in the Northern Hemisphere and is related to the monsoonal circulation. It was not seen above the 700 mb level in the data of Peixoto (loc. cit.), presumably because of the longer season and the paucity of data over the Asian continent. The anomalous heating over the continents is shown clearly in Figs. 4.1-4.3 and will be described later in more detail.

(vi) At mid-latitudes the temperature variations in the lower stratosphere are in the opposite sense to those in the troposphere

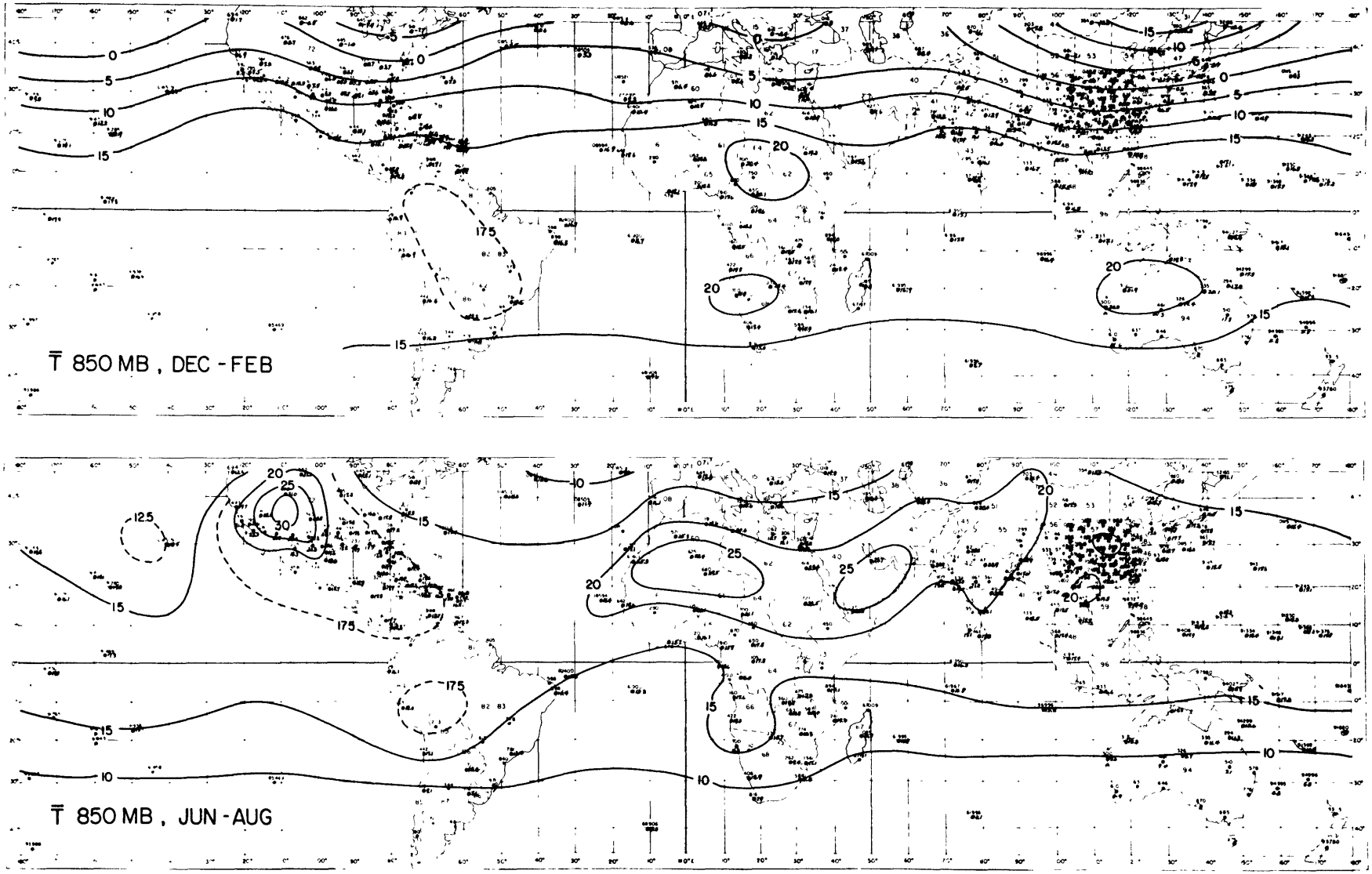

Fig. 4.1: Temperature maps at 850 mb for December-February and June-August.

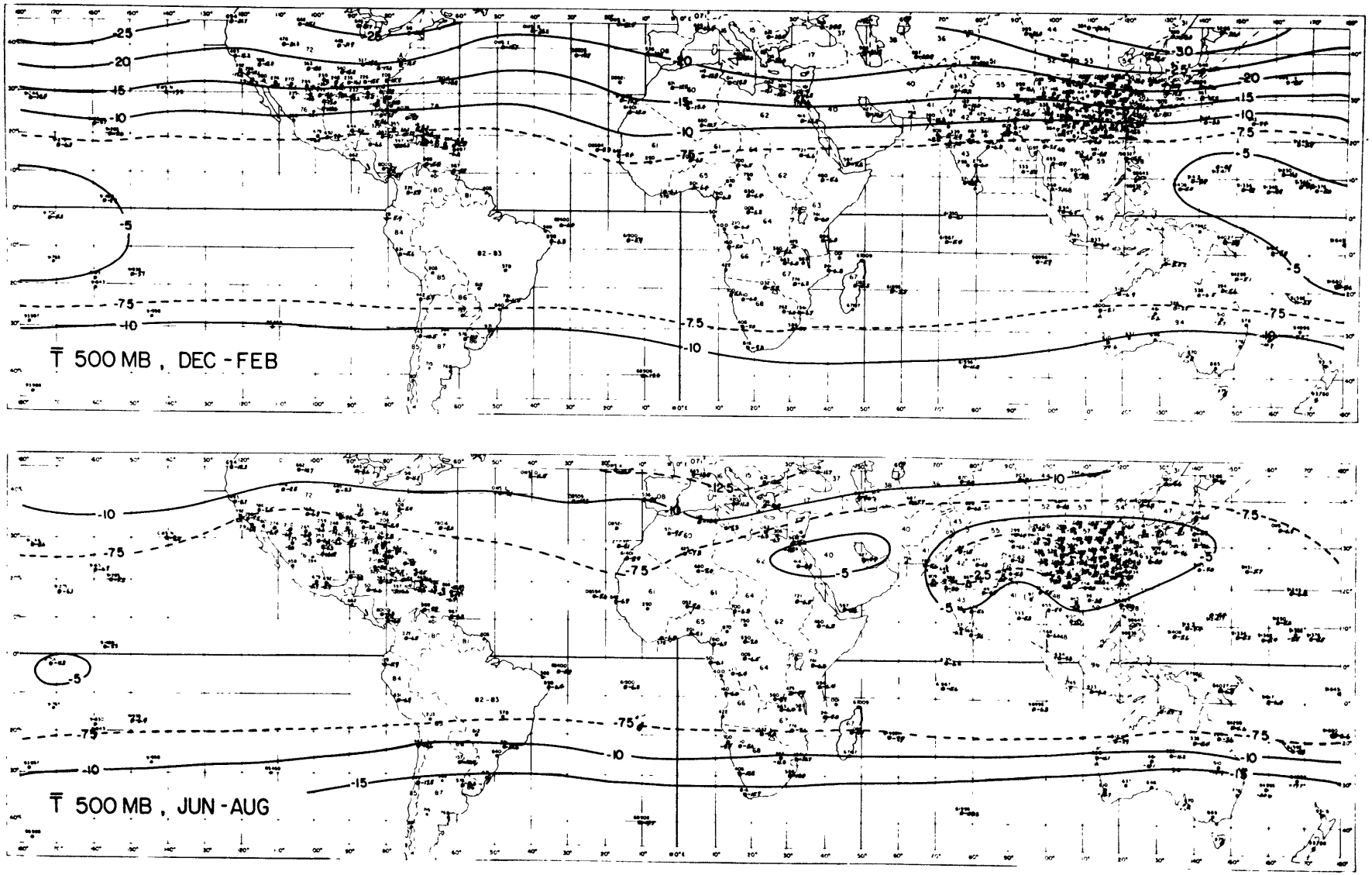

Fig. 4.2: Temperature maps at 500 mb for December-February and June-August.

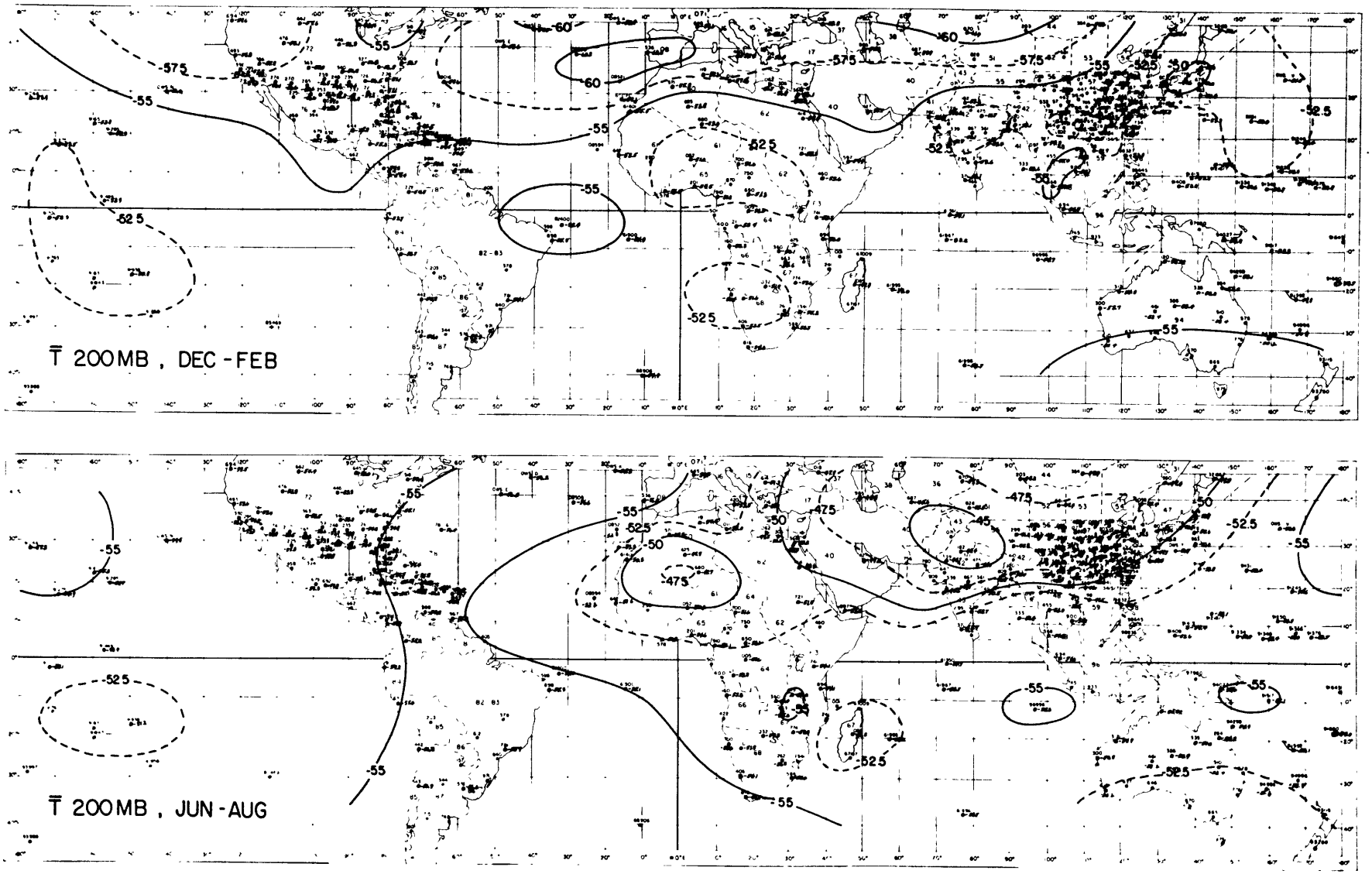

Fig. 4.3: Temperature maps at 200 mb for December-February and June-August.

with warmer temperatures immediately above the tropopause in winter. The predominant change in the tropical lower stratosphere is from colder temperatures during December-May to warmer temperatures in June-November. The largest changes occur at 70 mb and reach 7^{o} at 10^{o}N and 20^{o}N although they are more or less symmetric about the equator and also appear at the equatorial tropopause. At 40^{o}N the pattern changes again by the 10 mb level where the trend is for warmer temperatures in summer.

The analysed maps at the 850, 500 and 200 mb levels are shown in Figs. 4.1-4.3 for the December-February and June-August seasons.

At 850 mb (Fig. 4.1) the lowest temperatures are observed over Siberia in Dec.-Feb. with the highest temperatures over the African, South American and Australian continents. The highest mean temperature observed is approximately 22^{o}. In contrast, the highest temperatures in the June to August period reach 29^{o} over the Sahara and Saudi Arabia. The high values over the western U.S. in June-August result from a relatively high surface elevation and the 00Z observation time being close to the time when the daily maximum is observed. This warm anomaly is likely to be considerably reduced on averaging over a 24 hour period but the other maxima are present during the night and early morning hours.

At 500 mb (Fig. 4.2) the cold area over Siberia remains and there are signs of another over the northern U.S. in December-February. Highest temperatures occur over the equatorial western Pacific. In the June-August period the maximum over the U.S. is no longer present and the highest temperatures are found further eastward over India and China. The maximum over the Sahara has largely disappeared.

As can be seen from the cross sections in Table 4.1 the 200 mb level shows the smallest latitudinal temperature gradients. The December-February map in Fig. 4.3 does not show such well-defined features as the June-August map where the monsoonal heating is very much in evidence over the African and Asian continents. Highest temperatures are again found over the Sahara and in a broad belt north of India extending from the Black Sea area to China.

4.2 THE MEAN ZONAL WIND

The mean zonal wind cross sections are presented in Tables 4.3 and 4.4 and in Fig. 4.4. In the troposphere they show the familiar pattern of a westerly vortex in each hemisphere separated by a belt of easterlies in the tropics. While the easterlies extend approximately from 30^{o}N to 30^{o}S at the surface, their latitudinal extent decreases to a minimum at 200 mb of 30 degrees latitude in the June to

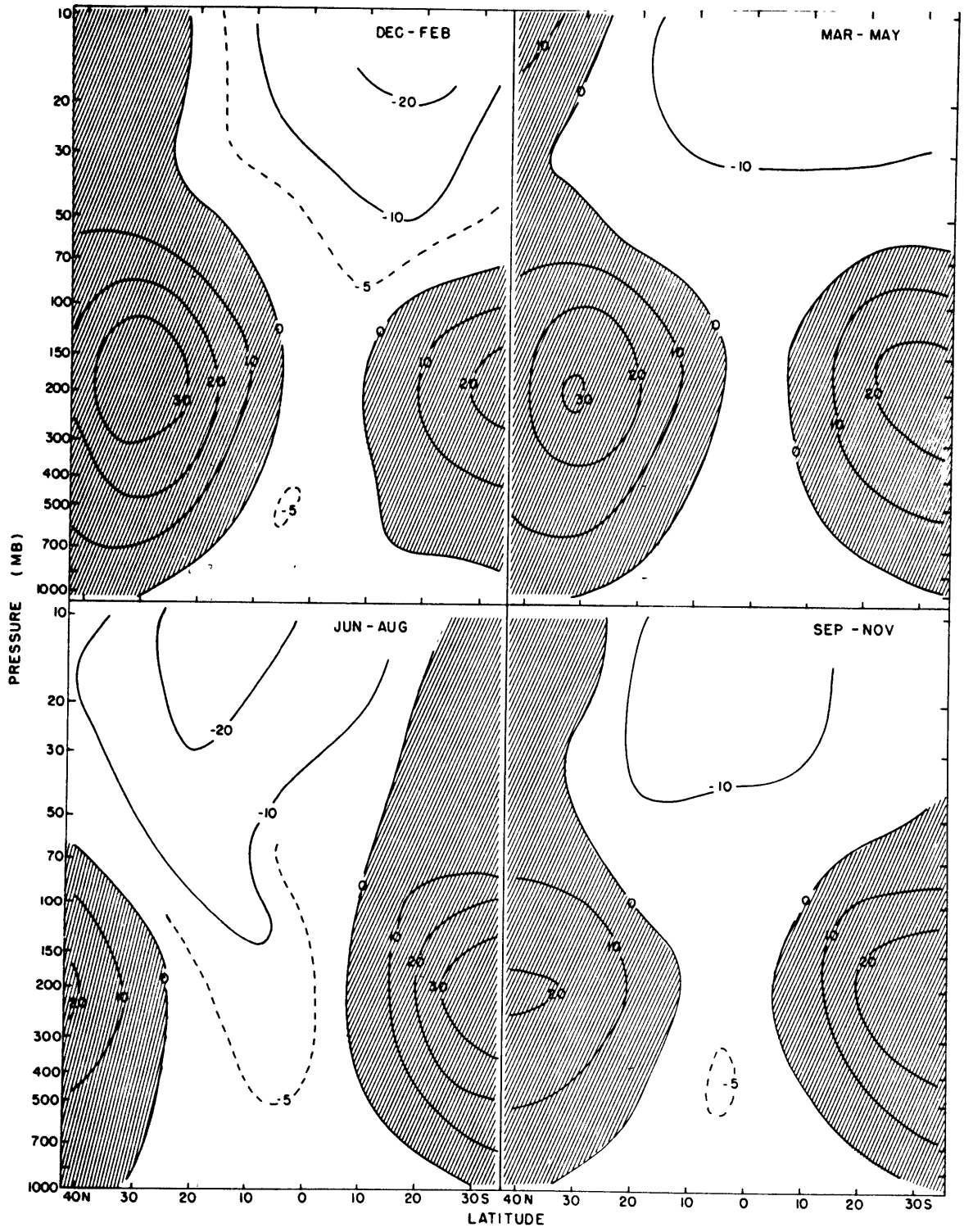

Fig. 4.4: Mean zonal wind cross sections for the four seasons in units of m · sec^{-1}. Westerlies shaded.

August period and to little more than 10 degrees in the March-May period. Above this level they gain both in width and strength as they merge with the easterly circulation of the stratosphere.

The axis of the subtropical jet is outside the area of analysis for the Northern Hemisphere during the June-August and September-November periods and for the Southern Hemisphere during all seasons except possibly March-May. The Northern Hemisphere jet reaches an average strength of 39 m/sec during December-February with its axis at 200 mb and 30^{o} N. In the northern summer its strength is at least 22 m/sec. The Southern Hemisphere jet exceeds a strength of 38 m/sec in the winter and 25 m/sec in the summer. These values are at least as large as those of Obasi (1963a). The westerly flow over the equator during his 6 month summer period is not supported by these results which show patterns similar to those of Mintz (loc. cit.) but with weaker easterlies.

Unfortunately the data coverage in the stratosphere is poor in equatorial regions and in the Southern Hemisphere but the boundaries between easterlies and westerlies with the biennial component removed are fairly well delineated up to the 20 mb level. One possible exception is the ten degree band centered on the equator where there appears to be a westerly bias in the statistics and some liberties have been taken in drawing the cross sections in Fig. 4.4.

In the tropical troposphere the strength and latitudinal extent

of the easterlies is greatest during the June-August period. This is due for the most part to the presence of the Tropical Easterly jet which extends from the Philippines across northern Africa to the Atlantic. Maximum wind speeds are observed to the south of the Asian continent, the highest value of approximately 30 m/sec occurring at the 150 mb level.

The seasonal changes in the strength and position of the jet streams are best seen by reference to the four maps in Fig. 4.5 which show the zonal wind component at 200 mb for each season. The map for the Dec.-Feb. period shows a three wave pattern similar to that found by Krishnamurti (1961) although the maximum over Arabia is much less marked. The speeds are also lower, with a maximum of 60 m/sec occurring over the south of Japan. The most probable reason for the difference is that the position of the jet fluctuates between different winters so that the long term maximum is weaker and more diffuse. This certainly appears to be the case to the east of the U.S. The westerly jet is still marked in the March-May period but weak and poorly defined in the other two seasons. The tropical easterlies are at minimum strength during March-May but increase to a maximum of 25 m/sec over southern India during June-August. The Southern Hemisphere westerly jet is seen most clearly in the June-August and September-November periods with a maximum of some 47 m/sec over Australia during the former.

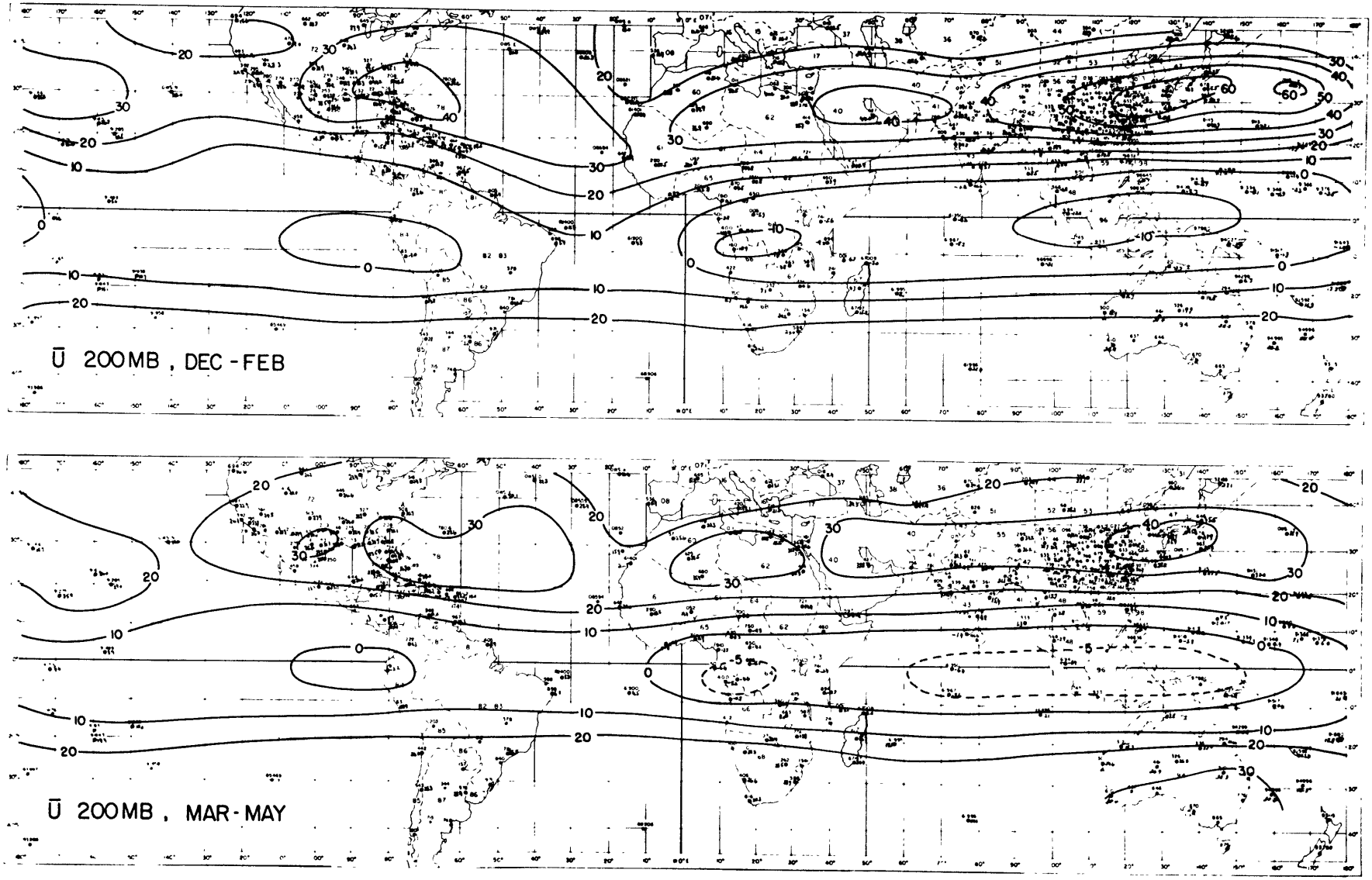

Fig. 4.5a: Mean zonal wind at 200 mb for December-February and March-May.

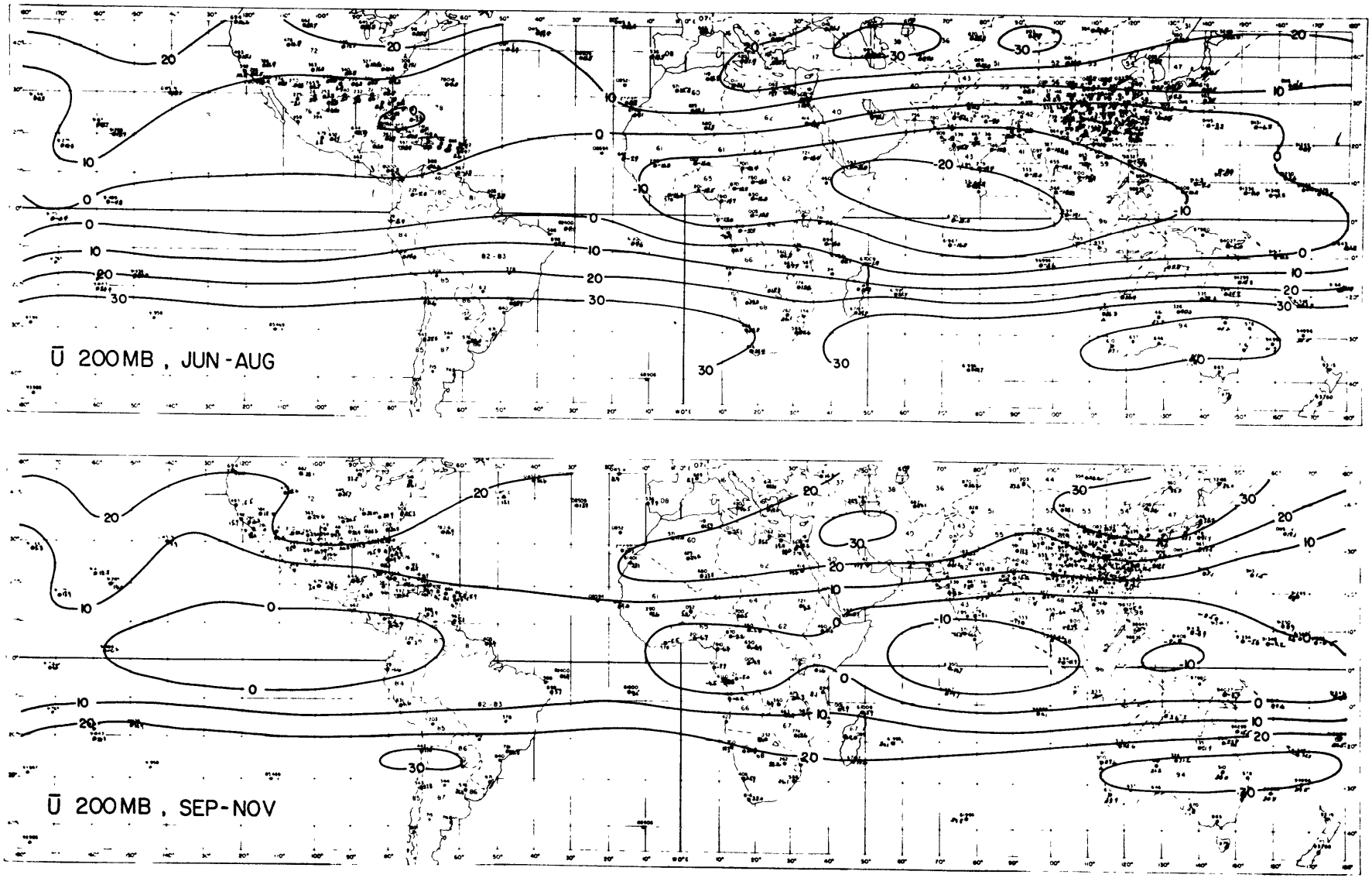

Fig. 4.5b: Mean zonal wind at 200 mb for June-August and September-November.

4.3 THE MEAN MERIDIONAL CIRCULATION

In contrast to the zonal wind and temperature the mean meridional circulation is very difficult to measure and earlier workers have obtained uncertainties of the same order as the mean values in middle latitudes. The results presented in Table 4.5 for the four seasons were obtained from the machine analyses as described in Chapter 3. The maps in Figures 4.6-4.9 show the 850 mb and 200 mb patterns for each season and these levels are representative of the upper and lower branches of the Hadley circulation. The uncertainty in the analyses used for deriving $[\bar{v}]$ cannot be obtained as in the original Eddy scheme but the upper limit is known from the within group variance before the regression analysis is carried out. As an example we take the 200 mb level for the December-February period which is characterized by quite large southward speeds in mid latitudes (Table 4.5). In isolated areas the standard deviation for the grid point value is approximately 4 m/sec which implies 95% confidence limits of $\pm$ 8 m/sec. In areas of good data coverage the regression technique leads to about a 90% reduction in variance of the predictand for quantities such as the temperature and this is a larger reduction than can be expected for wind fields. If however we assume a 90% reduction, the 95% confidence limits in the above example would be $\pm$ 2.4 m/sec. If averaging is then carried out over 36 such independent points to ob-

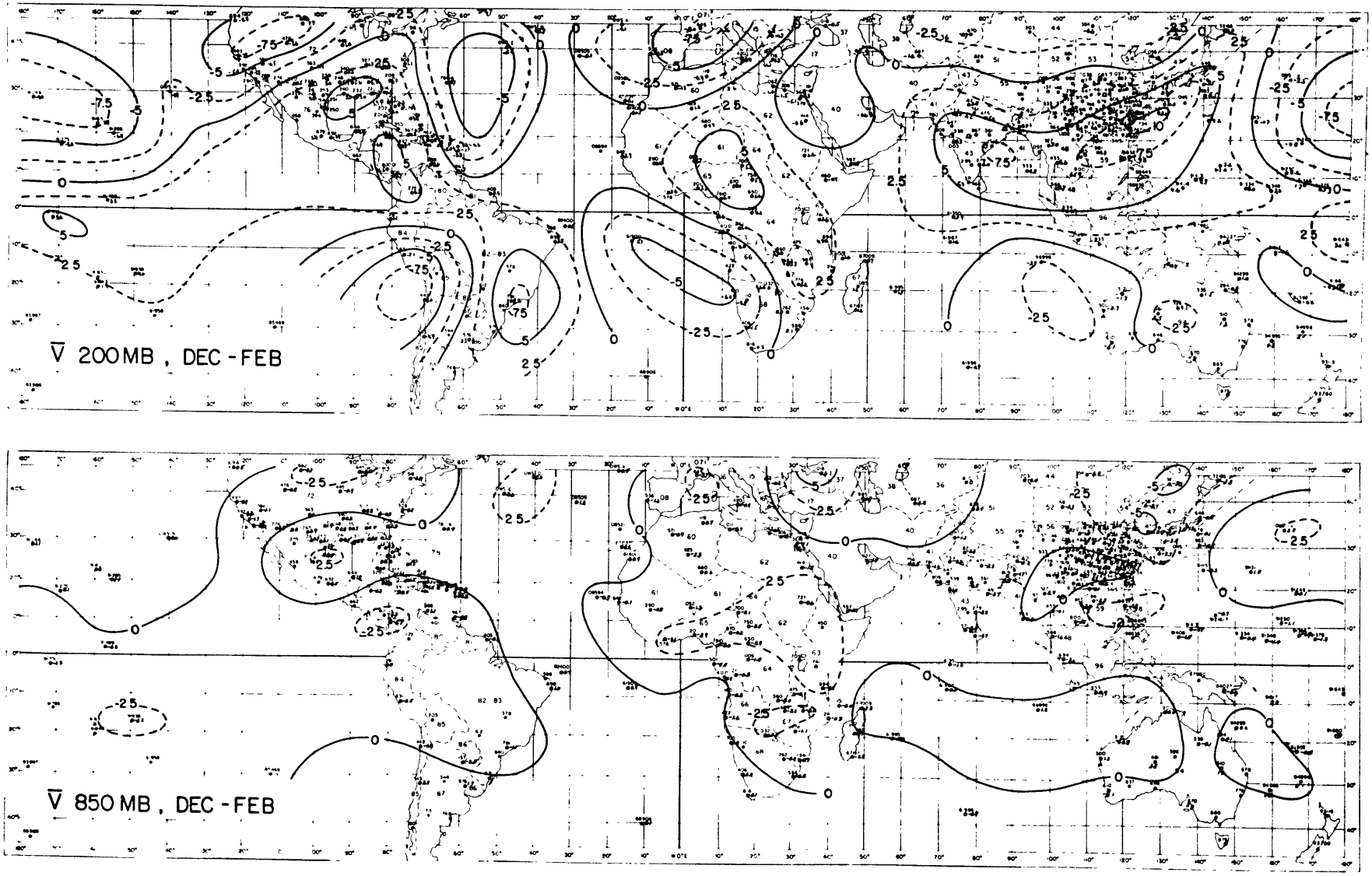

Fig. 4.6: Mean meridional wind components at 850 mb and 200 mb for December-February.

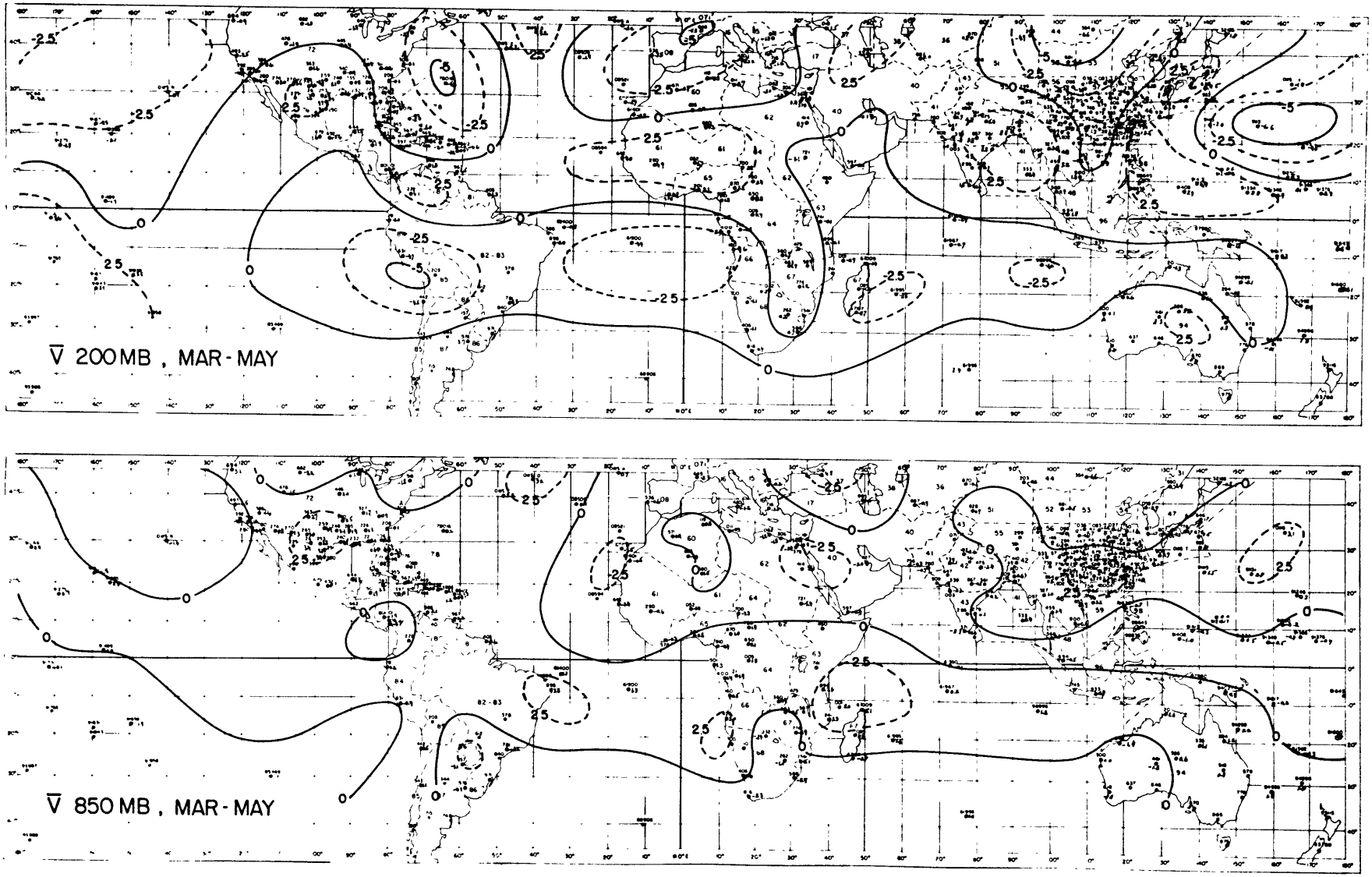

Fig. 4.7: Mean meridional wind components at 850 mb and 200 mb for March-May.

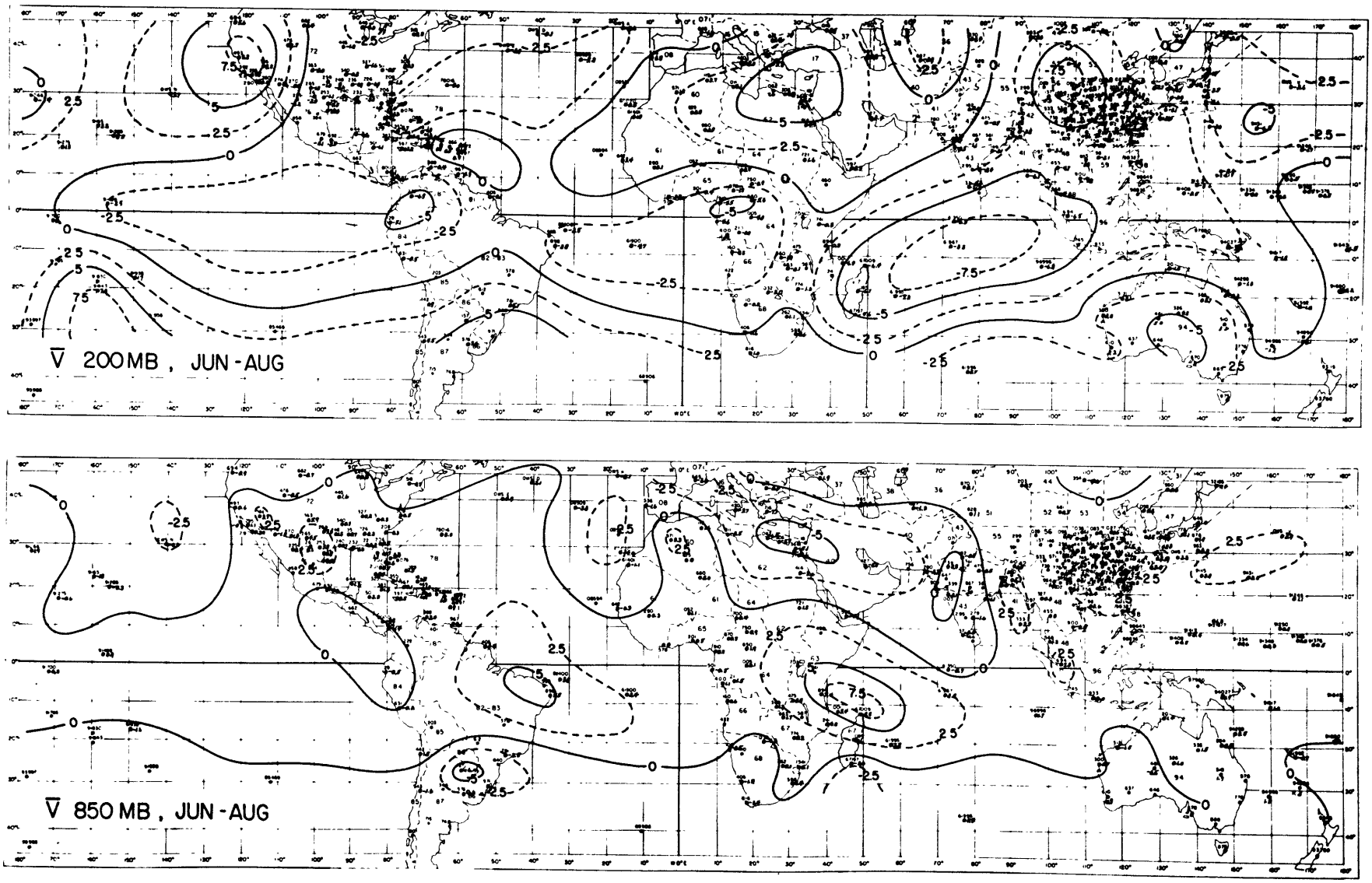

Fig. 4.8: Mean meridional wind components at 850 mb and 200 mb for June-August.

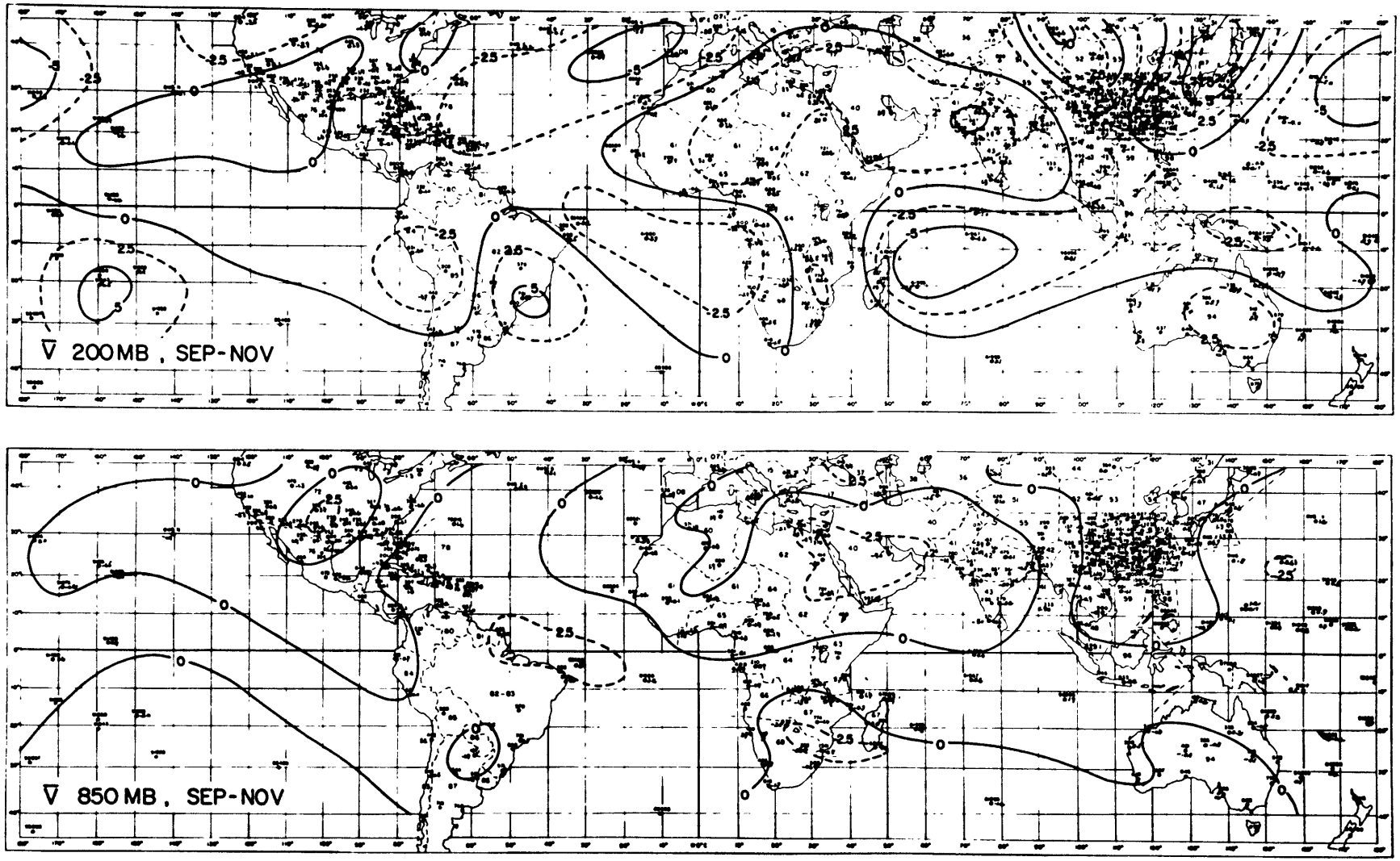

Fig. 4.9: Mean meridional wind components at 850 mb and 200 mb for September-November

tain the zonal mean, the 95% confidence limits for this mean would be $\pm$ 40 cm/sec. This figure, which represents an upper limit on the accuracy of the analysis is still comparable to reasonable values of $[\bar{v}]$ at mid latitudes, implying that it is impossible to measure $[\bar{v}]$ directly with sufficient precision in mid-latitudes, even in areas with good data coverage. In practice the confidence limits will be larger than this since in areas of poor coverage the errors at adjacent grid points are quite well correlated because they derive their values from the same station or stations.

With these difficulties in mind it will be appreciated that the mid-latitude values are not very well determined but the larger mean values in the tropics can be treated with more confidence. The values at 20^{o}S and 30^{o}S are based on rather few stations and little reliance can be placed on them. The pressure-weighted vertical integrals are also included in the tables and represent the net mass transport between 1000 and 100 mb. If no strong compensating flow is present above the 100 mb level then these vertically averaged values should not differ greatly from the complete integral to the top of the atmosphere. Typical values for the complete integral averaged over a season are of the order of a few millimeters per second (eg. Gordon 1953) so mean values much larger than this are indicative of deficiencies in the analyses. An examination of the vertical means in Table 4. 5 shows most of the values to be less than 20 cm/sec except at

33^{o}N and 41^{o}N where the analyses can not be considered reliable. The main problem appears to be the large southward components near the 200 mb level which are especially prominent during the December-February period. The map in Fig. 4.6 has been drawn by hand but it is difficult to reduce the value of -3.13 metres per second from the machine analysis while still fitting the plotted station values. Reading off grid point values at 41^{o}N from the hand analysis gives a value of -2.6 m/sec. In view of the comprehensive studies of the Northern Hemisphere circulation presently being undertaken by Prof. V.P. Starr and colleagues at M.I.T. and our main area of interest being the tropical region no further attempts were made at improving the analysis at mid-latitudes. Quite possibly our results are biased through the selection of stations in the 35^{o}N-45^{o}N band and analyses prepared for the same season in the five year study of the Northern Hemisphere give a much smaller mid-latitude circulation while the results in the tropics are comparable.

The analyses in Figs. 4.6-4.9 show the Intertropical Convergence Zone (ITC) to be best developed over Africa where it can be seen in all four seasons. The lack of stations in the eastern Pacific makes it impossible to show properly the well defined ITC which appears in data from satellite and ship observations etc. The ridges at 200 mb over the eastern U.S. and Japan show clearly in the December-February and March-May maps but there is not much evidence

for the trough over India seen in the data of Krishnamurti (1961). The monsoonal flow over Asia during June-August appears very clearly with a southerly inflow at 850 mb and a northerly return flow at 200 mb. As Flohn (1964) has shown it is this strong direct circulation which is responsible for the maintenance of the Tropical Easterly Jet.

The mean meridional mass circulations have also been computed from the $[\bar{v}]$ values given in Table 4. 5. The procedure followed was to subtract the vertical means from the components at each level and form a stream function by integrating the mass flux upward from the surface

$$\Psi(p) = -\frac{2\pi R \cos\phi}{g} \int_{1000}^{p} [\bar{v}]\, dp$$

The effect of subtracting the vertical integral is to confine the flow between the 1000 and 100 mb levels or within the troposphere. Indirect calculations of $[\bar{v}]$ (Murgatroyd 1968, Vincent 1968) suggest that the circulation in the upper troposphere extends in the same sense through the tropopause but the observations show the strength of the circulation to decrease above the 200 mb level, and probably only a small fraction of the mass transport occurs above the 100 mb level. The circulation patterns obtained are, of course, not representative of the flow at individual meridians and the structure of the ITC is blurred. The cross sections in Fig. 4. 10 do show however the main features of the meridional circulation which is dominated by the Had-

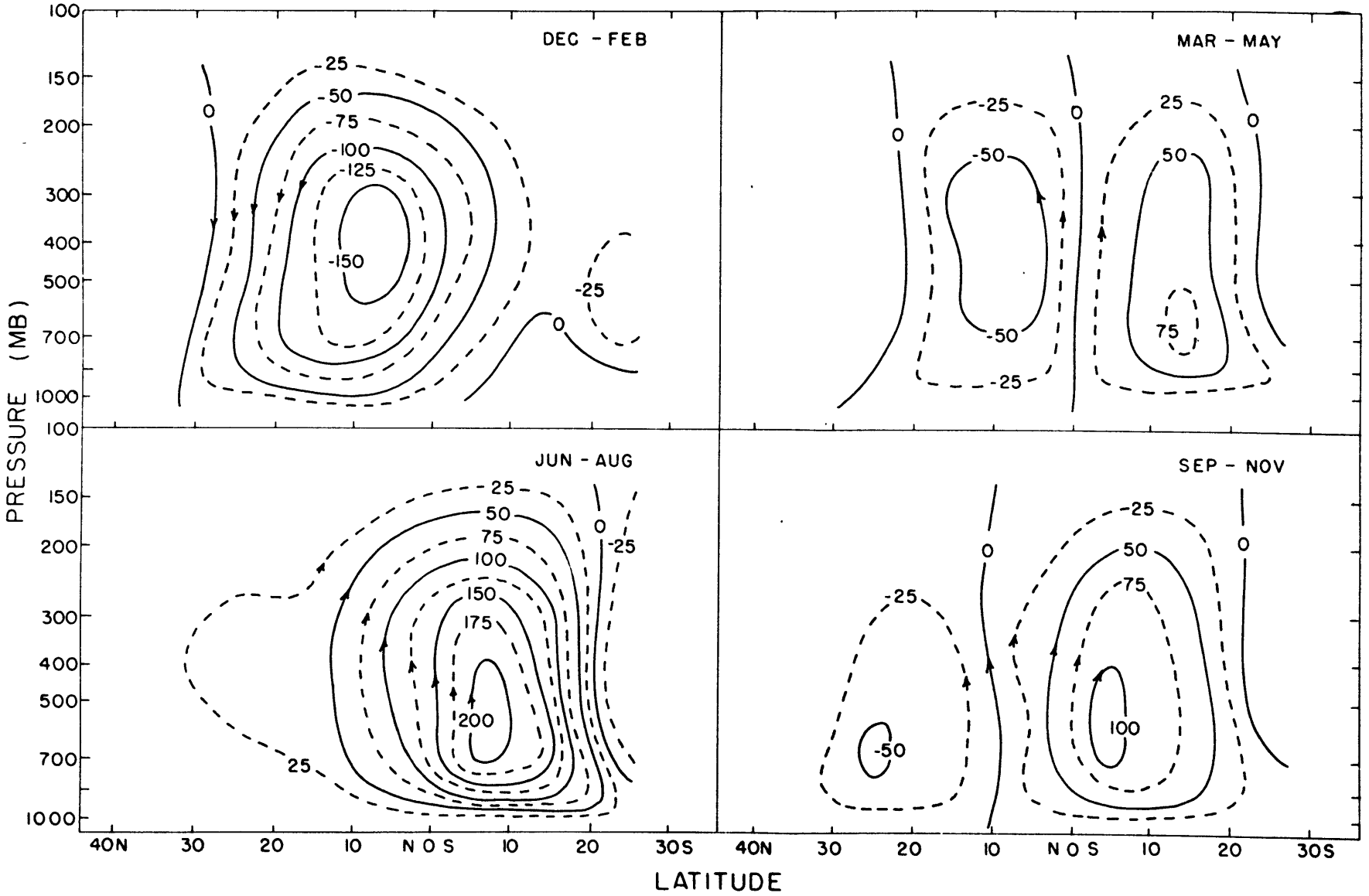

Fig. 4.10: Mean meridional circulation for each season. Streamlines at intervals of 10^{12} gm sec^{-1}.

ley cell of the winter hemisphere. In the December-February and June-August periods the winter Hadley cells are of comparable strengths and extend about 10^{o} into the summer hemisphere. The mass circulation of the northern winter cell is approximately 1.7×10^{14} g/sec and for the southern winter cell about 2.0×10^{14} g/sec. Considering the uncertainties involved these compare favorably with the earlier values of 2.3×10^{14} and an estimated 1.8×10^{14} obtained by Palmén and Vuorela (1963) and Vuorela and Tuominen (1964) respectively. They are also in reasonable agreement with the value of 1.4×10^{14} obtained in the numerical experiment of Manabe and Smagorinsky (1967).

In the intermediate seasons two Hadley cells are present. For the March-May period their strengths are comparable at 0.7 and 0.9×10^{14} g/sec for the northern and southern cells respectively. During September-November the southern cell, with a strength of 1.1×10^{14} g/sec, is twice as strong as the northern cell whose strength is 0.5×10^{14} g/sec. It is interesting to note that the total mass circulation in the two Hadley cells is roughly the same in each season. The mid-latitude meridional velocities lead to strong indirect cells but because of the difficulties mentioned previously little credence should be placed in them.

CHAPTER 5.

MOMENTUM TRANSPORTS

With mean easterly surface winds in the tropics and mean westerlies at middle and higher latitudes, the frictional torque at the earth's surface provides a source of westerly angular momentum in the tropics and a sink at higher latitudes. Since the long term mean angular momentum of the atmosphere remains constant, a fundamental balance requirement to be fulfilled by the atmospheric circulation is the poleward transport of angular momentum between the source and sink regions.

The time-averaged total flux of angular momentum across a latitude circle may be written as

$$\frac{2\pi R^2 \cos^2\phi}{g} \int \left[(\Omega R \cos\phi)\,\bar{v} + \overline{uv} \right] dp \qquad 5.1$$

where the first term in the integral represents transport due to the net mass flux and the second, the transport of relative angular momentum. Although the first term vanishes in taking long term annual means, it is not identically zero in individual seasons. Inserting a vertically averaged $[\bar{v}]$, however, gives a typical magnitude of the order of 1 m^2/sec^2 and it may be neglected in comparison to the transport of relative angular momentum. The second term in the in-

tegrand may be further resolved into three components:

$$[\overline{uv}] = [\bar{u}][\bar{v}] + [\bar{u}^* \bar{v}^*] + [\overline{u'v'}] \qquad 5.2$$

where a bar denotes a time mean and brackets a zonal mean. Deviations from these are indicated by a prime and a star respectively. The first term on the right hand side represents the contribution of the zonally averaged meridional circulation and may be referred to as the toridal component. The second or standing eddy term results from the spatial correlation of the time means of u and v around a latitude circle and the third from the time correlation of the wind components at individual stations.

The first comprehensive studies of the momentum fluxes in the Northern Hemisphere using actual wind data were made by Starr and White. Their results were obtained from averaging over groups of stations centred on particular latitude circles and in most cases the period of study was the year 1950. Their results, summarized in Starr and White (1954), show the following essential points:

1. The transport of relative angular momentum was northward throughout the Northern Hemisphere to about 65N and reached a maximum near the boundary between surface easterlies and westerlies at 30^{o}N.

2. The majority of the transport was due to eddy processes and the role of the mean motions was small, even at 13N.

3. The transports during the winter were about twice as strong as in summer and occurred at a slightly lower level.

Subsequently, the analysis was repeated by Buch (1954) who obtained the zonal means and standing eddies from analysed maps. His results confirmed those for the year 1950, obtained by Starr and White, but the values obtained by dividing the year into two seasons were not considered sufficiently reliable to be presented.

The first attempt to obtain the corresponding figures for the entire Southern Hemisphere was by Obasi (1963b) who used data for the year 1958 divided into two 6 month seasons. Again the transient eddies were found to be primarily responsible for the poleward transport of relative angular momentum. In contrast to the Northern Hemisphere the seasonal change in the vertically integrated momentum flux was insignificant equatorward of 50^{o}S. While the standing eddy transports were very small in comparison to the transient eddy transports in mid-latitudes, they were found to give the main contribution to a transport of relative angular momentum across the equator from the winter hemisphere to the summer hemisphere as predicted earlier by Widger (1949).

The annual mean vertically integrated flux was found to be comparable to Buch's values in the Northern Hemisphere, reaching a max-

imum near 30^{o} latitude but, as mentioned previously, the standing eddy contribution was smaller. Although the role of the mean motions appeared to be small, it could not be evaluated with much accuracy.

More recently the momentum fluxes at the equator have been examined by Tucker (1965) using a string of seven stations regularly reporting up to higher levels. He found a pronounced seasonal variation peaking at 200-150 mb with strong fluxes into the summer hemisphere. The patterns of all three components were remarkably similar with the transient eddies giving the smallest contribution. The standing eddy flux was particularly large and apparently due mostly to the monsoonal changes in the Indian Ocean region.

5.1 MOMENTUM FLUX CROSS SECTIONS

The results obtained for the momentum flux are presented in Tables 5.1-5.5 for the four three month periods. The values up to 100 mb were taken from the objective analyses using the long term station means as input. For the stratosphere only the transient eddy flux is presented and this was obtained from the latitude band means, giving equal weight to data from odd and even years over the period 7/57-6/63. The individual values are given simply as the covariances of the velocity components but the integrals have been multiplied by the factor in equation 5.1 to give the relative angular momentum

transports over the complete latitude circle.

The total flux is shown as a composite in Fig. 5.1 for the four seasons. In the tropical troposphere the sum of all three components was taken over the region of the main Hadley circulation between 24°N and 15°S except during March-May when the northern limit was 15°N. Because of the large errors in determining $[\bar{v}]$, the sum of the transient and standing eddies only was taken over the remaining area. The total flux can therefore be expected to differ slightly at mid-latitudes from the patterns shown but in view of the relatively minor role of the mean motion term established in earlier studies, the change is expected to be small. In the main tropical cell, however, the strength of the mean motions is in agreement with previous studies and the values obtained for the momentum flux are realistic.

For the stratosphere only the transient eddy flux is available from the latitude band means and there is little prospect of obtaining the other terms with the present observational network. For the most part the standing eddy contribution appears to be decreasing with height toward 100 mb and it is probable that this trend continues. Indirect estimates of $[\bar{v}]$ seem to give the best chance of obtaining the mean motion contribution (cf. Vincent 1968). Despite the checking procedure outlined in Chapter 3 and the use of three month seasons the stratospheric fluxes are still erratic and it is difficult to draw many firm conclusions.

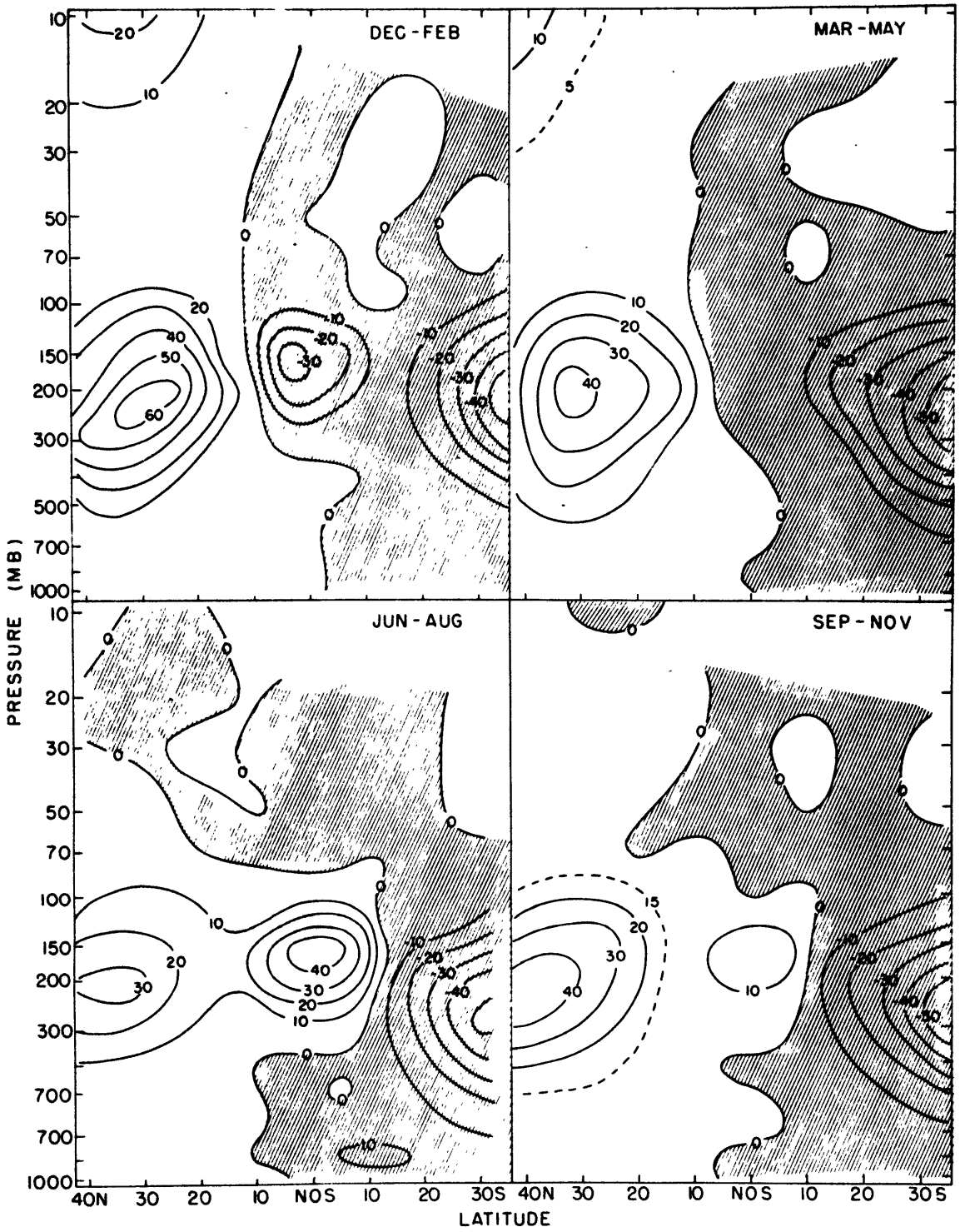

Fig. 5.1: Momentum flux cross sections. All terms included in tropical troposphere; otherwise eddy terms only as discussed in Section 5.1.

Table 5. 5 shows that in the stratosphere the transient eddies are generally weak and directed polewards in each hemisphere. At high levels in the Northern Hemisphere they reach their peak in the December-February season while during the June-August period the area of southward flux extends some distance into the Northern Hemisphere. The modulation of the stratospheric momentum flux throughout the biennial oscillation has already been examined in detail by Wallace and Newell (1966) as noted earlier. At this time it was thought that the horizontal flux convergence could satisfactorily account for the change between easterly and westerly regimes but more recently Wallace and Holton (1968) have decided against this on the basis of modelling experiments. In the view of the writer the observations are inadequate for a detailed study of this kind but the matter will be treated in more detail in subsequent chapters. The patterns for the troposphere in mid-latitudes are similar to the results obtained by Starr and White, Buch, and Obasi if the two eddy terms alone are considered. In both hemispheres a strong flux is seen in the upper troposphere directed towards the westerly jet, and this is mostly contributed by the transient eddies. As noted in the earlier studies, the role of the standing eddies in the extratropical Northern Hemisphere is comparatively small and they are limited to about one half the magnitude of the transient eddies in all seasons except March-May when they are appreciably smaller. In the Southern Hemisphere their contribu-

tion is negligible in the December-May period while in the June-November period they weakly oppose the transient eddy flux. These results probably demonstrate a real reduction in the importance of standing eddies in the Southern Hemisphere but it should be borne in mind that the data network there is generally too poor for an adequate resolution of standing eddy components. The objective analysis scheme does not draw in wave patterns over areas with no data as might occur in a knowledgeable hand analysis so that the standing eddy contributions will tend to be smaller.

In the Northern Hemisphere the seasonal variation in strength of the total flux noted by Starr and White (1952) at 30^{o}N is seen also in our data with the peak values in the winter being approximately twice those in the summer. They are also found at a lower latitude and a slightly lower level. The peak fluxes during spring and fall have a strength about midway between the summer and winter extremes. The sharp decline of the northward flux at 41^{o}N during March-May is apparently related to a similar decrease in the zonal wind although the jet axis is at about the same latitude as in the winter season. The seasonal changes in the Southern Hemisphere pattern are generally similar to those found by Obasi with the transient eddy flux in the winter season having a comparable magnitude to that in the summer and occurring at a lower level. The magnitudes in the vicinity of 30^{o}S are larger than Obasi's.

The most interesting results are obtained in the upper tropical troposphere where there is a strong flux directed into the summer hemisphere. A flux of this magnitude was not suspected in the earlier studies although Obasi (1963b) found a small flux in the same sense mainly due to the standing eddies and more prominent in the southern summer. Tucker (1965) however found an even stronger flux in his study based on seven equatorial stations for the years 1961 and 1962. The total transport reached a maximum near 200-150 mb of about $+ 70\ m^2\ sec^{-2}$ in July and $-50\ m^2 sec^{-2}$ in January. The values obtained in this study are lower, approximately +40 and $-35\ m^2 sec^{-2}$ for the June-August and December-February periods respectively. While there is no significant transport over the equator in the March-May period, the northward transport during the southern winter persists into the September-November period with a magnitude of $14\ m^2 sec^{-2}$. Some reduction is to be expected in the peak values since our figures apply to a three month period but the main difference appears to lie in the standing eddy contribution which was the largest of the three in Tucker's results. Our peak values of the toroidal and transient eddy fluxes are comparable to Tucker's but in both summer and winter seasons our standing eddy flux is only one half as large with a magnitude of approximately $20\ m^2\ sec^{-2}$. Nevertheless, it is comparable to the other terms in contrast to its role in mid-latitudes. While the longer averaging periods employed may have reduced our standing

eddy contribution, it is doubtful whether seven stations are sufficient for a determination of a standing eddy flux and our analyses in this region have been based mostly on the 39 stations within 10^{o} latitude of the equator. The reinforcement of the three terms in equation 5.2 noted by Tucker is also seen in our results for the upper equatorial stratosphere.

Fig. 5.2 shows the covariance $\overline{u'v'}$ at 200 mb for the December-February and June-August seasons. This level is slightly above the level of maximum poleward flux in mid-latitudes and slightly below the level of maximum flux across the equator so that both are well represented. The areas of maximum poleward transport during the northern winter are clearly related to the jet maxima shown in Fig. 4.5, except over China where values are apparently too small and based on very few stations. Nearly all stations near the equator show a southward momentum flux with maximum values occurring in the central Pacific and in the sector between South America and India. In the June-August period the relation between the poleward momentum transport and the jet maxima is not clearly defined in either hemisphere. The strongest northward transport across the equator again extends from South America to the east of the Indian Ocean.

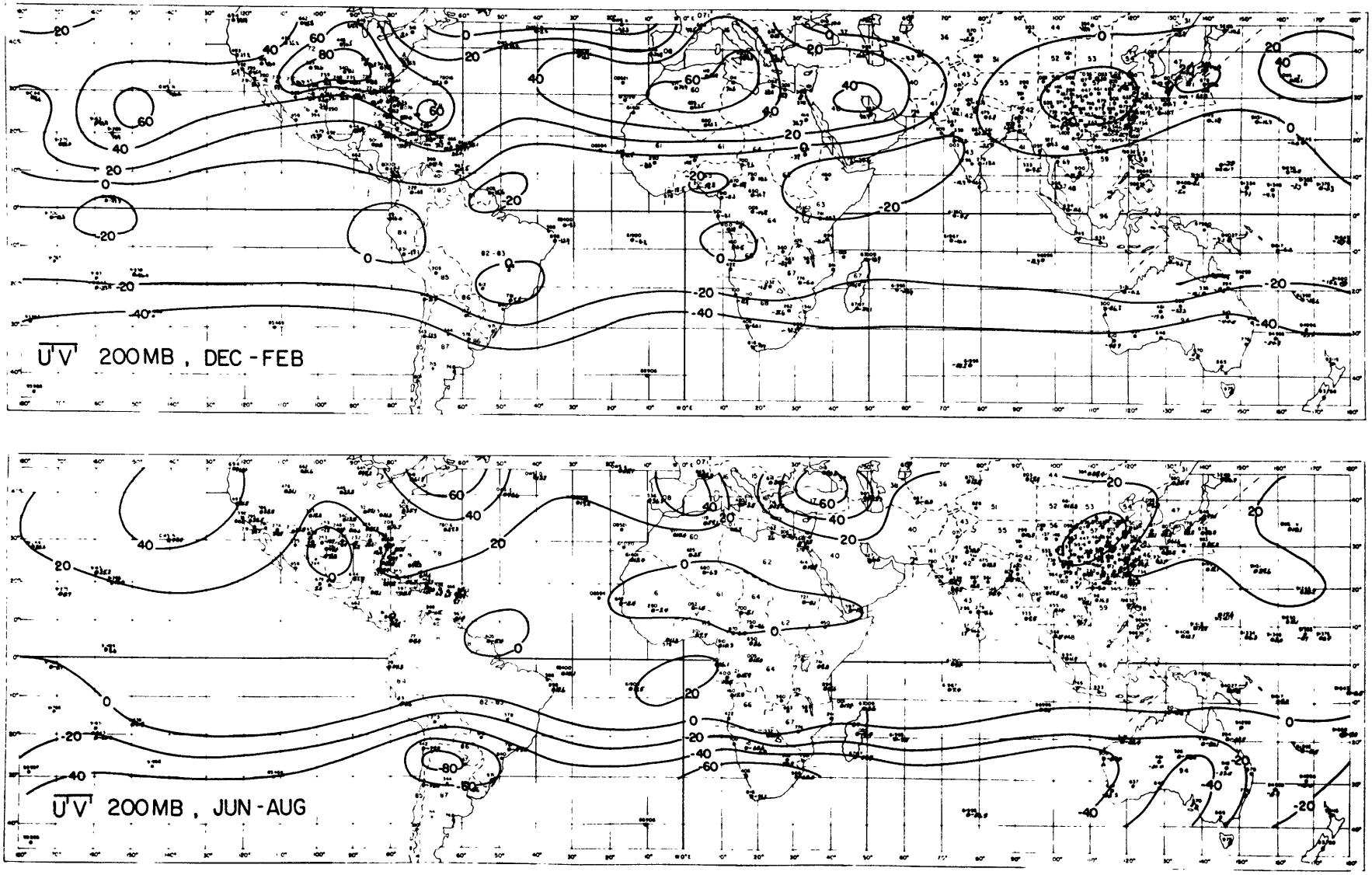

Fig. 5.2: Momentum flux by transient eddies at 200 mb for December-February and June-August.

5.2 VERTICAL INTEGRALS

The vertical integrals of the three flux components and their total are displayed in Fig. 5.3 together with the mean surface zonal wind component. The mean meridional term has been omitted from the total outside the main Hadley circulation as explained in the previous section. The limits of integration are 1000 to 100 mb and since the fluxes in the stratosphere and lower troposphere are weak the error introduced by this approximation is small.

In the December-February period the poleward flux in the Northern Hemisphere peaks near 30^{o}N with a value of approximately 41×10^{25} cgs units. Both the transient and standing eddy terms reach their peak near this latitude with the standing eddies contributing about one quarter of the total flux. In the Southern Hemisphere the total flux is predominantly due to the transient eddies and appears to be still increasing at 33^{o}S. During the June-August season the latitude of the maximum flux in the Northern Hemisphere moves slightly poleward to about 33^{o}N. The strength is less than half of the winter value at 17×10^{25} cgs units. The mean of the summer and winter values is in good agreement with Buch's results poleward of 10^{o}N. In contrast to the results of Obasi (1963b) who found no significant seasonal difference, the poleward flux is about 30% larger than in the December-February period. Measurements over the Australian sector alone at

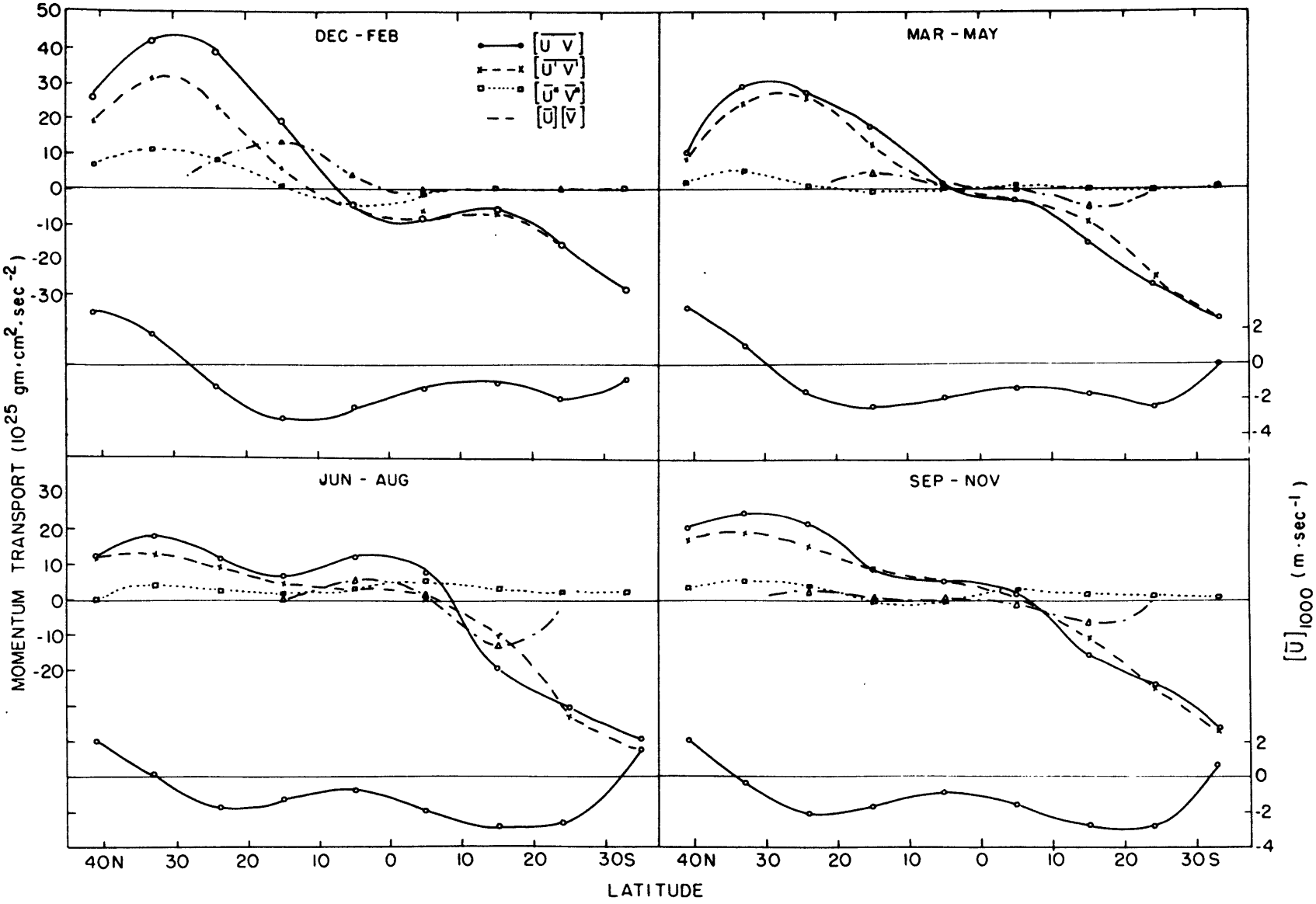

Fig. 5.3: Momentum flux integrals and the 1000 mb zonal wind for each season.

30^{o}S (Yoshida 1967) show maximum southward transports in the autumn and winter, approximately 50% larger than those in spring and summer. In the intermediate seasons the fluxes lie between the winter and summer extremes in both hemispheres.

The transport of momentum across the equator in each season represents a significant part of the peak flux into the westerly vortex of the summer hemisphere. Although the transport into the Southern Hemisphere during December-February is only about 25% of the poleward flux at 30^{o}S, in the June-August period the northward transport across the equator is nearly two thirds of the maximum flux at 30^{o}N. The flux across the equator is negligible during March-May but during the September-November period it is approximately 15% of the maximum near 30^{o}N.

The flux across the equator appears to be related to the relative strengths of the Hadley cell and the surface easterlies in each hemisphere . Because of the non-linear nature of the surface stress it is not possible to make a quantitative estimate of the momentum generation in each hemisphere from the data presented here. It can be shown for a normally distributed u component that the surface stress is proportional to $\bar{u}$ if the ratio $\bar{u}/\sigma u$ is less than ~ 1. For large normalized departures the stress is proportional to $\bar{u}^{2} + (\sigma u)^{2}$ so that the stress is proportional to a power of $\bar{u}$ ranging from 1 to 2 as $\bar{u}$ increases relative to σu. On this basis we would expect the

surface stress or momentum generation to be approximately proportional to $[\bar{u}]$ since the mean and standard deviation of u are comparable at individual grid points. (The torque is also proportional to the cosine of the latitude but this is approximately constant for the area considered.) The meridional profile of $[\bar{u}]$ is shown in Fig. 5.3 and it can be seen qualitatively that considerably more angular momentum is generated in the winter hemisphere than in the summer hemisphere. During the March-May period the generation is approximately equal in each hemisphere but in the September-November season the Southern Hemisphere Hadley cell and surface easterlies are stronger. It appears that the generation of momentum in the easterlies of the winter hemisphere exceeds the dissipation in the westerlies at higher latitudes with the surplus being transported into the summer hemisphere. The strong circulation in the southern winter persists into the southern spring with a continuing but weaker flow of momentum into the Northern Hemisphere. The corresponding effect is not seen during the northern spring, when the Hadley circulations in each hemisphere are of comparable intensity.

The decrease in the total transport at 10-15^{o} latitude in the summer hemisphere presents something of a problem since it implies a sink, or convergence of westerly angular momentum in a source region of surface easterlies. The integrated transient eddy flux does not show this decrease and it is probably due to insufficient contribu-

tions by the mean motion and the standing eddies. Alternatively, the fluxes measured at the equator may be too large and errors in the totals of 25-30% in the opposite sense would be sufficient to eliminate the convergence.

5.3 VERTICAL FLUXES

At any given latitude the vertical transport of momentum may be resolved into three components in a similar way to the horizontal flux:

$$[\bar{\omega}\bar{u}] = [\bar{\omega}][\bar{u}] + [\bar{\omega}^*\bar{u}^*] + [\overline{\omega'u'}] \qquad 5.3$$

where ω is the vertical velocity in pressure coordinates. The third term on the right hand side is due to transient eddies and requires daily omega values for its evaluation. No such calculations were made during the course of this study but the terms due to the mean motion and the standing eddies can be obtained from the seasonal mean wind field with the aid of the continuity equation. The mean vertical velocity $[\bar{\omega}]$ is obtained from the $[\bar{v}]$ cross section through integration of the continuity equation starting at the surface. The mean meridional velocities were adjusted by subtracting out the vertical mean, as in the stream function calculation of section 4.3 so that $[\bar{\omega}]$ was zero both at the 1000 and 100 mb levels. Although this gives better results for the troposphere the approximation cannot be used to

estimate momentum fluxes into the stratosphere. The standing eddy term was evaluated by computing $\bar{\omega}$ over the 10^{o} squares of the analysis grid, using the $\bar{u}$ and $\bar{v}$ components from the analyses without any adjustment. The $\bar{u}$ value in each case was the average over the four values at the corners of the grid square. Typical values of $[\bar{\omega}^{*}\bar{u}^{*}]$ reach a maximum of the order of 10^{-1} m sec^{-1} · mb sec^{-1} and although some coherent patterns were obtained in the cross sections they were not considered to be sufficiently reliable for presentation.

5.4 MOMENTUM BALANCE

Some idea of the consistency of the various terms involved in the momentum budget may be obtained through the use of the zonal momentum equation

$$\underbrace{\frac{1}{R\cos^{2}\phi}\frac{\partial}{\partial\phi}\left[\overline{u'v'}+\bar{u}^{*}\bar{v}^{*}\right]}_{(1)}+\underbrace{\frac{\partial}{\partial p}\left[\bar{\omega}^{*}\bar{u}^{*}\right]}_{(2)}+\underbrace{\left[\bar{\omega}\right]\frac{\partial[\bar{u}]}{\partial p}}_{(3)}$$

$$+\underbrace{\frac{[\bar{v}]}{R\cos\phi}\frac{\partial}{\partial\phi}[\bar{u}]\cos\phi}_{(4)}-\underbrace{f[\bar{v}]}_{(5)}=d-\frac{\partial[\bar{u}]}{\partial t}-\frac{\partial}{\partial p}\left[\overline{u'\omega'}\right] \qquad 5.4$$

The five terms on the left have been evaluated from the grid point analyses and a reasonable estimate of the magnitude of $\frac{\partial[\bar{u}]}{\partial t}$ may be made from a comparison of the values in adjacent seasons. As mentioned previously the transient eddy term in the vertical was not computed and it is difficult to obtain estimates of its magnitude. From the results of Miller (1966) it appears that the largest values occur-

ring in the lower stratosphere are about 10^{-6} m sec^{-2}. The combined vertical eddy transports of Smagorinsky et al. (1965) show a maximum divergence of 10^{-5} m sec^{-2} at the mid-latitude tropopause but in the tropics the divergence is about an order of magnitude smaller. The dissipation term d due to the smaller scale eddies may be written approximately

$$d = k_z \frac{\partial^2[\bar{u}]}{\partial z^2}$$

where k_z is a diffusion coefficient that is rather poorly determined. Estimates for the troposphere range from 1 to 20 $m^2 sec^{-1}$. Maximum values of $\frac{\partial^2[\bar{u}]}{\partial z^2}$ are of the order of 10^{-6} m^{-1} sec^{-1} near the axis of the subtropical jet and away from the jet may be an order of magnitude less. This implies an upper limit of about 2×10^{-5} m sec^{-2} for the dissipation term. Maximum values for the time derivative are of the order of 10 m/sec over a three month period leading to a typical maximum value of 10^{-6} m $\cdot$ sec^{-2}.

The requirement then to be satisfied by the five terms on the left is that their sum should not be more than about 5×10^{-5} m $\cdot$ sec^{-2} in mid-latitudes while in the tropics a reasonable value is probably about an order of magnitude less.

Summation of the five terms on the L. H. S. of equation 5. 4 gives for the December-February period values ranging up to 8.7×10^{-5} m $\cdot$ sec^{-2} at 150 mb at 37°N while in the June-August period the largest values occur at 29°S with a maximum of 15.8×10^{-5} at the

200 mb level.

Extreme values for the March-May and September-November were both 7.6×10^{-5} m · sec^{-2} at 29^{o}S and 150 mb. In all four seasons the largest degree of imbalance, as indicated by the sum of the five terms in equation 5.4 was to be found in the strong indirect cells at latitudes 29^{o} and 37^{o}. From the estimates for reasonable values of the remaining terms in the momentum equation it appears that the residues are larger than can be accepted. The most probable reason for the discrepancy is the large contribution from terms (4) and (5) which involve $[\bar{v}]$. In the example quoted for the December-February period the coriolis term is -10.2×10^{-5} m · sec^{-2}, while the horizontal advection term is $+1.9 \times 10^{-5}$ m · sec^{-2} and these two terms alone account for most of the sum in equation 5.4. As a reasonable guide to the proper magnitude of $[\bar{v}]$ we can assume that the R.H.S. of equation 5.4 is zero and solve for $[\bar{v}]$ after substitution of values for the remaining terms (eg. Vincent 1968). At latitudes 29^{o} and 37^{o} the largest values in each season are of the order of 30-40 cm/sec.

In view of the uncertainties involved a detailed analysis of the momentum balance will not be presented although the following example may be of some interest. Referring to the cross sections of the total momentum transport in Fig. 5.1 it will be seen that during the winter season in each hemisphere there is a strong centre of divergence near 200 mb at 10^{o} latitude. Evaluating the five terms in

equation 5.4 we obtain (in units of 10^{-5} m · sec^{-2}):

	(1)	(2)	(3)	(4)	(5)	Total:
10N Dec.-Feb.	1.9	-0.6	0.0	4.1	-7.1	-1.7
10S June-Aug.	1.4	-0.4	0.0	3.8	-6.9	-2.1

In both cases the shape of the zonal wind profile implies a negative sign for the dissipation d and typical values of $\frac{\partial[\bar{u}]}{\partial t}$ are $\sim .1$ in these units. The contribution from the divergence of the vertical transient eddies is unknown but it can be seen that in each case the return branch of the Hadley cell generates more than sufficient momentum through the coriolis torque to balance the horizontal eddy divergence and its own horizontal advection of the zonal wind.

CHAPTER 6.

HEAT AND ENERGY TRANSPORTS

Radiation calculations (eg. London 1957, Albrecht 1931, Gabites 1950) show that on the average the tropics receive considerably more solar radiation than the polar regions but the outgoing long wave radiation is more uniformly distributed. The net result is a heat surplus in the tropics and a deficit at higher latitudes. In order to maintain approximate temperature equilibrium there must be energy transfer through the atmosphere and oceans from the source region in the tropics.

Following Starr (1951) we may write the time averaged energy flux over a latitude circle in the form

$$H = h + \frac{2\pi R\cos\phi}{g}\int\left[\overline{v\left(\Phi + c_pT + Lq + c^2/2\right)}\right]dp \qquad 6.1$$

where h is the flux due to transport processes in the oceans, Φ is the geopotential, T is the temperature, q the specific humidity and $c^2/2$ the kinetic energy per unit mass. L is the latent heat of evaporation and c_p the specific heat of air at constant pressure. The heat transport h in the oceans is generally considered to be about 10% of that in the atmosphere but the exact values are not known. Estimates by Jung (1952) indicate the percentage could be higher. The kinetic energy of large scale motions is about two orders of magnitude smaller than the kinetic energy of molecular motions and the flux of kine-

tic energy may be neglected in comparison to the flux of sensible heat.

The three main terms to be considered then are the fluxes of sensible heat and latent heat and the flux of geopotential at constant pressure surfaces. Each of these may be resolved into the contributions from the mean motion, from standing eddies and from transient eddies in the same way as the momentum flux in Chapter 5.

The earliest measurements of the eddy fluxes of sensible heat over the entire Northern Hemisphere were made by White, whose results are also conveniently summarized in Starr and White (1954) for the complete year 1950. Geostrophic calculations for the winter of 1945-1946 (White 1951a) showed the poleward flux of sensible heat to reach a maximum of 34.9×10^{21} ergs/sec at 55^{o}N. The flux of latent energy was computed from evaporation and precipitation data and a maximum poleward flux of 17.8×10^{21} erg/sec was obtained at 35^{o}N. The combined flux was found to be comparable to that required by radiation calculations. Over the North American continent White (1951b) also computed the transport of latent heat and sensible heat from soundings grouped into latitude bands for February and August 1949. The sensible heat flux was strongest during February with maximum polewards values occurring in the middle and upper troposphere in the vicinity of 55^{o} N. Strong equatorward fluxes were observed in the lower stratosphere at mid-latitudes and throughout the tropical troposphere. The overall pattern of latent heat and sensible heat transport

was similar to that for sensible heat during February. Subsequently, White (1954) calculated the eddy flux of sensible heat for the entire Northern Hemisphere over the year 1950 using stations grouped into latitude bands from 31°N to 70°N. The pattern obtained was somewhat changed from the North American results and in the troposphere the flux was found to be strongest at the 850 mb level with a weaker maximum near the tropopause. The maximum poleward flux was again found at 55°N. The major change however was a reversal in direction of the flux in the lower stratosphere so that it was poleward at all levels up to 100 mb. With minimum temperatures observed in the tropics the poleward flux was directed towards warmer temperatures or against the gradient, as had been observed earlier for the momentum fluxes.

This was the first discovery of the countergradient heat flux on a hemispheric basic although it had been noted by Priestley (1949) in the data for a single station. Later investigations by Murakami (1962) and Peng (1963, 1965) for the 18 months of the IGY period showed that the stratospheric heat flux by transient eddies was predominantly poleward except at high latitudes. The implications of this countergradient flux will be discussed in later chapters.

More recently the Northern Hemisphere data for 1950 have been examined in greater detail by Peixoto (1960a) whose results also include the tropical regions. Statistics were obtained from grid point

values read from analyzed maps for six month winter and summer seasons as well as for the complete year. The results obtained did not differ greatly from White's but the tropical analyses showed the transient eddy flux to be predominantly equatorward south of 30^{o}N. The winter fluxes were approximately twice as strong as those in the summer and the average poleward flux for the year reached a value of $\sim 20 \times 10^{21}$ ergs/sec at 50^{o}N. The equatorward fluxes in the tropics were also discussed in more detail by Peixoto (1960b) and Starr and Wallace (1964) who pointed out the similarity of the countergradient fluxes there to those of the lower stratosphere.

No results have yet been published for the complete Southern Hemisphere although an analysis comparable to that by Peixoto (1960a) is currently being undertaken by the writer's colleagues for the year 1958. The tropical analyses have been based for the most part on data supplied by the writer and the counter gradient heat fluxes found by Kidson, Vincent and Newell (1969) were subsequently noted by Robinson (1968).

6.1 EDDY FLUXES OF SENSIBLE HEAT

The contributions of the transient and standing eddy terms to the transport of sensible heat are presented in Tables 6.1-6.3 for the four seasons. The covariances $[\overline{v'T'}]$ and $[\overline{v}^{*}\overline{T}^{*}]$ were obtained for the levels up to 100 mb by objective analysis of the long term means

and for the stratosphere from latitude band means.

The transient eddy flux patterns are similar in each season with areas of equatorward flux predominating in the tropical troposphere and giving way to poleward fluxes at higher latitudes. The fluxes in the stratosphere appear to be poleward in each hemisphere, and stronger in the winter with the possible exception of the June-August period but the values tend to be erratic. The data coverage in the Southern Hemisphere is inadequate to draw any firm conclusions there. The poleward fluxes in the mid-latitude troposphere show a double maximum with peak values at low levels near 850 mb and at the tropopause. They are strongest during the winter months although the upper maximum in the Northern Hemisphere during March-May is stronger than during the winter season. This may be due to a southward displacement of the area of maximum flux compared to its winter position and related to the sharper decrease in the zonal wind speed and momentum transport on the poleward side of the jet during the period.

Despite the uncertainties in the analysis the areas of equatorward heat flux in the tropics appear to be directly related to the Hadley circulation. In each case the boundary between the southward fluxes in the Northern Hemisphere and their counterpart in the Southern Hemisphere leads to a convergence of the heat flux near the centre of the ascending motion in the Hadley cell or cells. The poleward

limit of the equatorward fluxes is found in the descending branch of the Hadley cell, except in the summer hemisphere where there is no identifiable Hadley circulation. With the lapse rate being less than dry adiabatic, ascending motion corresponds to cooling while descent is associated with heating. The effect of the equatorward fluxes in each hemisphere therefore is to conduct heat away from the source regions in the descending branch of the Hadley cell and into the sink associated with the ascending branch. The transient eddy heat flux analysis at 500 mb is shown in Fig. 6.1 for the December-February and June-August seasons. The equatorward heat fluxes predominate in both seasons in the tropics except over Asia during the summer monsoon when poleward fluxes are more common. This is in keeping with the reversal of the mean circulation as the heat flux is directed northward into the rising branch over the Asian continent and away from the region of descent toward the equator.

The standing eddies are smaller in most cases than the transient eddies and weaker in the Southern Hemisphere. They are most prominent near the subtropical tropopause in the Northern Hemisphere where they reverse the equatorward flux due to the transient eddies, but otherwise the pattern of the total eddy flux is the same as for the transient eddy flux alone. Although the horizontal temperature gradients are weak in the tropics the results of Chapter 4 show that the equatorward heat flux in the troposphere is not always counter-gra-

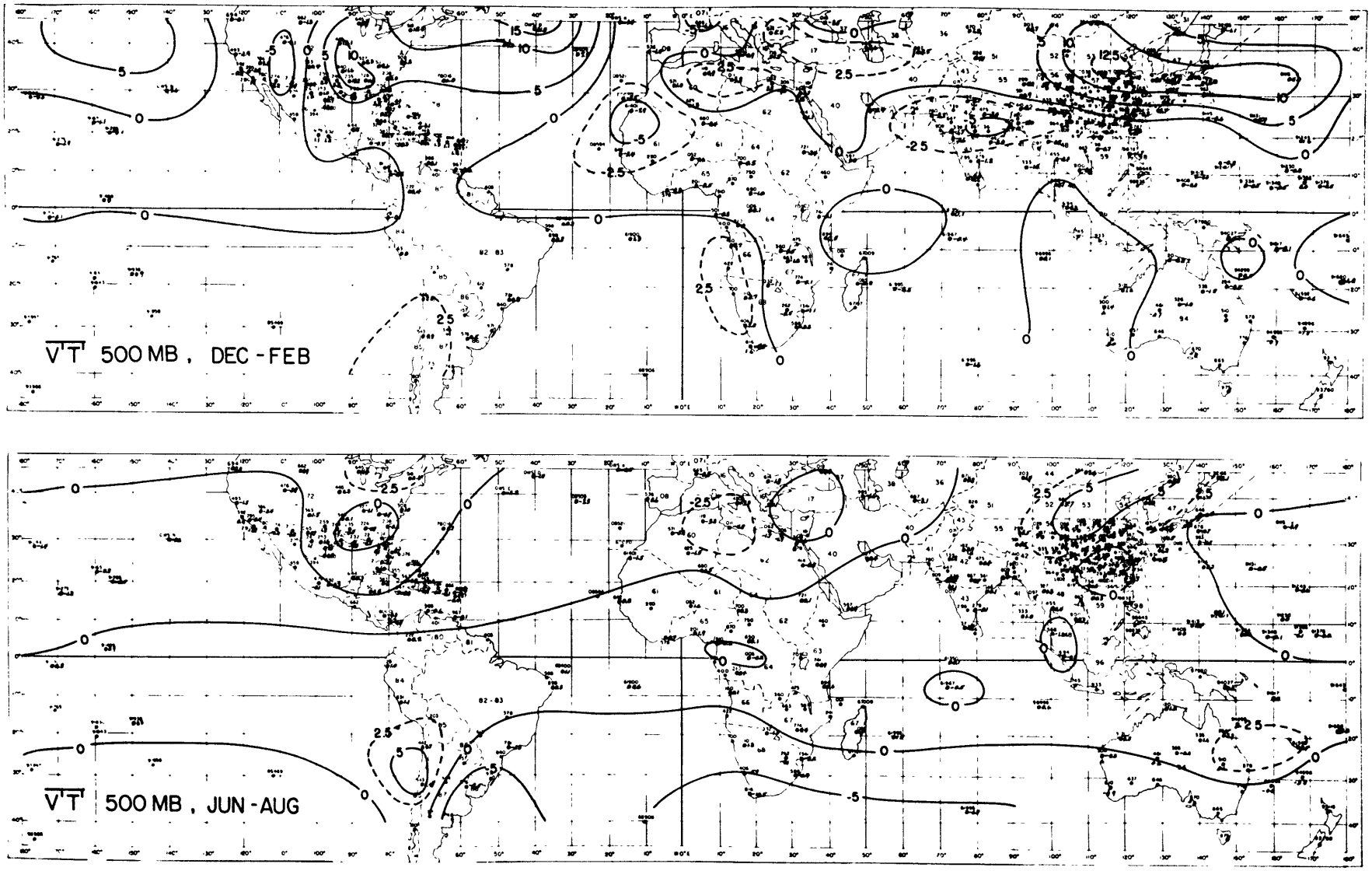

Fig. 6.1: Sensible heat flux by transient eddies at 500 mb for December-February and June-August.

dient. In the June-August period when the temperature maximum in the troposphere moves to 20°N the Northern Hemisphere flux is actually down a weak temperature gradient. The earlier temperature cross section of Peixoto (loc. cit.) showed the temperature maximum moved this far north only at lower levels and consequently it was thought that the equatorward fluxes were countergradient throughout the year.

6.2 EDDY FLUXES OF GEOPOTENTIAL

Transient and standing eddy fluxes of potential energy were computed in the same way as the fluxes of sensible heat. The covariances $[\overline{v'z'}]$ and $[\overline{v}^*\overline{z}^*]$ are shown for tropospheric levels in Tables 6.4 and 6.5. The transient eddy flux is predominantly equatorward in all seasons with magnitudes decreasing toward the equator. Maximum values occur in the upper troposphere and reach their peak during the winter. In the Northern Hemisphere the maximum values occur at 41°N in all seasons except March-May when the peak is reached at 33°N. The standing eddy fluxes are smaller in magnitude and show no well-defined patterns. It may well be that the analyses are not sufficiently good to bring the true pattern out of the noise level. As with the standing eddy fluxes of sensible heat, gradients are small in the tropics and errors introduced by using different types of radiosonde become important. In view of the relatively small contribution

of the eddy fluxes of geopotential to the energy budget of the tropics demonstrated in Section 6.5 it does not seem worthwhile to comment further.

6.3 THE ROLE OF THE MEAN MOTIONS:

The major contribution to the energy transport in the tropics is from the mean meridional circulation. In the poleward branch of the Hadley cell the air is colder than in the equatorward flow at low levels so that there is a net transport of heat towards the equator. On the other hand the potential energy of the air in the poleward branch is greater so that the net flux of potential energy is polewards. In an atmosphere with an adiabatic lapse rate the two fluxes would cancel but in practice lapse rates are less than dry adiabatic so that the flux of geopotential outweights the flux of sensible heat and the Hadley cell transports energy poleward.

The two fluxes were computed between the 1000 and 100 mb levels using the objective analyses of temperature, geopotential and the meridional wind component to obtain the zonal means. The meridional wind component was again adjusted so that the vertical mean was zero. The results obtained for each season are included in Table 6.6 which is a compilation of all contributions to the energy flux of equation 6.1. The mean meridional velocities are too large away from the main Hadley circulation of the tropics and attention should be

confined to the region between 24°N and 15°S where the results are considered reliable. In each season the flux of potential energy is about 50% larger than the flux of sensible heat so that the net transport is poleward. Both are considerably larger than the corresponding eddy fluxes in the tropics although it will be assumed that the eddy processes are responsible for most of the flux in mid-latitudes. The flux across 15°N during December-February is approximately half that found by Palmén et al. (1958) for the winter of 1955-1956.

6.4 TRANSPORT OF LATENT ENERGY

As mentioned earlier, water vapour analyses have not been attempted during this study but the station data have instead been forwarded to Dr. E. G. Rasmusson of ESSA. Some preliminary statistics are now available for the mid-season months January, April, July and October and these have been used to obtain the latest energy fluxes in Table 6.6. The analyses extended only to 16°S and no attempt has been made to estimate the values at 24°S and 33°S. Because the atmospheric water vapour content is concentrated in the lower layers the effects of topography become more important in estimating total transports. The cross sections of $[\overline{Q}]$, $[\overline{Q}^*\overline{v}^*]$ and $[\overline{Q'v'}]$ supplied were corrected for this by setting $\overline{Q}$ to zero at grid points where the surface elevation was above the pressure level in question.

The mean specific humidity [Q] was used in conjunction with mean meridional velocities of Table 4.5 after subtraction of their vertical mean to obtain the mean motion transport between 1000 and 100 mb. The flux quantities had already been integrated assuming a lower pressure limit of 1012.5 mb. A value of 590 cal gm^{-1} deg^{-1} was used to convert the water vapour flux to the flux of latent energy in equation 6.1.

Examination of Table 6.5 shows that the latent energy flux due to the mean motion can be comparable to the difference between the toroidal fluxes of sensible heat and geopotential. It is in the same sense as the sensible heat flux since the water vapour is concentrated in the lower portion of the Hadley circulation. The eddy fluxes are comparable to those of sensible heat with the standing eddy flux of latent heat during the summer monsoon being particularly prominent.

6.5 A REVIEW OF THE ENERGY FLUXES

The contributions to the energy transport within the 1000-100 mb layer of the atmosphere defined in equation 6.1 are presented in Table 6.6, with the transport of each quantity divided between the toroidal, standing eddy and transient eddy components. The eddy fluxes of sensible heat will be slightly overestimated at higher latitudes in the Northern Hemisphere since no correction was made

for the surface elevation.

The mean motion contribution is not included outside the area of the Hadley circulation for reasons discussed previously and the total flux is represented by the eddy components only. In practice, a small indirect cell is to be expected at mid-latitudes and this would cause a slight reduction in the poleward flux. The truncation of the integrals at 100 mb could lead to an appreciable error in the potential energy transport by the mean cell since the potential energy becomes infinite as p approaches zero. Substituting a linear profile of v between p = 0 and p = 100 mb and assuming isothermal conditions however leads to a finite value of the integral as follows:

For T constant

$$\Phi(p) = \Phi_{100} + RT \int_{p}^{p_{100}} d\ln p$$

$$= \Phi_{100} + RT \ln (p_{100}/p)$$

now assume $v = v_{100} \times p / p_{100}$

so that the geopotential flux becomes

$$G = \frac{2\pi R \cos\phi}{g} \int_{0}^{p_{100}} v_{100} (p/p_{100}) \left[\Phi_{100} + RT \ln\left(\frac{p_{100}}{p}\right) \right] dp$$

$$= \frac{2\pi R \cos\phi}{g} \left[\frac{p_{100} v_{100} \Phi_{100}}{2} + \frac{RT v_{100}}{p_{100}} \times \frac{p^2}{2} \ln \frac{p_{100}}{p} \Big|_{0}^{p_{100}} + \int_{0}^{p_{100}} \frac{p^2}{2} \cdot \frac{1}{p} dp \right]$$

$$= \frac{2\pi R \cos\phi}{g} \times \frac{p_{100} v_{100}}{2} \left[\bar{\Phi}_{100} + \frac{RT}{2} \right]$$

The integral of the sensible heat flux is

$$S = \frac{2\pi R \cos\phi}{g} \times \frac{p_{100} v_{100}}{2} \times c_p T$$

so that $$S/G = \bar{\Phi}_{100} / c_p T + \frac{\kappa}{2}$$

Substituting typical values for $\bar{\Phi}$ and T at the 100 mb level and taking $\kappa = .286$ gives a ratio for S/G of the order of 1. This indicates that although the geopotential tends to infinity for $p \rightarrow 0$, the integral of the geopotential flux above 100 mb by the mean motions is probably of the same order as the sensible heat flux. The error involved by truncating the mean motion integral at the 100 mb level is therefore not too serious. Inspection of Table 6.6 shows that the eddy fluxes of potential energy are insignificant in comparison to the other eddy fluxes but that the geopotential flux by the mean motion is larger than that of sensible heat or latent heat. The standing eddy fluxes of sensible heat and latent heat are of comparable magnitude except during the northern summer when the flux of latent heat is much larger than that of sensible heat. The transient eddy fluxes predominate at higher latitudes with similar contributions from the latent heat and sensible heat fluxes.

Fig. 6.2 shows the contribution to the total flux by the toroidal standing eddy and transient eddy components averaged over the four

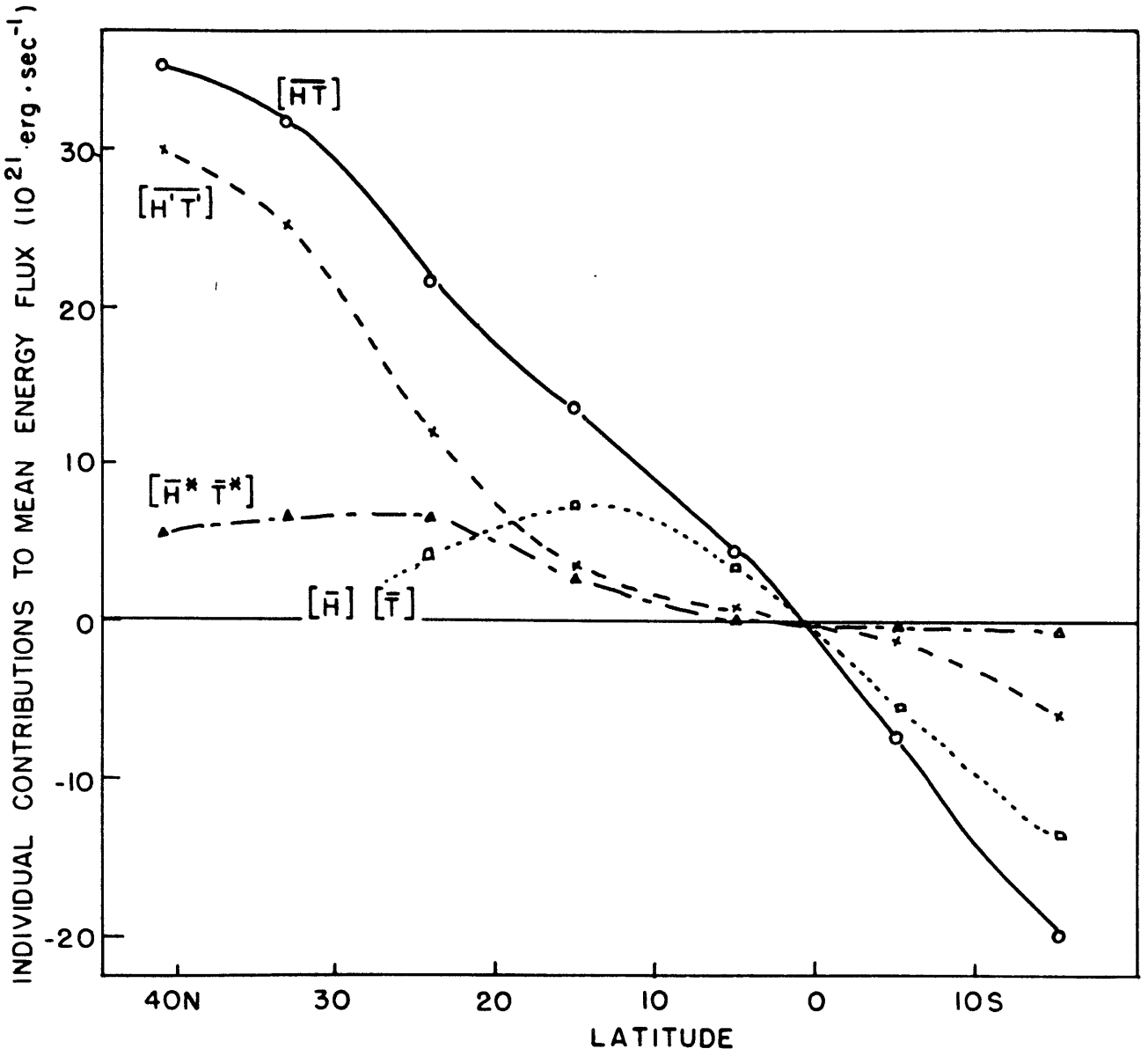

Fig. 6.2: Annual mean contributions to energy transport by mean motion and eddy terms.

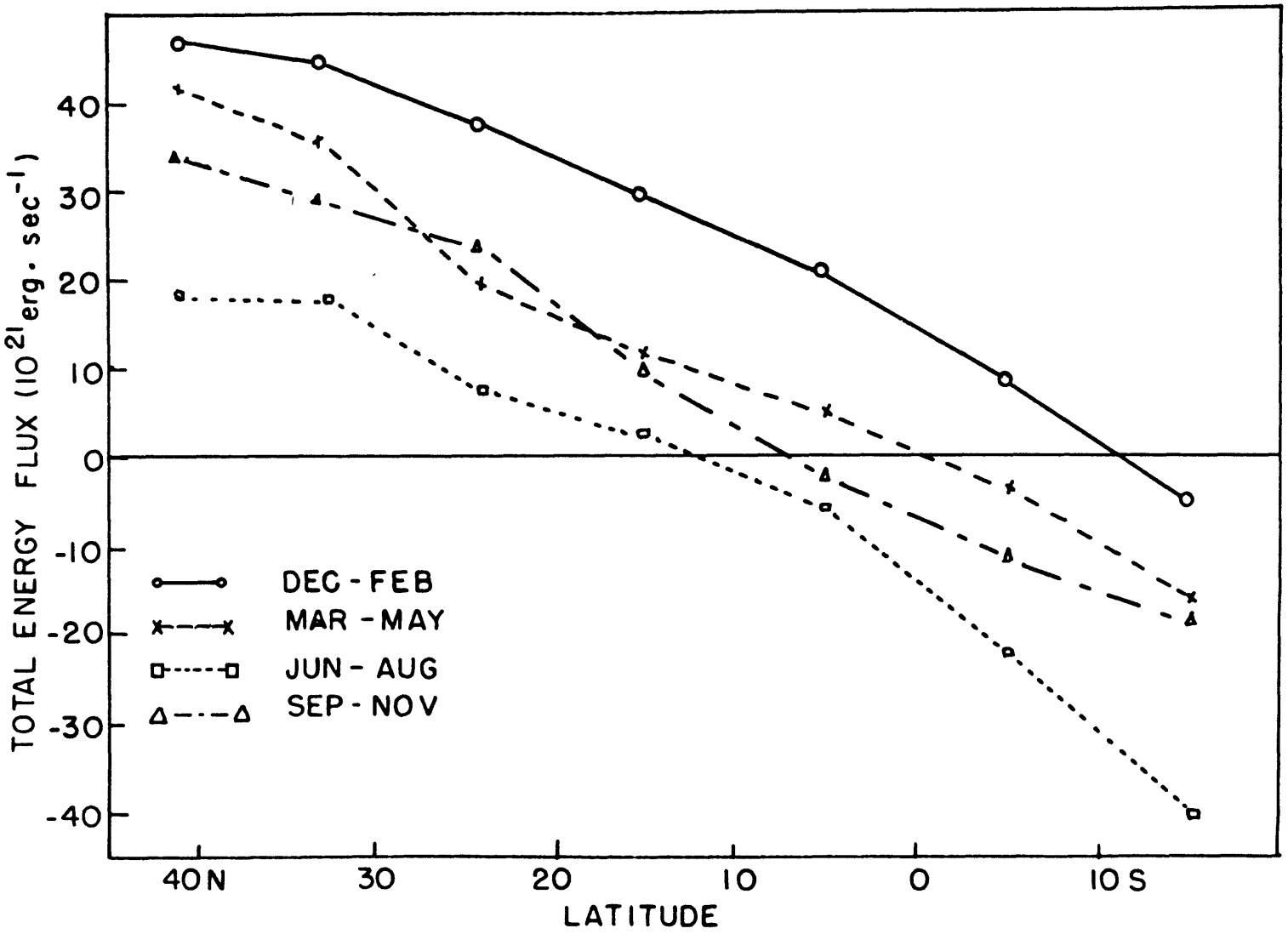

Fig. 6.3: Total atmospheric energy transport in each season.

seasons. The flux due to the mean motion reaches its peak at 15^{o} latitude and equatorward of this is larger than the sum of the eddy fluxes. The standing eddy fluxes are comparable to or larger than the transient eddy fluxes within 15^{o} of the equator but by 30^{o} latitude the transient eddy fluxes are responsible for most of the energy transports. In individual seasons the pattern changes with the Hadley circulation and in the northern winter would appear more like that given by Palmén (1964) although his Hadley flux appears to extend too far northward.

The seasonal variation of the total energy transport is presented in Fig. 6.3. The boundary between northward and southward energy transport is centred a little to the north of the equator on the average and during the winter seasons moves to about 10^{o} latitude in the summer hemisphere. The flux across the equator is about -14×10^{21} ergs/sec into the winter hemisphere during December-February and June-August. It is close to zero during the northern spring but still -6×10^{21} ergs/sec during the September-November period.

Although calculations of the radiation balance of the earth can lead to appreciably different results depending on the approximations used it is of some interest to compare the energy fluxes obtained here with those required to satisfy radiation balance requirements. Another check is provided by satellite measurements of outgoing radiation over the entire globe although the absolute calibration of satellite

radiometers is something of a problem. At 40^{o}N the estimates of the energy flux averaged over the year from radiation data range from 28×10^{21} ergs/sec (Albrecht 1931) to 44×10^{21} ergs/sec (Gabites 1950). The mean value obtained here of 35×10^{21} ergs/sec lies within these limits but since no estimates have been made of the energy flux in the oceans a direct comparison is not possible. Riehl and Malkus (1958) have made estimates of the energy flux required in a similar way for summer and winter seasons. Their calculations were made for periods toward the end of each season when the ocean temperatures reach their extreme values. In this way the problem of heat storage is eliminated and more realistic values for the fluxes are obtained. Their winter maximum of $\sim 40 \times 10^{21}$ ergs/sec occurred near 35^{o}N with the poleward flux originating near 10^{o} latitude in the summer hemisphere. The peak summer flux was half as large and was found about 45^{o} latitude. These values are in quite good agreement with those in Table 6.6. The radiational imbalance of the Northern Hemisphere during the June-August period is a surplus of about 125×10^{21} ergs/sec according to London (1957). Nimbus II satellite measurements for a shorter period show a larger surplus of some 178×10^{21} ergs/sec (Raschke and Pasternak 1967). The measured flux of energy across the equator during the June-August period is therefore only about 10% of the Northern Hemisphere surplus. Undoubtedly the ocean currents will contribute to the energy flux across

the equator but it appears that most of the radiational surplus is stored in the ground and in the oceans.

CHAPTER 7.

THE ENERGY CYCLE

The conversion from potential energy generated initially by solar heating to the kinetic energy of atmospheric motions and its ultimate dissipation by friction is best discussed in terms of the formulation by Lorenz (1955). Lorenz was able to express the concept of "available potential energy" in quantitative form and after dividing both the available potential energy and the kinetic energy into mean and eddy terms derived the expressions for the conversions between them. The four energy types are shown in Fig. 7.1 together with the permissible conversions between them.

The exact form of the energy integrals and the conversions between them depends on the averaging system employed and three possible schemes have been summarized in a review of Oort (1964), together with various estimates of their magnitude. The form appropriate to the statistics obtained in this study is the "space-time" domain and the individual terms will be examined in detail in the following sections. The equations used in the following section differ from those in Oort's review in that the time variant parts of the kinetic energy and available potential energy are omitted. The results of previous studies will be reviewed in the following sections and for the present the discussion will be limited to a general description of the pro-

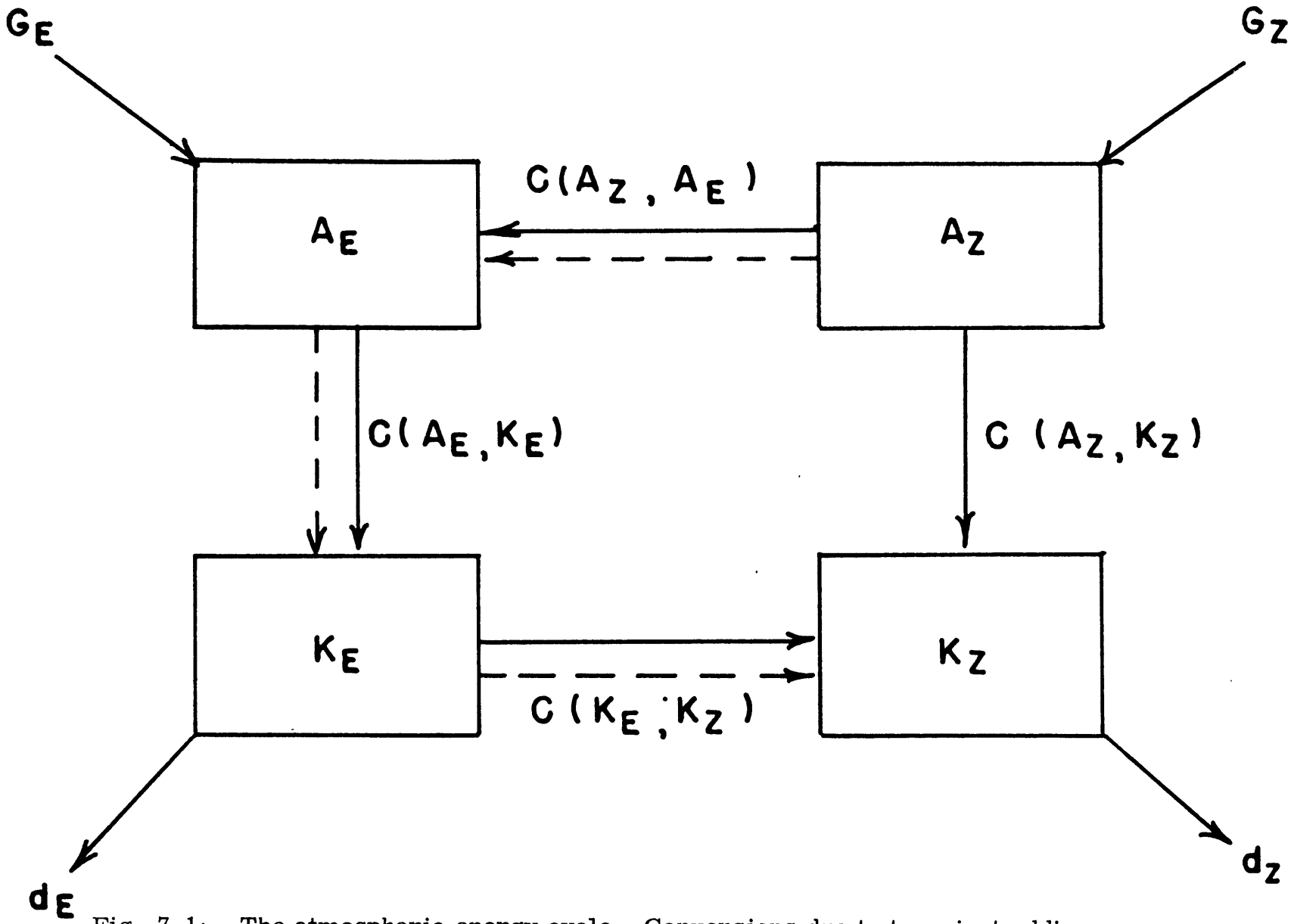

Fig. 7.1: The atmospheric energy cycle. Conversions due to transient eddies or mean motions shown with continuous lines. Standing eddy conversions drawn with dashed lines.

cesses involved.

Available potential energy is defined in terms of the temperature variance over complete isobaric surfaces and represents the portion of the potential energy that could be converted into kinetic energy if the atmosphere were to become horizontally stratified. The temperature variance may be partitioned into two components represented by the latitudinal trend and by the variance within latitude circles. The former is known as zonal available potential energy (A_Z) and the latter as eddy available potential energy (A_E). Conversion from A_Z to A_E takes place when the eddy fluxes of sensible heat flow down a meridional temperature gradient. Generation of A_Z results from a positive correlation between the zonal averages of temperature and diabatic heating. Similarly, generation of A_E requires a positive correlation between diabatic heating and temperature around individual latitude circles.

The kinetic energy is partitioned in the same way with conversion from K_E to K_Z resulting from an eddy flux of angular momentum against a zonal gradient of angular velocity. Conversion from A_E to K_E takes place when warmer air rises and cooler air sinks on the average around latitude circles, and conversion from A_Z to K_Z is due to a similar correlation between the zonally averaged vertical motion and the temperature. Dissipation of K_E and K_Z results from internal friction and from friction at the earth's surface.

Previous investigators have shown that on the average the operation of the energy cycle in the troposphere is from A_z to A_E by down gradient heat fluxes, from A_E to K_E by baroclinic distrubances and from K_E to K_Z by counter gradient momentum fluxes. The ultimate energy source is the generation of A_z by heating of the warm tropical regions and cooling of the polar regions as a consequence of the pattern of incoming solar radiation. In the lower stratosphere a so-called "refrigerator" exists where the counter gradient heat fluxes predominate. A_z and A_E are destroyed by radiation and kinetic energy has to be supplied from the troposphere.

7.1 AVAILABLE POTENTIAL ENERGY

The zonal and eddy available potential energies are defined as

$$A_z = \tfrac{1}{2} c_p \int \gamma \left[\overline{T}\right]''^2 dm$$

$$A_E = \tfrac{1}{2} c_p \int \gamma \left[\overline{T}^{*2}\right] dm$$

and their generation by

$$G_z = \int \gamma \left[\overline{Q}\right]'' \left[\overline{T}\right]'' dm$$

$$G_E = \int \gamma \left[\overline{Q}^* \overline{T}^*\right] dm$$

where a double prime denotes a departure from the global mean and the bars and brackets denote time means and zonal means respectively. An asterisk indicates a departure from a zonal mean. The integrals are over the atmospheric mass. The stability factor γ is defined in this case as

$$\gamma = -\left(\frac{\theta}{T}\right)^2 \frac{R}{c_p \times 900} \int_{100}^{1000} \left(\frac{T}{\theta}\right) \frac{1}{p} \left(\frac{\partial \tilde{\bar{\theta}}}{\partial p}\right)^{-1} dp$$

where θ is the potential temperature and ($\tilde{}$) indicates a global mean.

Although the eddy available potential energy can be computed for a restricted range of latitudes the same is not true of the zonal available potential energy which depends on the zonal departures in temperature from the global average. If for example, the "global" average is obtained from the tropical regions only, then it will be too high in the lower and middle troposphere and the zonal departures will be too small. The net effect is a reduction in A_z over that for the entire globe. However, in the case of the tropics, the principle energy conversion is found to be that between A_z and K_z by the Hadley circulation. Since the Hadley circulation in the tropics appears to be quite well separated from the indirect circulation of mid-latitudes, and the conversion between A_E and A_z depends on the zonal temperature gradient it seems quite reasonable to obtain the global averages

of T and ω for the tropics alone. The generation term G_z would be incorrect in that it would not reflect the overall heating in the tropics and cooling at the poles but would represent the relative heating over the area of the main Hadley circulation and consequently its driving force. The following discussion of the energy integrals will be in terms of units of 10^{25} ergs, and they will be shown in Fig. 7.2 also with the same scaling.

The zonal available potential energy can be obtained directly from the temperature statistics in Chapter 4 and its magnitude depends very strongly on the area chosen. In the 15^{o}N-15^{o}S band the magnitudes are only of the order of 2 units for each season because of the nearly uniform temperature of the tropics. Doubling the area to 33N-33S increases A_z about a factor of 50 to $\sim$100 units. Cross sections of $[\overline{T}^{*2}]$ are presented in Table 7.1 for the summer and winter seasons. The temperature variance is seen to be increasing towards lower levels and higher latitudes during the northern winter with a secondary maximum in the lower stratosphere at mid-latitudes. In the northern summer the large temperature variance seen in Fig. 4.8 is reflected in the 850 mb values but largest values occur in the upper troposphere in association with the monsoonal effects discussed earlier. Estimates of A_E from these figures range from about 6 units in the 15^{o}N-15^{o}S band to $\sim$ 20 units in the 33 N- 33 S band where the largest value occurs during the northern summer. Since

the integrals of A_E and A_z presented in Fig. 7.2 do not extend to high latitudes the values obtained are considerably smaller than for the entire hemisphere. Estimates of these two integrals from the data of Peixoto (1960a) for the year 1950 are 676 units for A_z and 376 units for A_E. The available potential energy for the tropical circulation is therefore only a small fraction of that for the entire hemisphere.

7.2 KINETIC ENERGY

The zonal and eddy kinetic energy integrals are

$$K_z = \frac{1}{2} \int [\bar{u}]^2 + [\bar{v}]^2 \, dm$$

$$K_E = \frac{1}{2} \int [\bar{u}^{*2} + \bar{v}^{*2}] \, dm$$

and their dissipation is represented by

$$d_z = \int [\bar{u}][\bar{F}_x] + [\bar{v}][\bar{F}_y] \, dm$$

$$d_E = \int [\bar{u}^* \bar{F}_x^* + \bar{v}^* \bar{F}_y^*] \, dm$$

where F_x and F_y are the x and y components of the frictional force. K_z may be obtained directly from the cross sections (in Tables 4.3 and 4.5) and the eddy kinetic energy integrand is presented in Table 7.2 for the summer and winter seasons. Both K_z and K_E show maximum values in the upper troposphere which appear to be directly related to the subtropical jet in the December-February period. In the June-August period the maximum values of K_E occur in the region

of the tropical easterly jet at 150 mb and decrease away from the tropics. However, the values of K_z increase away from the equator as the subtropical jets are approached. The integrals of K_z for each season range from about 10 units in the 15N-15S band to $\sim$100 units in the 33N-33S band. Values for K_E are smaller and the corresponding magnitudes are of the order of 8 and 16 units respectively. For the latitude range 10°N-70°N Murakami (1960) obtained values of approximately 65 units for K_E and 190 units for K_z.

Since the 33N-33S region includes at least part of the subtropical jet in each season the fraction of the total kinetic energy contained in it is higher than the fraction of the available potential energy, relative to the Northern Hemisphere as a whole.

7.3 CONVERSIONS BETWEEN EDDY AND ZONAL AVAILABLE POTENTIAL ENERGY

The conversion from A_z to A_E is given approximately by

$$C(A_z, A_\epsilon) = -c_p \int \gamma \left[\overline{v'T'} + \bar{v}^* \bar{T}^*\right] \frac{\partial T}{R \partial \phi} \, dm$$

The conversion rates obtained for the summer and winter seasons by transient eddies and the sum of the transient and standing eddies are presented in Table 7.3. Positive values indicate conversions from zonal to eddy potential energy and negative values appear in the so-

called "refrigerator" regions associated with counter gradient heat fluxes. Conversions are seen to be small throughout the tropics with some negative areas associated with the equatorward heat fluxes although they disappear in the averaging and are not found in the northern summer as explained previously. The largest values occur at mid-latitudes reaching maximum intensity during the winter months. Large positive conversions are found in the lower troposphere and the negative conversions associated with the counter gradient flux in the lower stratosphere are particularly prominent. The conversion integrals appear in Fig. 7.2 in units of 10^{20} ergs/sec so that dividing the energy contents by the conversion rate gives a time constant measured approximately in days. Between 33^{o}N and 33^{o}S the largest conversion rates occur during the northern winter, reaching a value of 10 units or 10×10^{20} ergs/sec. Between 24N-24S the conversion rates are an order of magnitude smaller, while in the band 15N-15S they are two orders of magnitude smaller. The transient eddy conversions predominate except close to the equator where the standing eddies are of equal importance and tend to cancel the transient eddy contribution.

For the entire Northern Hemisphere the conversion rates based on the data of Starr and White (1954) is 31×10^{20} ergs/sec so that the tropical region below 33^{o} latitude accounts, at most, for roughly one sixth of the total conversion.

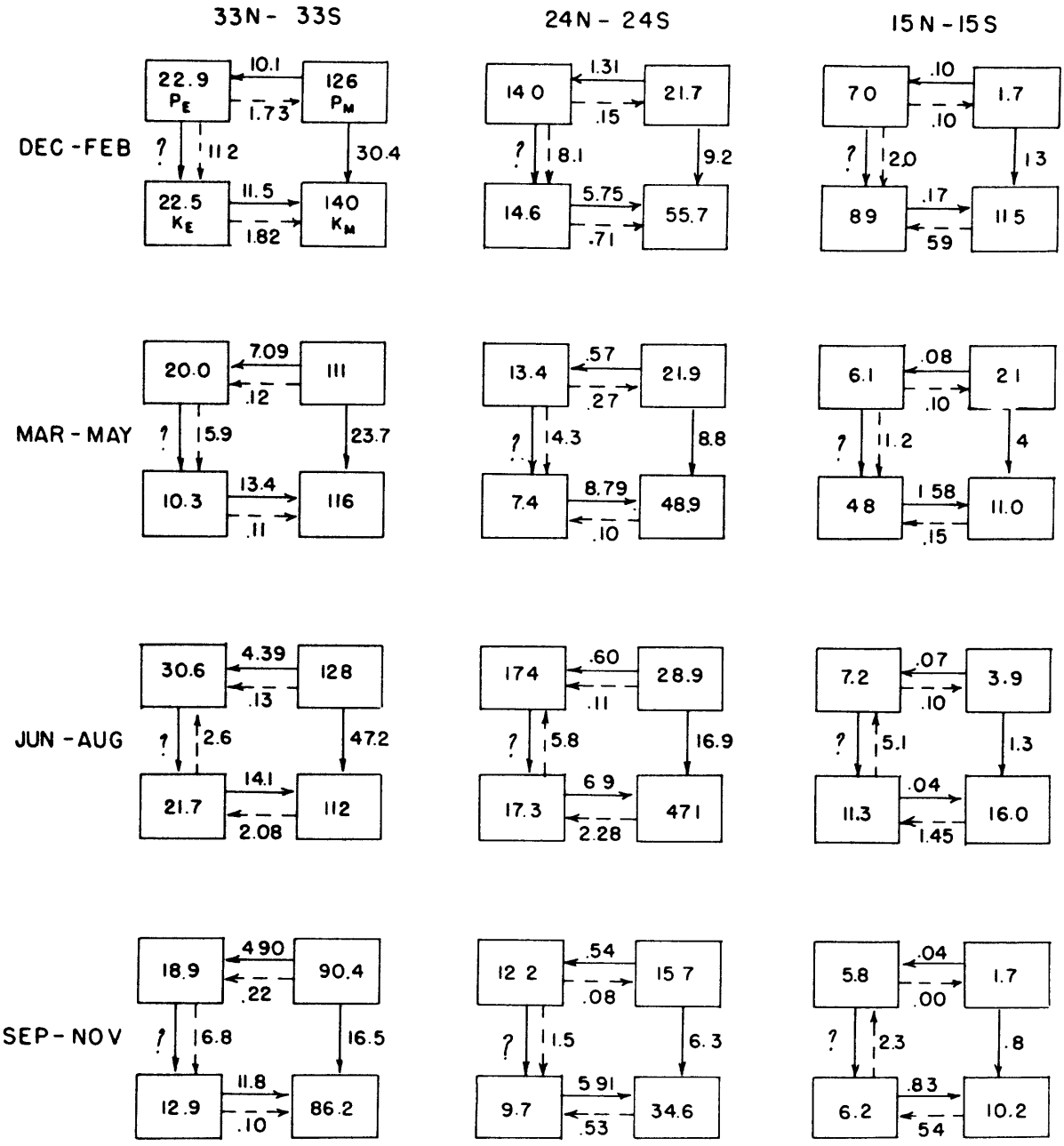

Fig. 7.2: Estimates of the tropical atmospheric energy cycle for three latitude ranges, following the format of Fig. 7.1. The conversion by transient eddies between A_E and K_E cannot be evaluated. Energy contents are in units of 10^{25} erg and conversion rates in units of 10^{20} erg sec^{-1}.

7.4 CONVERSIONS BETWEEN EDDY AND ZONAL KINETIC ENERGY

The conversion from eddy to zonal kinetic energy is approximately

$$C(K_E, K_Z) = \int \left[\overline{u'v'} + \bar{u}^* \bar{v}^*\right] \cos\phi \frac{\partial}{R\partial\phi}\left(\frac{[\bar{u}]}{\cos\phi}\right) dm$$

and the conversion rates due to the transient eddies alone and the sum of the transient and standing eddies are presented in Table 7.4 for the summer and winter seasons. The conversion is mostly positive in the troposphere within 30^{o} of the equator, with the largest contribution to the maintenance of the mean zonal flow occurring on the equatorward side of the subtropical jet in the upper troposphere, as found previously by Kuo (1951), Starr (1953). A negative region appears in the upper troposphere associated with the momentum flux across the equator. The standing eddy conversions are comparable to the transient eddy conversions at low latitudes but diminish in importance polewards. On the poleward side of the jet axis the conversion is from zonal to eddy kinetic energy. The stratospheric fluxes in Table 5.5 are counter gradient and a source of kinetic energy for the zonal flow. The integrals between 15^{o}N and 15^{o}S are of the order of 10^{20} ergs/sec but the contribution between 33^{o}N - 33^{o}S is ten times as large and shows little change between the seasons.

For the entire hemisphere, the estimate from Buch's data for the year 1950 is 5.6 units, or about the same as the conversion rate from 33°N to the equator. A smaller value might of course be expected because of the downgradient flux on the poleward side of the jet which is only partly included in the integral to 33°N. Obasi's (1965) conversion integral for the Southern Hemisphere is larger, about 9 units in both summer and winter seasons, but positive conversion rates appear to predominate over the entire hemisphere with little sign of the negative conversions on the poleward side of the jet. His choice of six month seasons however may have blurred the pattern.

7.5 CONVERSIONS BETWEEN POTENTIAL AND KINETIC ENERGY

The conversion from zonal available potential energy to zonal kinetic energy is given by

$$C(A_z, K_z) = -\int [\bar{\omega}]'' [\bar{\alpha}]'' \, dm$$

where $\alpha = RT/P$ is the specific volume and the double primes denote departures from the global average. This term has been evaluated using the mean vertical motions computed from Table 4.5 and the temperature profiles of Table 4.1. The "globally averaged" values of $\overline{\omega}$ and $\overline{\alpha}$ were defined only over the region of integration so that the pattern of departures from the mean changed with the area of integra-

tion. The integral between 33°N and 33°S, which covers all the Hadley circulation is largest during the summer and winter seasons when the cell in the winter hemisphere predominates. The conversion rates range from 16.5 units in September-November to 47.2 units in June-August and over the 24°N-24°S band from 6.3 units to 16.9 units in the same seasons. For a comparison, the value obtained by Palmén et al. (1958) for 0-30°N over the winter was 30 units while Tucker (1959) obtained a figure of over 100 units for the low latitude cell in winter. The values obtained here are in reasonable agreement with those of Palmén et al. but Tucker's appear to be too high. Starr (1959) gives an average value of about -2.5 units for the entire hemisphere for the years 1950 and 1951 with the contribution from the indirect cell in mid-latitudes outweighting a weak positive conversion in the Hadley cell. This conversion integral was evaluated in a different form and this apparently led to an underestimate of the conversion in the tropics.

The conversion from eddy available potential energy to eddy kinetic energy is given by

$$C(A_E, K_E) = -\int [\bar{\omega}^* \bar{\alpha}^* + \overline{\omega' \alpha'}] \, dm$$

Since no daily ω values were computed only the standing eddy contribution could be evaluated. The mean vertical motions were calculated using the equation of continuity as described in Chapter 5. The results are not considered very reliable. As the area of integration increases,

there is a greater tendency for positive values or generation of eddy kinetic energy.

7.6 A REVIEW OF THE ENERGY CONVERSIONS WITHIN THE TROPICS

The energy integrals and energy conversions within the tropics have been summarized for convenience in Fig. 7.2 for the four seasons and three latitude ranges. The main features are summarized in the following remarks:

(i) Eddy energy contents are smaller than the mean energy contents but their importance increases towards the equator and in the $15^{o}N$-$15^{o}S$ band the eddy available potential is larger than the zonal available potential energy.

(ii) At low latitudes the kinetic energy is about twice as large as the available potential energy but the two forms are comparable in size when the area is increased to $33^{o}N$-$33^{o}S$.

(iii) Except in the narrow $15^{o}N$-$15^{o}S$ band, the largest energy conversion rate is the generation of zonal kinetic energy by the mean meridional circulation. The rejuvenation time is about 3-5 days.

(iv) Transient eddy conversions are larger than the standing eddy conversions except in the band $15^{o}N$ -$15^{o}S$. The sense of the standing eddy conversions of available potential energy fluctuates between seasons and latitude ranges, indicating that they may not be very

accurately determined. The variation of the standing eddy conversion between eddy and zonal kinetic energy seems to be better defined. It appears that conversions from zonal to eddy kinetic energy predominate in the tropics while at higher latitudes the conversion is largely due to the counter gradient flux in the Northern Hemisphere. As the Northern Hemisphere jet weakens and moves northward the negative conversions predominate so that in the northern summer the standing eddy conversion is from zonal to eddy kinetic energy even in the 33^{o}N-33^{o}S band.

(v) Except for the 33^{o}N-33^{o}S band, the conversions associated with momentum fluxes are appreciably larger than those involving heat fluxes.

(vi) The seasonal variation in the energy contents and conversions for individual hemispheres cannot be determined from the integrals in Fig. 7.2 but inspection of the integrands for the Northern Hemisphere shows that in nearly every case maximum values occur in the winter and minimum values in summer. This is in agreement with the findings of Wiin-Nielsen (1968), apparently for the portion of the Northern Hemisphere covered by the NMC grid which extends from the pole to 15-20^{o}N.

As a consequence of the small temperature variation in the tropics the eddy heat fluxes and the conversions by them between the forms of available potential energy is also small. The negative

conversions therefore do not contribute materially to the hemispheric conversion rate, or to the dynamics of the tropical troposphere. This area of negative conversions in the tropics can not be regarded in the same way as that in the lower stratosphere where counter gradient heat fluxes are also found, because unlike the stratosphere the tropics generate sufficient kinetic energy to fulfill balance requirements. Whereas the lower stratospheric circulation is maintained by advection of kinetic energy from below (Starr 1960, Newell 1963) the tropics generate their own kinetic energy in situ. The kinetic energy budget of the tropics has been reviewed by Palmén (1964) who estimates that an average rate of at least 32×10^{20} ergs/sec is required to balance the advection of kinetic energy at 30^{o}N. This is the total generation rate which is the sum of the two conversions $C(A_z, K_z)$ and $C(A_E, K_E)$. Turning again to Fig. 7.2 it can be seen that the conversion between 33^{o}N and 33^{o}S due to the mean motion and standing eddies alone is close to this value. The transient eddy conversion rate can not be determined observationally but the results of Manabe et al. (1965) for the 9 level general circulation model with a simulated hydrological cycle show a strong conversion from eddy available potential energy to eddy kinetic energy in the tropics. This is due in large part to the release of latent heat and is responsible for the maximum of eddy kinetic energy found in the model tropics. The sub-synoptic scale disturbances which cannot be properly represented by the usual obser-

vational network may also contribute to the generation of kinetic energy. It appears likely then that there is a sufficient supply of kinetic energy to account for the poleward transport and the dissipation within the tropics. The poleward transport should also be added to the dissipation integrals of Section 7.2 since the areas under investigation do not extend over the entire globe. It is of course possible that the estimates of the poleward flux of kinetic energy are too large and Pisharoty's figure of 20×10^{20} ergs/sec quoted by Palmén (loc. cit.) is one tenth of the mean energy flux at 30°N, about an order of magnitude greater than usually assumed. The advection term can not be evaluated without returning to the daily observations, although its magnitude might be inferred from the dissipation rates and the conversion from available potential energy to kinetic energy over the remainder of the Northern Hemisphere.

The conversion by the indirect cell from zonal kinetic energy to zonal available potential energy has been estimated by Starr (1959) to be 2 to 3×10^{20} ergs/sec which is an order of magnitude less then the conversion from available potential energy to kinetic energy in the tropics. It appears that the poleward flux of kinetic energy at 30^{0}N could easily supply this amount but estimates of the generation of eddy kinetic energy are not sufficiently precise to permit an accurate evaluation of the total flux of kinetic energy out of the tropics.

CHAPTER 8.

FURTHER COMMENTS ON THE MEAN CIRCULATION

The results presented in Chapters 4 - 7 provide a consistent picture of the tropical circulation, with a clear relation between the different parameters analysed. The pattern emerges of a dominating Hadley circulation which acts as a source of momentum and heat for the poleward transports in each hemisphere. It appears that the strength of the Hadley circulation remains approximately constant throughout the year but that the centre of the rising motion follows the sun into the summer hemisphere. The displacement of the centre of rising motion apparently also determines whether one strong cell is present extending into the summer hemisphere or two are observed as in the spring and fall periods when the rising motion is centred near the equator. The summer Hadley circulation is too weak to be seen in our analyses and apparently it does not make an important contribution to the zonal mean energy fluxes and energy conversions within the tropics.

The yearly variation of the centre of rising motion of the Hadley circulation is also a function of longitude. As can be seen from Figs. 4.6 - 4.9 the ITC is well developed over Africa. Although the pattern of relative humidity there does not change much throughout the year the effect of predominantly rising motion at the ITC is clearly

seen in the rainfall distribution (Thompson 1963). The seasonal variation of the mean Hadley circulation also reflects an asymmetry between the two hemispheres which can be observed in other features. While the March-May cross sections show the northern and southern Hadley circulations to be of comparable strength, in the September-November period the Southern Hemisphere cell is appreciably stronger. This indicates that the winter circulation of the Southern Hemisphere is slower to give way to the summer time conditions and the surplus generation of momentum is reflected in the northward flux of momentum across the equator during this period.

The Hadley cell is seen to be the source of the momentum flux which diverges from the upper troposphere at 15^{o} latitude in the winter hemisphere. Although the ultimate source is at the earth's surface it is transferred upward through the action of the Hadley cell where the poleward flow in its upper branch generates westerly momentum through the coriolis torque. In the two cases examined in Section 5.4 it was shown that the generation at the 200 mb level was apparently sufficient to counter the strong eddy flux divergence between the poleward flux in the winter hemisphere and the flux across the equator into the summer hemisphere. The flux across the equator seems to be quite well explained by an excess generation in the winter Hadley cell although as yet no quantitative estimates of the generation at ~~its~~ the surface have been made. It appears to be a fundamental part of the

global circulation system.

Although further refinement in the computations is necessary before a detailed energy balance can be made for individual latitude belts, the pattern of the sensible heat fluxes is in qualitative agreement with the heat sources and sinks associated with the Hadley circulation. Taking the December-February and March-May periods for example, the vertical velocity in the mid-troposphere associated with the rising branch of the Hadley cell is 3-4 mm/sec. At 20^{o}N in the descending branch the vertical velocity has about the same magnitude. The heating rates associated with the vertical motion are of the order of 1^{o} per day cooling at the equator and 1^{o} per day warming at 20^{o}N. The horizontal eddy flux convergence into the ascending branch gives a heating of $\sim .07^{o}$ C/day and divergence from the descending branch produces cooling at the rate of $\sim .15^{o}$ C/day. The diabatic heating rates can not be very accurately determined. In the mid-troposphere the radiational effects combine to cause a cooling of about 1.5^{o} C/day according to Rodgers (1967) and the values of Katayama (1967) appear to be comparable, Riehl (1962) also gives a measured value of this magnitude over the Caribbean in the lower troposphere. Adding these three terms together we are left with a deficit of $\sim .7^{o}$ C/day at 20^{o}N and 2.6^{o} C/day at the equator.

The contributions to the diabatic heating from convection and latent heat release are difficult to estimate. For the 0^{o} - 10^{o}N belt,

which should be reasonably typical of conditions in the vicinity of the ITC, Budyko and Kondratiev (1964) have obtained figures for the atmospheric heat balance components on an annual basis. The net heating rate was 52 k cal cm^{-2} $year^{-1}$ resulting from the supply of 119 units by latent heat release and 9 units by conduction and the loss of 76 units by radiative flux divergence. If the release of latent heat is confined between the 850 and 200 mb levels the heating rate corresponds to 2.0 degrees per day and the radiative cooling averaged over the whole atmospheric depth is .85°C/day. The model calculation of Manabe and Smagorinsky (1967) shows similar contributions from radiational and latent heat terms at 3°N but their convection term of approximately 2°/day is considerably larger, while the adiabatic cooling is twice as large at 2°/day. If we retain the radiative cooling rate of 1.5°/day and the adiabatic cooling of 1°/day then an approximate balance would be achieved in the mid-troposphere against 2°/day latent heat release and small contributions from the horizontal eddy conversions and vertical eddy flux.

In the latitude belt 20°N-30°N, which may be taken to represent the downward branch of the Hadley circulation, Budyko and Kondratiev obtain an overall cooling rate of 14 k cal cm^{-2} $year^{-1}$. The radiative cooling rate remains approximately the same at 82 units while the reduction in the latent heat release to 44 units is only partially offset by the increase of the conduction from the surface to 24

units. The net heating in the mid troposphere by latent heat release and conduction is therefore of the order of $1^{o}C$/day. The radiative cooling rate according to Rodgers (loc. cit.) remains at approximately 1.5^{o} C/day. Adding the subsidence heating of $1^{o}C$/day and subtracting the eddy flux divergence of $.15^{o}C$/day leads to a rough balance.

The results for the heat fluxes are therefore not as clear cut as those for the momentum fluxes because the diabatic terms are not adequately known. It does seem however that the pattern of heat fluxes is not inconsistent with the observed meridional circulation. Furthermore the counter gradient heat fluxes represent only a small term in the tropical heat budget and do not appear to be of fundamental importance to the tropical circulation. It is interesting to note that they also appear in the results of Manabe et al. (1965).

As can be seen from the heat budget terms quoted above, the release of latent heat of condensation is the dominant term in the generation of zonal available potential energy, which is converted to zonal kinetic energy by the mean meridional circulation. This is in agreement with the finding of Manabe and Smagorinsky (1967) that without the release of latent heat in their general circulation model, the circulation of the Hadley cell in the tropics was approximately equal to that of the small indirect cell at mid-latitudes. In the moist model, the Hadley circulation increased to a realistic value of 140 x 10^{12} gm/sec while the mid-latitude cell fell to half its former value.

More recently Charney (1968) has found the release of latent heat to be the main driving force in his simplified model of the ITC. The release of latent heat has also been found by Manabe and Smagorinsky to be the major source of eddy available potential energy and this applies not only to the tropics but middle and high latitudes also. This result is in agreement with the calculations of Katayama (1967) who found a net destruction of available potential energy by radiative processes which was opposed by the generation due to latent heat release and a small contribution from conduction leading to an overall generation.

It is unfortunate that the limitations of the data have not allowed the presentation of an equally satisfactory picture for the tropical stratosphere. The latitude band means of the zonal wind and the temperature generally appear satisfactory although they do not match perfectly with the analysed values at 100 mb. The momentum fluxes and heat fluxes are more susceptible to error but it appears that the long term averages have brought out the main features. The mean meridional circulation of the stratosphere, which is of great importance to the prediction of the spread of radioactive debris etc., can not be determined directly from the wind observations. The best hope for its evaluation lies in observing the motion of tracers and in indirect calculations based on heat sources and sinks or the momentum fluxes and the zonal wind equation of Section 5. (eg. Murgatroyd and Singleton 1961, Murgatroyd 1968, Vincent 1968.)

These indirect calculations suggest that the mean meridional circulation of the lower stratosphere is an upward extension of the tropospheric cells. If this is so, the coupling of the tropospheric and stratospheric circulations may have a direct bearing on the cause of the biennial oscillation. The implications will be discussed in more detail in the following chapters.

CHAPTER 9.

THE BIENNIAL OSCILLATION

No description of the general circulation of the tropics can be considered complete without some mention of the biennial oscillation which is seen most clearly in the mean zonal wind and temperature fields of the tropical stratosphere where it has an amplitude comparable to the seasonal change.

Since its discovery by Reed (1960) the oscillation has attracted considerable attention and its observable properties are now quite well established. The ultimate cause of the oscillation is still unknown however and even the dynamics of its downward propagation are still imperfectly understood. The oscillation has also been detected at higher latitudes and in other parameters such as ozone concentrations and may be related to a two year periodicity in the sudden warmings of the Arctic stratosphere. In addition, evidence has been found for a two-year periodicity in the troposphere which may be directly related to that in the stratosphere.

The present study has been directed towards a description of the biennial oscillation based on a larger data sample in the tropics and Southern Hemisphere than was available for the earlier study of Wallace (1967) and a search for possible linkages between the troposphere and stratosphere. The present status of the oscillation will be

reviewed in the following sections and some of the results of this investigation presented. In the following chapter the tropospheric data are examined in greater detail and possible linkages between the tropospheric and stratospheric oscillations discussed.

9.1 OBSERVATIONAL RESULTS

The biennial oscillation appears most clearly in the zonal wind reversals of the tropical stratosphere. The pattern observed is a succession of zonally symmetric downward propagating easterly and westerly regimes centred near the equator. The oscillation appears to originate above the 30 km level, reaches maximum amplitude of about 20 m/sec at the 25 km level, and attenuates rapidly as the tropopause is approached. Rocket soundings at Ascension Island (Reed 1965) show the oscillation to be present with a decreasing amplitude up to the 50 km level. Its average rate of downward propagation decreases from about 2 km/mo. at this level to an average of 1 km/mo. below the 30 km level. Higher rates are observed for the westerly regimes. The period averages around 26 months but in individual cycles may range from about 21 to 30 months. As Wallace and Newell (1965) have shown, the phase has a tendency to lock on to the annual cycle with the transition to easterlies at the 20 mb level taking place around November at Canton Island. Occasionally a lapse of six months occurred with the changeover taking place in May. It appears that the basic period

is 24 months with the lapses in phase related to the intensity of the winter circulation in each hemisphere.

The amplitude of the oscillation falls off quite rapidly away from the equator with the phase apparently remaining the same. Probably the best known illustration of the biennial oscillation is the time-height cross section of the zonal wind at Canton Island (3^{o}S) which appears, for example, in the review by Reed (1965). The downward progression of the alternating easterly and westerly regimes is also clearly shown in the zonal cross sections of Wallace (1966) at two month intervals. Fig. 9.1 shows the latitude band means of $\bar{u}$ obtained for the four seasons during even and odd years which divide the biennial oscillation into eight phases. (Decembers are included with the January and February of the following year.) The average downward progression of the easterly and westerly regimes is clearly seen, together with their intensification near the 30 mb level. The eight cross sections give somewhat better coverage for the Southern Hemisphere than previously obtained and confirm the symmetry observed about the equator. The maximum amplitude of $\sim$20 m/sec is in agreement with previous studies.

The accompanying temperature oscillation has a maximum amplitude of approximately 2^{o}C and changes phase rather abruptly near 15^{o} latitude. As Reed (1962) has shown, the period of the oscillation is so long that the zonal wind is geostrophic to within a few tens of kil-

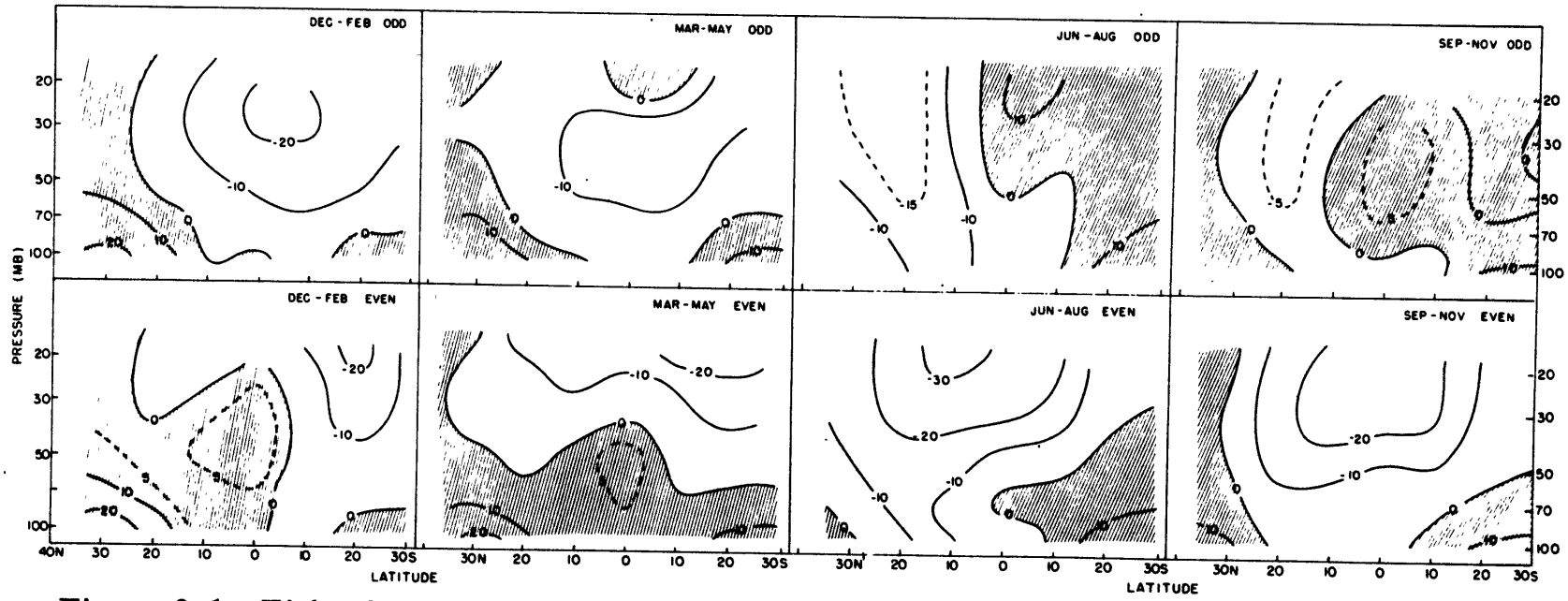

Figure 9.1: Eight phases of the biennial oscillation showing the downward propagation of easterly and westerly (shaded) wind regimes. Contours in m. sec^{-1}.

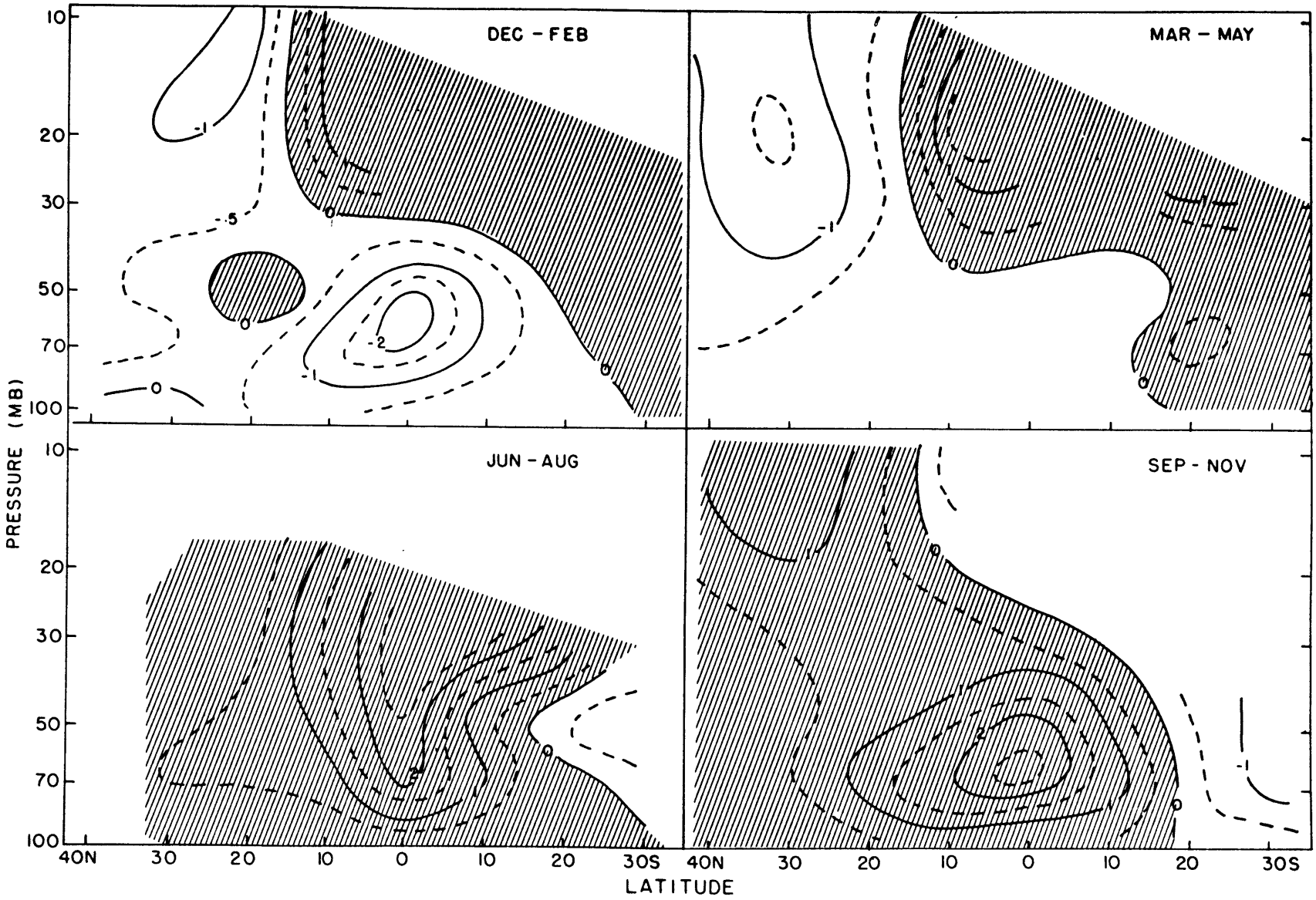

Fig. 9.2: Temperature anomalies during odd years showing downward propagation.

ometers from the equator. The pattern of the temperature anomalies is therefore related to the zonal wind anomalies by the thermal wind equation. Four of the corresponding eight phases of the temperature oscillation are shown in Fig. 9.2 in which the temperature anomalies plotted represent the difference between the mean for odd years and the seasonal mean. The downward propagation of temperature anomalies accompanying the wind anomalies can be quite easily seen.

Recognising that the temperature anomalies could be due to adiabatic heating and cooling, Reed (1964) has proposed a simple model (shown in Fig. 9.3) in which a succession of meridional cells of opposite sense are imbedded in a basic downward current. Although this gives quite a good picture of the wind and temperature patterns it can not account for the supply of westerly momentum at the equator as will be discussed later. The model does however fit in with the ozone variations encountered during the cycle as Reed has pointed out. The total ozone amounts in a vertical column are higher when there is a downward cell velocity near 21 km and lower when it is upward, with the total concentrations in the equatorial regions and in the subtropics out of phase. As Newell (1964) has pointed out the observed relation between the variations of the zonal wind and the ozone concentrations may also result from modulations in the large scale eddy activity in the lower stratosphere. The lower stratosphere is driven from below and the eddies responsible for the counter gradient heat flux are in-

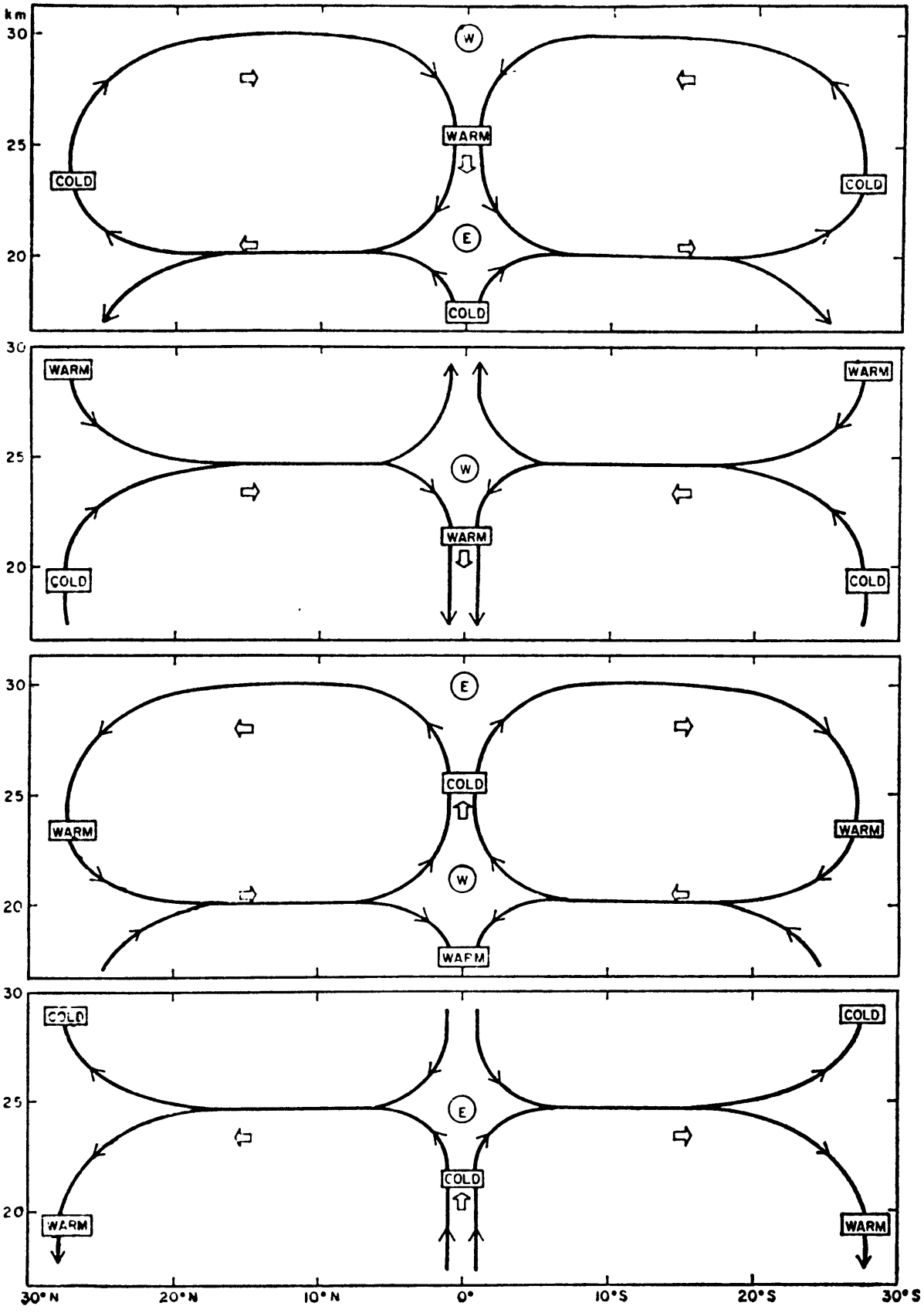

Fig. 9.3: Mean cell model of the biennial oscillation after Reed (1964).

clined more steeply than the isentropic surfaces. The effect of increased eddy activity is to transport more ozone than usual polewards and downwards while at the same time increasing the flux of angular momentum out of the tropics. In this way the presence of easterlies at the equator in the 20-30 km layer can be correlated with the higher ozone concentrations observed in mid-latitudes.

Observations of the oscillation in the extra-tropical stratosphere do not present a very clear pattern in the Northern Hemisphere due to its small amplitude in comparison to other variations. The Southern Hemisphere results show more consistency and a quasi-biennial oscillation can be readily identified. The results of Angell and Korshover (1964), Sparrow and Unthank (1964) and Tucker and Hopwood (1968) show the following features:

(i) When ozone concentrations and 50 mb temperatures are above normal in the tropics (with the westerly core at $\sim$ 30 mb) low ozone concentrations and temperatures are found at higher latitudes with stronger than normal westerlies.

(ii) While zonal wind anomalies of the same sign are observed at higher levels ($\sim$ 28 km) the phase is apparently independent of height at mid-latitudes.

(iii) The oscillation is well developed at Mc Murdo Sound (78^{o}S) where the temperature oscillation at 50 mb has an amplitude of 1^{o}, half that at Canton Is., and is in the opposite phase.

In the Northern Hemisphere, the spring warmings have been found by Labitzke (1966) to show a two year periodicity between 1958 and 1962 with a phase change in 1963. At the 10 mb level, the polar vortex remained centred over the Arctic during March with a considerable amount of zonal symmetry but during the odd years the vortex was displaced towards Siberia. Undoubtedly this change in the stratospheric circulation pattern is responsible for some of the periodicity observed in the temperatures (eg. Angell and Korshover 1964). It is probably also related to the biennial variation observed by Ebdon (1966) in the changeover date to summer easterlies at the 50 mb level at Shanwell.

9.2 THE BIENNIAL OSCILLATION IN THE TROPOSPHERE

Time series analysis of a variety of tropospheric parameters has shown evidence for an oscillation with a period near two years and a summary of these results has been presented by Landsberg (1962). More recently Landsberg et al. (1963) have used a band pass filter to examine the biennial oscillation in surface temperatures at a number of stations covering a wide range of latitudes. The study showed the pulse with a period slightly in excess of two years to be a world wide phenomenon, although contributing only a few percent to the variance of the monthly means. It showed a marked tendency to be locked in phase to the annual cycle with extreme values occurring

most frequently in the winter months. The phase appeared to differ between the tropics and higher latitudes with the changeover occurring at the axis of the subtropical highs but was also a function of the longitude. A weak oscillation in the variance of surface pressure over North America and Europe has also been found by Shapiro (1964) and again the winter months were seen to be largely responsible.

For the most part, upper air observations have not shown the oscillation with as much clarity as the surface data. There are indications however that the oscillation is quite wide-spread in the troposphere and some of the results presented by Wright (1968) show a clear difference between odd and even years. Some of the parameters appear to be quite clearly related to each other, eg. the jet axis at 0^{o} longitude is farther north in July of the even years, coinciding with less zonality in the flow over the Mediterranean and a greater frequency of westerlies at Scilly (50^{o}N, 6^{o}W). The 700 mb ridge axis over the Western Pacific was also further north. Another related set of phenomena are found in the Indian Ocean region. In even years the summer westerlies in the lower troposphere at Gan and Singapore were stronger than usual. At the same time, the Madagascan trades,which are one of the two main currents feeding the equatorial westerlies were better developed and the flow over Australia was more zonal than usual. For the examples given it was noted that the two year cycle is easily masked by other localized effects such as the monsoon and it

was most noticeable during seasons when these were weak.

A large two year periodicity has also been observed in the 500 mb momentum fluxes by Miller, Woolf and Teweles (1967) during the period 1956-65. Although the total transport did not show this variation, harmonic analysis revealed that pronounced variations in wave numbers 1 and 3 were consistently opposed by that in wave number 2. Again the oscillation appeared to be locked to the annual cycle with maximum transports for wave numbers 1 and 3 occurring during the winters of odd years.

Another example of the oscillation in surface temperature is found in a pilot study by the writer. 12-month running means were computed for a number of stations for records extending back nearly 100 years in most cases. It was found that the two year oscillation appeared very clearly over some shorter periods of the record but long intervals were found without any systematic year to year changes. During the periods when the oscillation was most marked a clear phase relation could be established between the variations at widely separated stations. Some of the better examples are shown in Fig. 9.4 where the surface temperatures at Woodstock, Md. (39^{o}N, 77^{o}W) and Stockholm (59^{o}N, 18^{o}E) are in phase and the temperature at Upernavik (73^{o}N, 56^{o}W) is in the opposite phase. The extreme values tend to occur in the winter months.

The evidence for the troposphere therefore suggests an oscil-

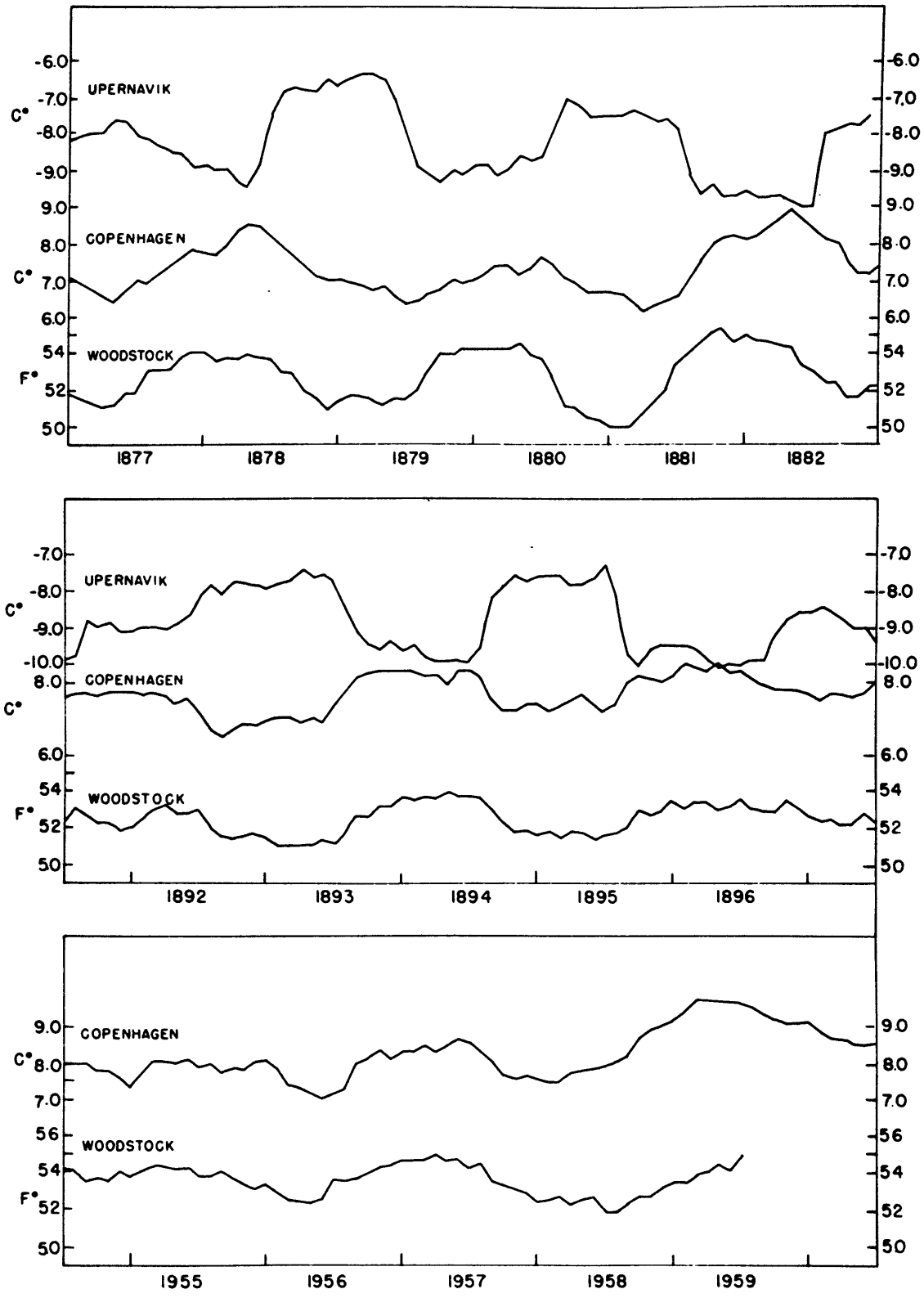

Fig. 9.4: 12-month running means of surface temperature at Upernavik, Copenhagen and Woodstock.

lation on a global scale with its phase linked to the annual cycle. Because of its small amplitude it is frequently masked by other features of the tropospheric circulation and quite long periods occur when it can not be detected at all.

9.3 THE DYNAMICS OF THE BIENNIAL OSCILLATION

Although the dynamics of the biennial oscillation have been the subject of a number of theoretical and modelling studies, no completely satisfactory explanation has yet been given of its downward propagation. Other factors to be explained are of course the approximately biennial periodicity and the generation of westerly momentum at the equator.

The most recent investigations have specified an external forcing function of heat or momentum and attempted to reproduce the downward propagation of the oscillation. Wallace and Holton (1968) have used a numerical model of a symmetric vortex in the tropical stratosphere with the diabatic heating rate and the diffusion parameterized. The unperturbed state was matched as far as possible to the observed tropical circulation, and was made to vary by heat or momentum forcing with a biennial periodicity. They were able to obtain time dependent solutions resembling the observed oscillation but these were embedded in a basically downward flow at the equator requiring a strong radiative heat sink. As calculations by Rodgers (1967) show

the lower equatorial stratosphere has on the average a small positive heating rate which is very difficult to reconcile with mean downward motion. A more serious difficulty seems to be that the downward propagation is restricted to too narrow a latitude range. Attempts to increase the horizontal extent by the choice of a larger horizontal diffusion coefficient resulted in too much attenuation below the 25 km level. Dickinson (1968) in an analytical study of zonally-symmetric stratospheric circulations has suggested that the Coriolis torques associated with downward-propagating meridional cells similar to Reed's 1964 model create the necessary changes in zonal momentum away from the vertical advection region close to the equator. This model did not however allow a latitudinal variation of the Coriolis parameter, f, and a value corresponding to 12^{o} lat. was chosen. Subsequent calculations by Holton (1968) have shown that the inclusion of the latitudinal variation of f caused a considerable increase in attenuation and a reduction in the rate of downward propagation. These results confirmed the earlier findings of Wallace and Holton that the Coriolis torque was too weak to be a primary cause of the downward propagation of the oscillation.

In each of the studies mentioned above a periodic forcing function of heat or momentum was assumed. While Staley (1963) concluded that the drive of the oscillation was due to varying solar ultra-violet radiation, Wallace and Holton (1968) could only obtain a rather un-

realistic downward propagating wave by assuming a very large variation in the diabatic heating. Momentum fluxes appear to be much more probable as the source of initial perturbation at high levels, and the convergence of the horizontal momentum fluxes has been studied in detail by Wallace and Newell (1965). Their principle findings were

(i) In the tropics at the 20 mb level and above the convergence of the horizontal transient eddy flux is of the proper size and phase to account for the zonal accelerations.

(ii) Below 30 mb there is little or no evidence for an oscillation in momentum transports in the tropics.

(iii) The oscillation in momentum transports is practically simultaneous at all levels and latitudes where it appears.

(iv) The oscillation is strong at mid-latitudes.

The oscillation in the momentum fluxes specified by Wallace and Holton (1968) was based on the pattern observed by Wallace and Newell and led to the difficulties discussed earlier. It was concluded by Wallace and Holton that the only successful way to model the downward propagation of alternating wind regimes would be to resort to a phase dependence with height in the momentum fluxes.

An ingenious approach has recently been suggested by Lindzen and Holton (1968) which relies on the interaction of long period vertically propagating gravity waves with the zonal wind. The convergence of the vertical eddy flux of momentum can, under certain conditions,

lead to a downward propagating zonal wind profile originating with the semi-annual oscillation above 40 km. A biennial oscillation in the flux at the lower boundary is not required since the absorption depends on the shear of the zonal wind. Their model appears to give an adequate representation of the oscillation both at the equator and at 12^{o} latitude and predicts a period which is a multiple of six months. So far no attempt has been made to compute the vertical fluxes of momentum in the tropics although the large scale disturbances considered responsible have been described in some detail by Maruyama (1967), and Wallace and Kousky (1968). In view of the difficulties in computing vertical motions, particularly in the tropics, it is unlikely that the vertical eddy flux will ever be obtained with sufficient accuracy to verify the model. It does appear however that the model is in reasonably good agreement with the observable features of the oscillation.

9.4 THE SOURCE OF THE OSCILLATION

In the previous sections the biennial oscillation has been presented as a global phenomenon which is most pronounced in the tropical stratosphere. The oscillation tends to be locked in phase to the annual cycle in both the troposphere and stratosphere with the difference between consecutive winters being responsible for most of the associated variance in atmospheric parameters. At present the ultimate source of the oscillation is still unknown and any theory devel-

oped to explain it should take account of its global extent, the apparent linkage between troposphere and stratosphere and its disappearance for quite long periods of time.

Initially it was thought that oscillation could be related to a fluctuating output of solar radiation absorbed at high levels in the stratosphere. Cycles with a period of approximately 26 months had been discovered (Shapiro and Ward 1962) in the sunspot number and the theory of Staley (1963) assumed a corresponding fluctuation of the incoming ultra-violet radiation. The weaknesses of this hypothesis lie in the fact that the much larger 11 year cycle does not produce changes in the stratospheric circulation of a comparable magnitude and that, as Wallace and Holton (1968) show, the change in solar output required would be unreasonably large. With an extra-terrestrial origin seemingly ruled out the most likely source for the origin is some naturally occurring cycle within the atmosphere. As far as the tropical stratosphere is concerned, the main requirement to be met is a periodic convergence in the momentum fluxes by either horizontal or vertical eddies. Newell (1964) has pointed out that the lower stratosphere up to about the 25 km level is driven by an upward flux of energy from the troposphere and consequently changes in the eddy activity in the stratosphere should originate in the upper troposphere at mid-latitudes. In view also of the small mass of the atmosphere above the 30 km level where the downward propagation originates and its attenu-

ation toward the tropopause it is most unlikely that an oscillation originating in the upper stratosphere could produce the observed changes in the troposphere.

An essential part of the oscillation is a suitable feedback mechanism or "memory" by which the state of the oscillation can be preserved over long periods. Unlike the tropical stratosphere where energy conversions are small and the zonal wind can remain relatively unchanged over a period of months, the conversions in the troposphere are large so that characteristic rejuvenation times are relatively short. The troposphere then cannot retain the perturbation sufficiently long to maintain an oscillation of biennial periodicity. A more likely solution is that of heat storage in the oceans which, as shown in Chapter 6, apparently takes up most of the radiational surplus during the summer and makes up most of the winter deficit.

Bjerknes (1966) has investigated a mechanism of this type operating in the central and eastern Pacific, showing that a positive water temperature anomaly at the equator was related to stronger westerlies over the northeast Pacific during November 1957 to February 1958. In explanation, it was suggested that the anomalous heating intensified the Hadley circulation, increasing the flow of momentum into the mid-latitude westerlies. The anomalous heating was, in turn, due to the lack of upwelling of colder water due to weaker surface easterlies. Further analysis over the period 1950-1967 (Bjerknes 1968)

failed to show any biennial periodicity in the sea surface temperature at Canton Island until 1963 afterwhich it was very pronounced over the rest of the period. It therefore seems unlikely that the anomaly in the equatorial Pacific could have been responsible for the biennial oscillation over the period of our study. However, for the reasons discussed above, air-sea interaction in some form may well be responsible for the biennial oscillation.

In view of the importance of the Hadley circulation to the atmospheric circulation as a whole the results of this study were examined for possible year to year changes. An increase in the strength of the Hadley cells for example will increase the poleward momentum flux into the subtropical jet, strengthening it and possibly increasing the energy flux upward into the mid-latitude stratosphere. (As Charney and Drazin (1961) have shown, a westerly zonal wind profile favours energy propagation upwards.) Another possible effect of an increased Hadley circulation would be a stronger meridional velocity in the lower stratosphere where the upper branch of the cell extends through the tropopause. The results are presented in the following chapter.

CHAPTER 10

OBSERVATIONAL EVIDENCE OF THE BIENNIAL OSCILLATION IN THE TROPOSPHERE

Following the determination of the average conditions reported in the previous chapters, attempts were made to find evidence of the biennial oscillation in the tropospheric radiosonde data. Two main techniques were used; twelve month running means of the latitude band averages and objective analysis of the long term means for odd and even years.

A twelve month running mean is equivalent to a low pass filter so that oscillations in the data with periods of the order of two years and longer are passed virtually unchanged. The large annual cycle is entirely filtered out and periods shorter than one year are strongly attenuated. Because the oscillations with longer periods than 24 months are also included it is possible to make a more realistic evaluation of the importance of biennial changes in comparison to longer term trends or climatic changes. While a narrow band filter centred on a period of 24 months would give a clearer representation of any existing biennial periodicity, the output from such a filter may be entirely due to noise in the observations and care is required in

its interpretation. Aside from the extra computing involved, it was felt that if a biennial oscillation did not show in the 12 month running means then it was unlikely to be of much significance to the circulation as a whole.

The long term means were recomputed for the four seasons further divided into odd and even years. Decembers were included with the January and February of the following year. Although the lapses in phase of the oscillation led to an average 26-month period over the interval 7/57-6/63 for which the means were computed, the variation in phase in each season is only one sixth of a cycle. Furthermore the phase of the oscillation tends to be locked to the annual cycle so that grouping the data by season should provide an insight into that variation between consecutive years which is apparently responsible for the biennial periodicity. Analyses were made of the five parameters, $\bar{u}$, $\bar{v}$, $\overline{u'v'}$, $\bar{T}$ and $\overline{v'T'}$ in order to detect any shift in the large scale wave patterns from year to year, and possible modulations in the energy conversion rates.

In view of the small amplitude of the tropospheric oscillation demonstrated in previous studies it was anticipated that it would be difficult to find in the radiosonde data. For the most part this proved to be the case but some of the results which point to a small biennial modulation in the strength of the Hadley circulation will be discussed in the following sections.

10.1 MODULATIONS OF THE ZONAL MEANS

A selection of the 12-month running means obtained is shown in Fig. 10.1. The values presented have been normalized by dividing by the standard deviation shown opposite each trace and their vertical separation is four standard deviations. The five traces in the lower part of the figure essentially confirm previous results and are included to show the phase of the stratospheric oscillation. Since the data coverage is better at 10°N than at the equator and the downward propagation is essentially the same at both latitudes, the running means at 10°N have been taken to represent conditions in the equatorial stratosphere. The downward propagation of the zonal wind at 10° can be clearly seen with the phase differing by about 90° between the 20 mb and 50 mb levels. The 30 mb temperature is almost in phase with the 20 mb zonal wind oscillation so that higher temperatures occur below the westerly regimes. The standard deviation of the meridional wind component at 40° N is a maximum during the winters whose Januarys fall in even years with the phase being independent of height. Higher temperatures at 40°N are associated with the stronger eddy activity, and as Wallace and Newell (1966) have shown, the divergence of momentum flux from the equatorial stratosphere is also a maximum at this time.

In the troposphere only a few of the zonal means showed signs of a biennial periodicity and these are presented in the upper part of

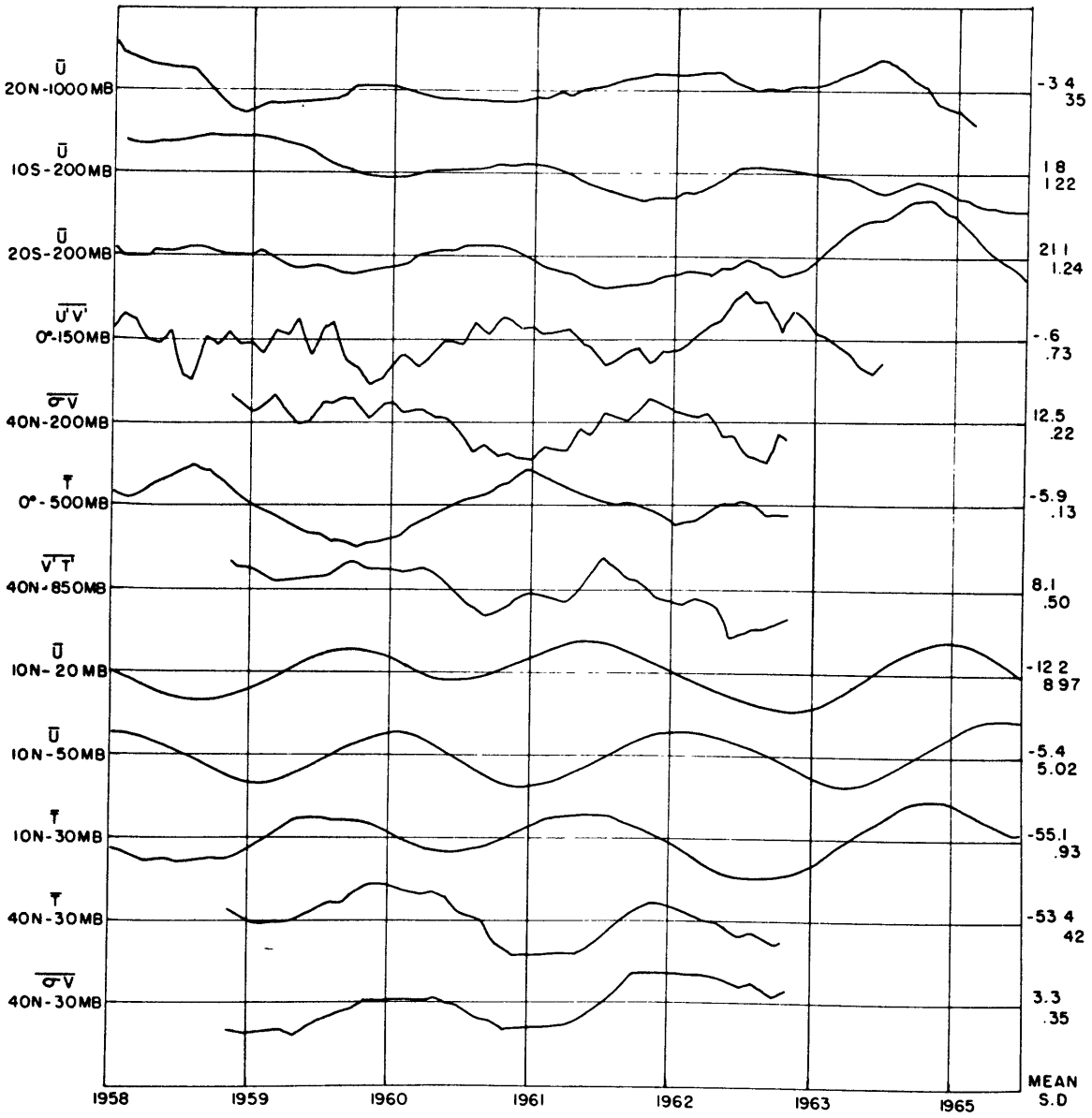

Fig. 10.1: 12-month running means of selected parameters normalized by the standard deviation opposite each. The vertical separation of the plots is four standard deviations.

Fig. 10. 1. The oscillations in the zonal wind component at 10°S and 20°S occurred at a number of tropospheric levels and have been represented by the values at the 200 mb level. The temperature oscillation at the equator occurred with the same phase at nearly all tropospheric levels and the 500 mb level has been used as an example. The oscillations observed in the other tropospheric parameters in Fig. 10. 1 could not be observed at adjacent levels.

In each case the amplitude of the biennial variation is small and is about 5 to 10% of the range of the seasonal means. Although the phase cannot be clearly determined in some of the examples shown, in most cases extreme values occur during the Northern Hemisphere winter. The main exception is the zonal wind component at 20°S for which maxima tend to occur in the Southern Hemisphere winters of even years. The other examples presented show that during the Northern Hemisphere winters of even years there is a tendency for weaker 1000 mb easterlies at 20°N while the eddy activity in the upper troposphere at 40°N is stronger and there is more southward transport of momentum across the equator. At the same time, temperatures in the equatorial troposphere are lower, and the poleward heat flux in the lower troposphere at 40°N is stronger.

In order to explore further the relation between these parameters the individual three-month seasonal means were examined for systematic year to year changes. For most of the running means

in Fig. 10.1 only one or two seasons of the year showed any clear biennial periodicity and in these cases the results obtained have been summarized in Fig. 10.2. The 1000 mb zonal wind component has been taken as an indicator of the strength of the northern Hadley cell on the assumption that stronger surface easterlies imply a stronger meridional circulation. In the same way the stronger westerlies in the upper troposphere at 10^{o}S and 20^{o}S have been taken as an indicator of a stronger Hadley circulation there. As Fig. 10.2 shows, the Hadley circulation is apparently weaker in both hemispheres during the northern summer and fall of odd years. At the same time the temperatures at the equator tend to be cooler, which suggests that reduction of the adiabatic cooling in the ascending branch is more than offset by reduced convective activity and latent heat release. While the greater than normal momentum flux by transient eddies across the equator in the southern spring might result from a greater proportional reduction in the strength of the northern Hadley cell it is not easy to account for the stronger poleward flux of sensible heat which might possibly indicate an earlier onset of winter conditions. The stronger Southern Hemisphere circulation during even years is apparently in agreement with the evidence presented by Wright (1968) and reviewed in Chapter 9. The weaker eddy activity at 40^{o}N in the upper troposphere during odd winters is consistent with the weaker fluxes observed in the stratosphere during this period

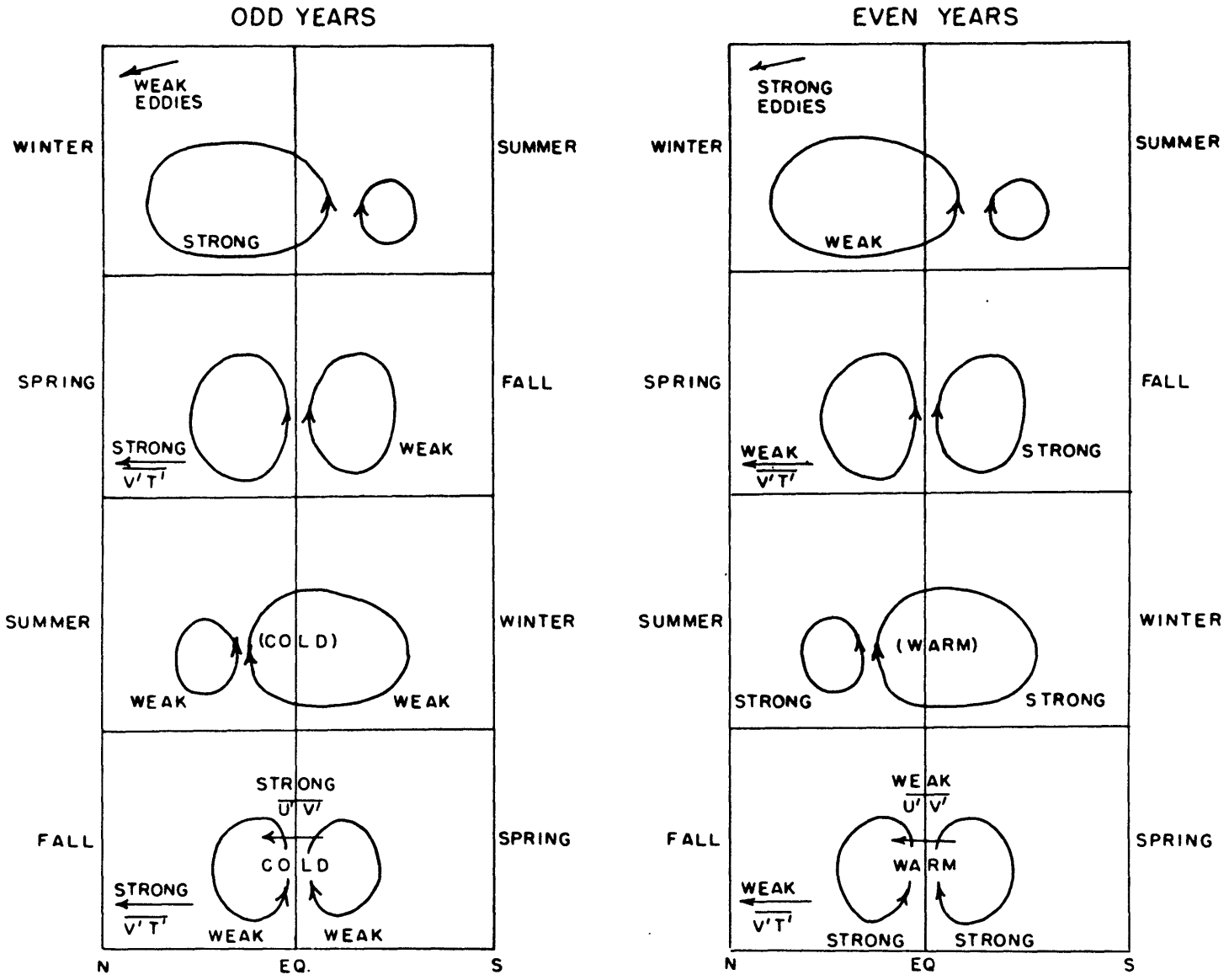

Fig. 10.2: Schematic diagram showing observed biennial periodicities in the troposphere.

and the recognition that the eddy kinetic energy of the lower stratosphere is supplied from below. No convincing explanation can be given at the present time of the remaining biennial changes shown in Fig. 10.2 and the possibility that they are due to sampling errors can not be ruled out.

10.2 ANALYSIS OF THE LONG TERM MEANS

The objective analyses of the seasonal means for odd and even years failed to show significant differences which could be attributed to the biennial oscillation. The main difficulty encountered lies in the fact that year to year differences are small and tend to be obscured by noise in the data and longer period trends. The longer period trends which are often observed in the twelve month running means can be caused not only by genuine climatic changes but by inhomogeneity in the data coverage. While longer period averages eliminate much of the trend, errors in the data may significantly influence the analysis, particularly if they occur at isolated stations.

In view of the uncertainty in the results, the discussion in this section will be limited to a comparison of the energy integrals and conversion rates in odd and even years between 33^{o}N and 33^{o}S (Fig. 10.3). In odd years the total available potential energy is larger during all seasons except September-November while the total kinetic energy is greater in summer and winter but slightly smaller in the

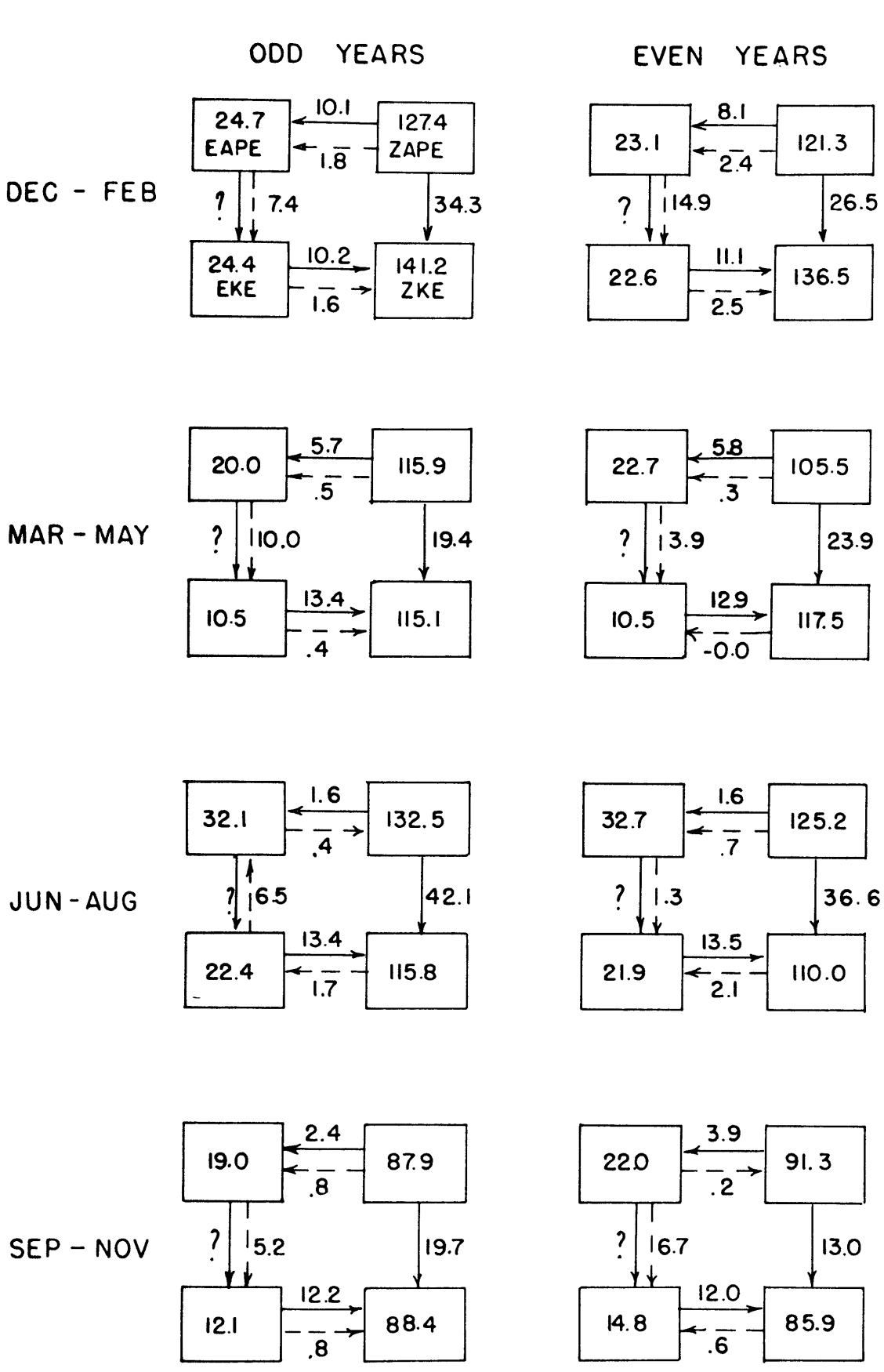

Fig. 10.3 Comparison of energy integrals between odd and even years.

spring and fall seasons compared to their values in even years. The conversion from zonal available potential energy to zonal kinetic energy is larger in odd years during all seasons except March to May, a result which agrees with the findings of the previous section during December-May and disagrees with them during the rest of the year. Because the integral involved in the conversion is strongly dependent on the mean meridional circulation it is unwise to attach too much importance to the year to year differences mentioned above. The conversions between the eddy and zonal forms of available potential energy and kinetic energy are probably not significantly changed, and in general it is difficult to gauge the significance of the observed year to year changes in Fig. 10.3. It may well be that the results presented in this section are unrelated to the biennial oscillation of the troposphere and serve only as an indication of the uncertainty in measuring the energy integrals.

In view of the difficulties discussed above, it seems desirable to filter the monthly station means to retain only those variations with periodicities near two years and in this way eliminate the longer period trends. The filtered output could then be grouped according to season as before and the analysis repeated. It is hoped that further investigations using this technique will lead to a consistent pattern of year to year changes.

10.3 FINAL COMMENTS

Despite the difficulty of observing the biennial oscillation in the troposphere the results presented in Section 10.1 show an apparently consistent variation in the strength of the Hadley circulation from year to year. It was not possible in all cases to fit the observed seasonal patterns of change into a consistent model of the tropospheric oscillation and it has been suggested that sampling errors may be responsible for the discrepancies.

Considering the time involved in preparation of the long term seasonal means and in their objective analysis the results obtained were rather disappointing. As mentioned in Section 10.2 the only hope of improvement apparently lies in filtering the station data before obtaining the seasonal means so that only the variations with a period near two years can contribute to the difference in the analyses.

Although a start has been made in the description of the tropospheric oscillation clearly much remains to be done before an adequate quantitative definition can be obtained and it would be premature at this stage to put forward any detailed theory concerning the interaction between troposphere and stratosphere. Further research should be directed toward a more complete description of the tropospheric oscillation using not only radiosonde data but the more accurate surface observations of temperature, pressure and rainfall

which are available at many more locations. The analysis of sea surface temperatures and their interaction with the atmospheric circulation should be extended as far as the existing observations permit. Hopefully the results obtained would lead not only to the answer of the long-standing question as to the source of the biennial oscillation but would prove invaluable in the study of climatic change and in its more practical aspect of long range forecasting.

REFERENCES

Albrecht, F., 1931: Uber die 'Glashauswirkung' der Erdatmosphare und das Zustandekommen der Troposphare. Met. Zeit., 48, 57-68.

Angell, J.K., and J. Korshover, 1964: Quasi-biennial oscillations in temperature, total ozone and tropopause height. J. Atmos. Sci., 21, 479-492.

Bjerknes, J., 1966: A possible response of the Hadley circulation to variations of the heat supply from the equatorial Pacific. Tellus, 18, 820-829.

Bjerknes, J., 1968: Atmospheric teleconnections from the equatorial Pacific. U.C.L.A. Dept. of Meteor., Progress Report on N.S.F. Contract GP-3193, 35 pp.

Buch, H.S., 1954: Hemispheric wind conditions during the year 1950. Final Report No. 2, M.I.T. Dept. of Meteor., Planetary Circulations Project, AF 19-122-153.

Budyko, M.I. and K.Y. Kondratiev, 1964: The heat balance of the earth. Solid Earth and Interface Phenomena, Vol. 2, M.I.T., pp. 529-554.

Charney, J.G., 1968: The intertropical convergence zone and the Hadley circulation of the atmosphere. To be published.

Charney, J.G. and P.G. Drazin, 1961: Propagation of planetary scale disturbances from the lower into the upper atmosphere. J. Geophys. Res., 66, 83-109.

Cressman, G.P., 1959: An operational objective analysis system. Mon. Weath. Rev., 87, 367-374.

Dickinson, R.E., 1968: On the excitation and propagation of zonal winds in an atmosphere with Newtonian cooling. J. Atmos. Sci., 25, 269-279.

Ebdon, R.A., 1966: A summer predictor? Weather, 21, p. 259.

Eddy, A., 1967a: The statistical objective analysis of scalar data fields. J. Appl. Met., 6, 597-609.

Eddy, A., 1967b: Two dimensional statistical objective analysis of isotropic scalar data fields. U. of Texas Atmos. Sci. Group, Publ. No. 5, 100 pp.

Efroymson, M. A., 1962: 'Multiple regression Analysis', Mathematical Methods for Digital Computers. Ed. A. Ralston and H. S. Wilf, Wiley and Sons, Vol. I, pp. 191-203.

Flohn, H., 1964: Investigations on the tropical easterly jet. Bonner Meteorologische Abhandlungen No. 4., 80 pp.

Gabites, J. F., 1950: Seasonal variation in the atmospheric heat balance. Sc. D. Thesis, M. I. T. Dept. of Meteor., Cambridge, Mass.

Gordon, A. H., 1953: Seasonal changes in the mean pressure distribution over the world and some inferences about the general circulation. Bull. Amer. Met. Soc., 34, 357-367.

Holton, J. R., 1968: A note on the propagation of the biennial oscillation. J. Atmos. Sci., 25, 519-521.

Jung, G. H., 1952: Note on the meridional transport of energy by the oceans. J. Mar. Res., 11, 139-146.

Katayama, A., 1967: On the radiation budget of the troposphere over the Northern Hemisphere (III) 'Zonal cross section and energy consideration'. J. Met. Soc. Japan, 45, 26-39.

Kidson, J. W., D. G. Vincent, and R. E. Newell, 1969: Observational studies of the general circulation of the tropics, I.'Long term mean values'. Quart. J. R. Met. Soc., 95, to be published.

Krishnamurti, 1961: The subtropical jet stream of winter. J. Met., 18, 172-191.

Kuo, H. L., 1951: A note on the kinetic energy balance of the zonal wind systems. Tellus, 3, 205-207.

Labitzke, K. B., 1966: The nearly two year cycle of the midwinter warmings of the stratosphere. Paper presented at the Symposium

on the Interaction between the Upper and Lower Layers of the Atmosphere, IUGG Meeting, Vienna.

Landsberg, H.E., 1962: Biennial pulses in the atmosphere. Beitr. Phys. Atmos., 35, 184-194.

Landsberg, H.E., J.M. Mitchell Jr., H.L. Crutcher and F.T. Quinlan, 1963: Surface signs of the biennial atmospheric pulse. Mon. Weath. Rev., 91, 549-556.

Lindzen, R.S., and J.R. Holton, 1968: A theory of the quasi-biennial oscillation. To be published.

London, J., 1957: A study of the atmospheric heat balance. Final Report, N.Y.U. Dept. of Meteorology and Oceanography, AF 19 (122)-165.

Lorenz, E.N., 1955: Available potential energy and the maintenance of the general circulation. Tellus, 7, 157-167.

Manabe, S. and J. Smagorinsky, 1967: Simulated climatology of a general circulation model with a hydrological cycle, Part II: Analysis of the tropical atmosphere. Mon. Weath. Rev., 95, 155-169.

Manabe, S., J. Smagorinsky and R.F. Strickler, 1965: Simulated climatology of a general circulation model with a hydrologic cycle. Mon. Weath. Rev., 93, 769-798.

Maruyama, T., 1967: Large scale disturbances in the equatorial lower stratosphere. J. Met. Soc. Japan, 45, 391-408.

Miller, A.J., 1966: Vertical motion atlas for the lower stratosphere during the IGY. Report No. 16, M.I.T. Dept. of Meteor., Planetary Circulations Project.

Miller, A.J., H.M. Woolf, and S. Teweles, 1967: Quasi-biennial cycles in angular momentum transports at 500 mb. J. Atmos. Sci., 24, 289-304.

Mintz, Y., 1954: The observed zonal circulation of the atmosphere. Bull. Amer. Met. Soc., 34, 208-214.

Murgatroyd, R.J., 1968: The inference of the mean meridional cir-

culation in the Northern Hemisphere from angular momentum transport data. To be published.

Murgatroyd, R.J. and F. Singleton, 1961: Possible meridional circulations in the stratosphere and mesosphere. Quart. J.R. Met. Soc., 87, 125-135.

Murakami, T., 1960: On the maintenance of kinetic energy of the large-scale stationary disturbances in the atmosphere. Sci. Report No. 2, M.I.T. Dept. of Meteor., Planetary Circulations Project, AF (604)-6108, 42 pp.

Murakami, T., 1962: Stratospheric wind, temperature and isobaric height conditions during the IGY period, Part I. Report No. 5, M.I.T. Dept. of Meteor., Planetary Circulations Project, AT (30-1) 2241 and AF 19 (604)-5223.

Newell, R.E., 1963: Preliminary study of quasi-horizontal eddy fluxes from meteorological rocket network data. J. Atmos. Sci., 20, 213-225.

Newell, R.E., 1964: A note on the 26-month oscillation. J. Atmos. Sci., 21, ~~572-573.~~ 320-321

Obasi, G.O.P., 1963a: Atmospheric momentum and energy calculations for the Southern Hemisphere during the IGY. Sci. Report No. 6, M.I.T. Dept. of Meteor., Planetary Circulations Project, AF 19 (604)-6108.

Obasi, G.O.P., 1963b: Poleward flux of atmospheric angular momentum in the Southern Hemisphere. J. Atmos. Sci., 20, 516-528.

Obasi, G.O.P., 1965: On the maintenance of the kinetic energy of mean zonal flow in the Southern Hemisphere. Tellus, 17, 95-105.

Oort, A.H., 1964: On estimates of the atmospheric energy cycle. Mon. Weath. Rev., 92, 483-493.

Palmén, E., 1964: General circulation of the Tropics. Symposium on Tropical Meteorology, Rotorua, 1963, pp 3-30, New Zealand Meteorological Service, Wellington, N.Z.

Palmén, E., H. Riehl and L.A. Vuorela, 1958: On the meridional circulation and release of kinetic energy in the tropics. J. Met., 15, 271-277.

Palmén, E. and L. A. Vuorela, 1963: On the mean meridional circulations in the Northern Hemisphere during the winter season. Quart. J. R. Met. Soc., 89, 131-138.

Peixoto, J. P., 1960a: Hemispheric temperature conditions during the year 1950. Sci. Report No. 4, M. I. T. Dept. of Meteor., Planetary Circulations Project, AF 19(604)-6108.

Peixoto, J. P., 1960b: Contribuição para o estudo dos campos médios da distribuição e do fluxo meridional da entalpia na atmosfera. Prize essay 'Artur Malheiros', Academy of Sciences of Lisbon.

Peng, L., 1963: Stratospheric wind, temperature and isobaric height conditions during the IGY period, Part II. Report No. 10, M. I. T. Dept. of Meteor., Planetary Circulations Project, AT (30-1) 2241 and AF 19 (604)-5225.

Peng, L., 1965: Stratospheric wind, temperature and isobaric height conditions during the IGY period, Report No. 15, M. I. T. Dept. of Meteor., Planetary Circulations Project, AT (30-1) 2241 and AF 19 (604)-5223.

Priestley, C. H. B., 1949: Heat transport and zonal stress between latitudes. Quart. J. R. Met. Soc., 75, 28-40.

Priestley, C. H. B., and A. J. Troup, 1964: Strong winds in the global flux of momentum. J. Atmos. Sci., 21, 459-460.

Raschke, E., and M. Pasternak, 1967: The global radiation balance of the earth atmosphere system obtained from radiation data of the meteorological satellite Nimbus II. Report No. X-622-67-383, Goddard Space Flight Center, Greenbelt, Maryland.

Reed, R. J., 1960: The circulation of the stratosphere. Paper presented at 40th Anniversary meeting of the A. M. S., Boston, January 1960, 12 pp.

Reed, R. J., 1962: Evidence of geostrophic motion in the equatorial stratosphere. Quart. J. R. Met. Soc., 88, 324-327.

Reed, R. J., 1964: A tentative model of the 26-month oscillation in tropical latitudes. Quart. J. R. Met. Soc., 90, 441-466.

Reed, R. J., 1965: The present status of the 26 month oscillation. Bull. American Met. Soc., 46, 374-387.

Riehl, H., 1962: Radiation measurements over the Caribbean during the Autumn of 1960. J. Geophys. Res., 67, 3935-3942.

Riehl, H., 1966: Upper air observations in the Tropics. World Weather Watch Planning Report No. 1, W.M.O., Geneva, 16 pp.

Riehl, H. and J.S. Malkus, 1958: On the heat balance in the equatorial trough zone. Geophysica, 6, 503-538.

Robinson, J.G., 1968: Mean meridional eddy flux of enthalpy in the Southern Hemisphere during the IGY. S.M. Thesis, M.I.T., Dept. of Meteor., 77 pp.

Rodgers, C.D., 1967: The radiative heat budget of the troposphere and lower stratosphere. Report No. A2, M.I.T. Dept. of Meteor., Planetary Circulations Project, N.S.F. Grant No. GA - 400.

Shapiro, R., 1964: A mid-latitude biennial oscillation in the variance of the surface pressure distribution. Quart. J.R. Met. Soc., 90, 328-331.

Shapiro, R., and R.F. Ward, 1962: A neglected cycle in sunspot numbers? J. Atmos. Sci., 19, 506-508.

Smagorinsky, J., S. Manabe and J.L. Holloway, Jr., 1965: Numerical results from a nine-level general circulation model. Mon. Weath. Rev., 93, 727-768.

Sparrow, J.G., and E.L. Unthank, 1964: Biennial oscillations in the Southern Hemisphere. J. Atmos. Sci., 21, 592-596.

Staley, D.O., 1963: A partial theory of the 26-month oscillation in the equatorial stratosphere. J. Atmos. Sci., 20, 506-515.

Starr, V.P., 1951: Applications of energy principles to the general circulation. Compendium of Meteorology, A.M.S., 568-576.

Starr, V.P., 1953: Note concerning the nature of the large-scale eddies in the atmosphere. Tellus, 5, 494-498.

Starr, V.P., 1959: Further statistics concerning the general circulation. Tellus, 11, 481-483.

Starr, V. P., 1960: Questions concerning the energy of stratospheric motions. Arch. F. Met., Geoph., u Biokl., Ser. A., 12, 1-7.

Starr, V. P. and R. M. White, 1952: Note on the seasonal variation of the meridional flux of angular momentum. Quart. J. R. Met. Soc., 78, 62-69.

Starr, V. P. and R. M. White, 1954: Balance requirements of the general circulation. Geophys. Res. Papers, No. 35, Geophys. Res. Directorate, AFCRC, Cambridge, Mass.

Thompson, B. W., 1963: The Climate of Africa. Oxford University Press, Nairobi, 132 pp.

Tucker, G. B., 1959: Mean meridional circulations in the atmosphere. Quart. J. R. Met. Soc., 85, 209-224.

Tucker, G. B., 1965: The equatorial troposphere wind regime. Quart. J. R. Met. Soc., 91, 140-150.

Tucker, G. B., and J. M. Hopwood, 1968: The 26-month zonal wind oscillation in the lower stratosphere of the Southern Hemisphere. J. Atmos. Sci., 25, 293-298.

Vincent, D. G., 1968: Mean meridional circulations in the Northern Hemisphere lower stratosphere during 1964 and 1965. Quart. J. R. Met. Soc., 94, to be published.

Vuorela, L. A. and I. Tuominen 1964: On the mean zonal and meridional circulations and the flux of moisture in the Northern Hemisphere during the summer season. Pure and Appl. Geophys., 57, 167-180.

Wallace, J. M., 1966: Long period wind fluctuations in the tropical stratosphere. Report No. 19, M. I. T. Dept. of Meteor., Planetary Circulations Project, 167 pp.

Wallace, J. M., 1967: On the role of mean meridional motions in the biennial wind oscillation. Quart. J. R. Met. Soc., 93, 176-185.

Wallace, J. M. and J. R. Holton, 1968: A diagnostic numerical model of the quasi-biennial oscillation. J. Atmos. Sci., 25, 280-292.

Wallace, J. M. and V. E. Kousky, 1968: Observational evidence of Kelvin waves in the tropical stratosphere. J. Atmos. Sci., 25,

(in press).

Wallace, J. M. and R. E. Newell, 1966: Eddy fluxes and the biennial stratospheric oscillation. Quart. J. R. Met. Soc., 92, 481-489.

White, R. M., 1951a: The meridional flux of sensible heat over the Northern Hemisphere. Tellus, 3, 82-88.

White, R. M., 1951b: The meridional eddy flux of energy. Quart. J. R. Met. Soc., 77, 188-199.

White, R. M., 1954: The countergradient flux of sensible heat in the lower stratosphere. Tellus, 6, 177-179.

Widger, W. K., 1949: A study of the flow of angular momentum in the atmosphere. J. Met., 6, 291-299.

Wiin-Nielsen, A., 1968: On the annual variation and spectral distribution of atmospheric energy. Tellus, 19, 540-559.

Wright, P. B., 1968: A widespread biennial oscillation in the troposphere. Weather, 23, 50-54.

Yoshida, K., 1967: An assessment of the transport of momentum in the Australian sector of the Southern Hemisphere. Tech. Report No. 7, International Antarctic Meteorological Research Centre, Commonwealth Bureau of Meteorology, Melbourne, Australia.

APPENDIX A: STATION LIST

The complete station list is shown in Table A1 which contains the following information:

(i) KN index: This index runs from 1 to 306 and indicates the order in which the stations appear on the covariance tapes.

(ii) WMO index: In some cases where the index has changes the more recent one is used. Chinese stations in blocks 51-59 are not listed in W. M. O. publications but a listing may be found in the weather station index published by the U. S. Naval Oceanographic Offices. *

(iii) Station name

(iv) Latitude

(v) Longitude

(vi) Height above sea level in meters

(vii) Observation times: Observations at 00, 06, 12, 18Z are indicated by a 1 in the respective columns. This 1 should not be interpreted as an indication that observations were obtained regularly at the time specified but rather that some observations were obtained at this hour. It may also indicate a change in the observing time during the study period.

---

* 'Weather Station Index', H.O. Pub. No. 119, 2nd Ed., U.S. Govt. Printing Office, Washington, 1963.

(viii) Report type: W indicates radar wind observation, T indicates radiosonde observations and WT indicates radiosonde and radar wind or pilot balloon observations.

(ix) Data source: The data sources listed are described briefly as follows:

TRC: A total of 229 stations was selected from the 704 processed by Travellers' Research Center for the 5 year period May 1958-April 1963. These stations have a KN index from 1-229 and include all TRC stations south of 35^{o}N together with selected stations in the 35^{o}N - 45^{o}N band. These data were obtained on 12 tapes with observations for all stations grouped by day. Observations were supplied where available at 50 mb intervals from the surface to 100 mb but the difficulties in processing the tapes and lack of data at intermediate levels for most stations made it worthwhile only to process the 10 mandatory levels: surface, 1000, 850, 700, 500, 400, 300, 200, 150 and 100 mb levels.

Above 100 mb, data for 250 stations had been obtained earlier from TRC by J. M. Wallace for the same period. 120 of these stations coincided with stations in the group of 229 obtained for the troposphere and included virtually all those with good data above 100 mb. Since the main mean and covariance terms had already been computed by Wallace and were readily available they were added directly to the monthly covariance tape. As TRC confined itself to decks used

by the National Weather Records Center at Asheville for preparation of the Northern Hemisphere data tabulations, a number of stations were missing from the 229 and few Indian wind observations were obtained. Where possible 12Z data or alternative sources were used and these are indicated instead of TRC in the source column of the station list.

ASHEVILLE: Data obtained from NWRC at first on cards and later on tapes. These were used to extend the Northern Hemisphere data beyond the main five year period, to fill gaps in the TRC data and to extend coverage into the Southern Hemisphere. The principal card decks used were numbers 524/5, 545/645 and 562 which are punched on a regular basis. Deck 616 provided Indian wind data and deck 612 provided Southern Hemisphere data mainly during the IGY-IGC period.

MCDS: Punching of data from the IGY microcards was undertaken at M.I.T. where it could not be obtained already punched from other sources. The overall period is limited to 7/57-12/59 and a number of stations gave only partial coverage of this period. The card format is similar to that of Asheville deck #525.

FOREIGN: Punched cards were obtained in many different formats from the Australian, British, French, New Zealand and South African Meteorological Services. The country of origin appears in the comments in the station list. The majority of the French sta-

tions reported only winds as did 2 of the 4 stations under New Zealand control. The quality and quantity of observations were both good and these stations were a valuable source for Africa, the Indian Ocean and the South Pacific.

FRN TAB: A limited number of stations were punched from tabulations by the Portugese and Mauritian Meteorological Services. The Mauritian data was kindly provided by Dr. A. D. Belmont of the Control Data Corporation. These stations included the Portugese territories in South Africa and the Indian Ocean Islands of Mauritius and Diego Garcia.

(x) Comments: Any comments of particular relevance are included. Typically they indicate whether any station has a particularly short record, and the country of origin for foreign sources.

Table A. 1

STATION LIST FOR TROPICAL STUDY

KN	WMO	STATION NAME	LAT	LONG	HT	00	06	12	18	TYPE	SOURCE	COMMENTS
1	07645	NIMES/CCURRESSANT	43.9N	4.4E	60	1				WT	TRC TAPES	
2	08509	LAJES (AZORES)	38.8N	27.1W	54	1				WT	TRC TAPES	
3	09521	FUNCHAL	32.6N	16.9W	110			1		T	ASHEVILLE	
4	09536	LISBOA/PORTELA	38.8N	9.1W	110	1				WT	TRC TAPES	
5	09594	SAL	16.7N	23.0W	55			1		T	ASHEVILLE	
6	15614	SOFIA	42.8N	23.4E	588	1				WT	TRC TAPES	
7	16420	MESSINA	38.2N	15.6E	54	1				WT	TRC TAPES	
8	16716	ATHINAI/HELLINIKON	37.9N	23.7E	9	1				WT	TRC TAPES	
9	31960	VLADIVOSTOK	43.1N	131.9E	138	1				WT	TRC TAPES	
10	32165	JUZNO-KURIL'SK	44.0N	145.8E	40	1				WT	TRC TAPES	
11	36870	ALMA ATA	43.2N	76.9E	847	1				WT	TRC TAPES	
12	37018	TUAPSE	44.1N	39.1E	78	1				WT	TRC TAPES	
13	37985	LENKORAN	38.7N	48.8E	-11	1				WT	TRC TAPES	
14	38687	CARDZOU	39.1N	63.6E	193	1				WT	TRC TAPES	
15	40181	BEER YAAQOV	31.9N	34.8E	63	1				WT	TRC TAPES	3 MONTHS' DATA ONLY
16	40627	BAHRAIN /MUHARRAQ	26.3N	50.6E	2	1				WT	TRC+ASHVL	
17	40597	ADEN/KHORMAKSAR	12.8N	45.0E	3	1				WT	TRC+ASHVL	
18	41780	KARACHI AP	24.9N	67.1E	22	1		1		WT	ASHEVILLE	1959-60 MISSING
19	41920	DACCA	23.8N	90.4E	8	1				T	TRC TAPES	STARTS 7/62 (MAY BE 41917)
20	42071	AMRITSAR	31.6N	74.9E	234	1				T	TRC TAPES	ENDS 5/60
21	42182	NEW DELHI/SAFDARJUNG	28.6N	77.2E	216	1		1		WT	TRC+ASHVL	
22	42339	JODHPUR	26.3N	73.0E	224	1		1		WT	TRC+ASHVL	
23	42361	GWALIOR	26.2N	78.2E	207	1				T	TRC TAPES	4 MONTHS' DATA
24	42910	GAUHATI	26.1N	91.7E	54	1				WT	TRC TAPES	
25	42411	GAUHATI	26.2N	91.8E	55	1				T	TRC TAPES	
26	43475	ALLAHABAD/RAMHRAULI	25.4N	81.7E	98	1		1		WT	MCDS+ASHVL	
27	43647	AHMADABAD	23.1N	72.6E	55	1				WT	TRC TAPES	STARTS 11/62
28	43809	CALCUTTA/DUM DUM	22.6N	88.4E	10	1		1		WT	TRC+ASHVL	
29	43867	NAGPUR/SONEGAON	21.1N	79.0E	310	1		1		WT	TRC+ASHVL	
30	43909	VERAVAL	20.9N	70.4E	8	1				T	TRC TAPES	ENDS 7/61
31	43003	BOMBAY/SANTACRUZ AP	19.1N	72.8E	15	1		1		WT	TRC+ASHVL	
32	43149	VISHAKHAPATNAM	17.7N	83.2E	3	1		1		WT	TRC+ASHVL	
33	43279	MADRAS/PINAMBAKKAM	13.0N	80.2E	16	1		1		WT	TRC+ASHVL	
34	43295	BANGALORE	13.0N	77.6E	921	1				T	TRC TAPES	8 MONTHS' DATA
35	43333	PORT BLAIR	11.7N	92.7E	79	1		1		WT	TRC+ASHVL	
36	43371	TRIVANDRUM	8.5N	77.0E	64	1		1		WT	TRC+ASHVL	
37	44354	YUGUDZYU	44.9N	110.1E	914	1				WT	TRC TAPES	
38	45004	HONG KONG/KING'SPARK	22.3N	114.2E	66	1				WT	TRC+ASHVL	
39	46692	TAIPEI	25.0N	121.5E	9	1				WT	TRC+ASHVL	
40	44697	TAOYUAN	25.0N	121.2E	48	1				WT	TRC+ASHVL	ENDS 5/60
41	46734	MAKUNG AO 1	23.5N	119.6E	22	1				WT	TRC+ASHVL	ENDS 1958
42	45747	TUNGKONG	22.5N	120.4E	8	1				WT	TRC+ASHVL	ENDS 5/60
43	47058	PYONGYANG	39.0N	125.8E	29	1				WT	TRC TAPES	
44	47187	MOSULPO AB	33.2N	126.2E	6	1				WT	TRC TAPES	
45	47646	TATENO	36.0N	140.1E	27	1				WT	TRC TAPES	
46	47678	MACHIJOJIMA/OMURE	33.1N	139.8E	156	1				WT	TRC TAPES	
47	47778	SHIONOMISAKI	33.4N	135.7E	75	1				WT	TRC TAPES	
48	47807	FUKUOKA	33.6N	130.4E	6	1				WT	TRC TAPES	
49	47827	KAGOSHIMA/YOSHINO	31.6N	130.6E	283	1				WT	TRC TAPES	
50	47909	NAZE/FUNCHATOGE	28.4N	129.6E	295	1				WT	TRC TAPES	
51	47931	KADENA AB	26.4N	127.8E	46	1				WT	TRC+ASHVL	
52	47963	TORISHIMA	30.5N	140.3E	83	1				WT	TRC TAPES	
53	48327	CHIANGMAI	18.8N	99.0E	313	1				WT	TRC TAPES	
54	48455	BANGKOK	13.7N	100.5E	12	1				WT	TRC+ASHVL	
55	48568	SONGKHLA	7.2N	100.6E	10	1				WT	TRC+ASHVL	
56	48694	SINGAPORE AP	1.4N	104.0E	10	1				WT	TRC+ASHVL	

STATION LIST FOR TROPICAL STUDY

KN	WMO	STATION NAME	LAT	LONG	HT	00 06 12 18	TYPE	SOURCE	COMMENTS
57	43819	LANG	21.0N	105.9E	5	1	WT	MCDS+ASHVL	ENDS 1/61
58	44855	DANANG/TOURANE	16.0N	108.2E	7	1	WT	TRC TAPES	STARTS 5/62
59	48900	SAIGON/TANSONNHUT	10.8N	106.7E	10	1	WT	TRC+ASHVL	
60	5[illegible]828	HOTIEN	37.1N	79.9E	1389	1	WT	TRC TAPES	
61	5[illegible]203	HAMI	42.8N	93.4E	735	1	WT	TRC TAPES	
62	5[illegible]681	MINCHIN	38.7N	103.1E	1368	1	WT	TRC TAPES	
63	5[illegible]299	HEIHE	32.0N	92.1E	4000	1	WT	TRC TAPES	
64	5[illegible]591	LASA	29.7N	91.0E	3658	1	WT	TRC TAPES	
65	5[illegible]029	YUSHU	33.1N	96.8E	3873	1	WT	TRC TAPES	
66	5[illegible]096	WUTOU	33.4N	104.7E	1090	1	WT	TRC TAPES	
67	5[illegible]137	CHANGTU	31.2N	97.3E	3200	1	WT	TRC TAPES	
68	5[illegible]146	KANTZE	31.6N	100.0E	3320	1	WT	TRC TAPES	
69	5[illegible]294	CHENGTU	30.7N	104.1E	498	1	WT	TRC TAPES	
70	5[illegible]492	YENPIN	29.9N	104.5E	286	1	WT	TRC TAPES	
71	5[illegible]533	TZUKEI	27.7N	98.4E	63	1	WT	TRC TAPES	
72	5[illegible]571	HSICHANG	27.9N	102.3E	1599	1	WT	TRC TAPES	
73	5[illegible]691	WEIYING	26.9N	104.2E	2235	1	WT	TRC TAPES	STARTS 1/60
74	5[illegible]739	TENG CHUNG	25.1N	98.5E	1628	1	WT	TRC TAPES	
75	5[illegible]778	KUNMING	25.0N	102.7E	1893	1	WT	TRC TAPES	
76	5[illegible]779	(KUNMING)	25.1N	102.8E	1905	1	WT	TRC TAPES	
77	5[illegible]964	SZEMAO	22.6N	101.0E	1319	1	WT	TRC+ASHVL	
78	5[illegible]999	HOKOU	24.4N	103.9E	134	1	WT	TRC+ASHVL	
79	57036	SIAN	34.2N	108.9E	400	1	WT	TRC TAPES	
80	57083	CHENG CHOW	34.7N	113.7E	110	1	WT	TRC TAPES	
81	57127	HANCHUNG	33.1N	107.2E	520	1	WT	TRC TAPES	
82	57447	ENSHIH	30.3N	109.4E	437	1	WT	TRC TAPES	
83	57461	YEHCHANG	30.7N	111.3E	707	1	WT	TRC TAPES	
84	57494	HANKOW	30.4N	114.3E	23	1	WT	TRC TAPES	
85	57515	SAPINPA	29.5N	104.6E	261	1	WT	TRC TAPES	CONTINUATION OF 57516
86	57516	PAISHIH TO	29.5N	106.3E	290	1	WT	TRC TAPES	ENDS 3/61
87	57679	CHANGSHA	28.2N	112.8E	49	1	WT	TRC TAPES	
88	57745	CHIHKIANG	27.4N	109.6E	268	1	WT	TRC TAPES	
89	57816	KWEIYANG	26.6N	106.7E	1071	1	WT	TRC TAPES	
90	57957	KWEILIN	25.2N	110.1E	156	1	WT	TRC TAPES	
91	57972	CHENGHSIEN	25.8N	113.0E	171	1	WT	TRC TAPES	
92	57993	KANCHOW	25.8N	114.9E	110	1	WT	TRC TAPES	
93	58027	HSUCHOW	34.2N	117.2E	45	1	WT	TRC TAPES	
94	5[illegible]150		33.9N	120.5E	2	1	WT	TRC TAPES	
95	5[illegible]203	FUYANG	32.9N	115.8E	32	1	WT	TRC TAPES	
96	5[illegible]238	YANCHING	32.1N	118.8E	72	1	WT	TRC TAPES	
97	5[illegible]321	HOFEI	31.9N	117.2E	28	1	WT	TRC TAPES	STARTS 1/60
98	5[illegible]367	SHANGHAI	31.2N	121.4E	5	1	WT	TRC TAPES	
99	5[illegible]606	JANCHANG	28.7N	116.0E	49	1	WT	TRC TAPES	
100	5[illegible]633	CHUNCHOW	29.0N	118.9E	80	1	WT	TRC TAPES	
101	5[illegible]636		29.5N	119.0E					
102	5[illegible]666	TACHEN TAO	28.4N	121.9E	199	1	WT	TRC TAPES	
103	5[illegible]725	SHAT WU	27.3N	117.5E	255	1	WT	TRC TAPES	
104	5[illegible]847	FUCHOW	26.1N	119.3E	88	1	WT	TRC TAPES	
105	5[illegible]912	CHANGTING	25.9N	116.4E	301	1	WT	TRC TAPES	10 MONTHS' DATA
106	5[illegible]965	DAOYUNG	25.1N	121.3E	49	1	WT	TRC TAPES	
107	5[illegible]082	CHUCHIANG	24.9N	113.5E	87	1	WT	TRC TAPES	ENDS 3/61
108	5[illegible]134	SHAMEN	24.4N	119.1E	39	1	WT	TRC+ASHVL	
109	5[illegible]135	CHIMEN	24.4N	118.3E	91	1	WT	TRC TAPES	PATCHY
110	5[illegible]137		24.3N	119.1E	23	1	WT	TRC TAPES	7 MONTHS ONLY
111	5[illegible]211	POSEH	23.4N	106.5E	198	1	WT	TRC+ASHVL	
112	5[illegible]265	WUCHOW	23.5N	111.4E	119	1	WT	TRC TAPES	

STATION LIST FOR TROPICAL STUDY

KN	WMO	STATION NAME	LAT	LONG	HT	00	06	12	18	TYPE	SOURCE	COMMENTS
113	59287	KUANGCHOW	23.2N	113.3E	19	1				WT	TRC+ASHVL	
114	59316	SWATOW	23.4N	116.7E	5	1				WT	TRC+ASHVL	
115	59345	NANKING	23.5N	119.5E	40	1				WT	TRC TAPES	ENDS 9/58
116	59431	NANNING	22.8N	108.3E	75	1				WT	TRC+ASHVL	
117	59559	HENGCHUNG	22.0N	120.9E	22	1				WT	TRC+ASHVL	
118	59758	HAIKOU	20.0N	110.4E	14	1				WT	TRC+ASHVL	
119	59981	SISHA	16.9N	112.3E	2	1				WT	TRC+ASHVL	
120	60020	SANTA CRUZ	28.5N	16.2W	37	1				WT	TRC TAPES	NO WINDS UNTIL 3/61
121	60119	KENITRA/PORT LYAUTEY	34.3N	6.6E	12	1				WT	TRC TAPES	
122	60571	COLOMB BECHAR	31.6N	2.2W	781			1		WT	ASHEVILLE	(FORMERLY 60570)
123	60625	AOULEF	27.0N	1.1E	290			1		WT	ASHEVILLE	
124	60680	TAMANRASSET	22.8N	5.5E	1378			1		WT	NCDS+ASHVL	
125	61052	NIAMEY	13.5N	2.2E	226	1				WT	TRC+ASHVL	
126	61401	FORT TRINQUET	25.2N	11.6W	360	1				WT	MICROCARDS	
127	61642	DAKAR/OUAKAM	14.7N	17.4W	39	1				WT	TRC+ASHVL	
128	61011	ANSELUS AFB TRIPOLI	32.9N	13.3E	4	1				WT	TRC TAPES	
129	61062	TOBRUK	32.1N	24.0E	14	1				WT	TRC TAPES	
130	61306	MERSA MATRUH	31.3N	27.2E	30	1				WT	TRC TAPES	
131	61366	CAIRO	30.1N	31.6E	74	1				WT	TRC TAPES	ENDS 7/60
132	61378	HELWAN	29.9N	31.2E	116	1				WT	TRC TAPES	STARTS 8/60
133	61414	ASSWAN	24.0N	32.9E	194	1				WT	TRC+ASHVL	
134	61721	KHARTOUM	15.6N	32.6E	380	1				WT	TRC+ASHVL	
135	64400	POINTE-NOIRE	4.8S	11.9E	17	1				W	FOREIGN	FR. STARTS 9/60
136	64650	BANGUI	4.4N	18.6E	381	1				WT	TRC+ASHVL	
137	64700	FORT-LAMY	12.1N	15.0E	295	1				WT	TRC+ASHVL	
138	64750	FORT ARCHAMBAULT	9.1N	18.4E	365	1				W	FOREIGN	FR. STARTS 11/61
139	65201	LAGOS/IKEJA	6.6N	3.3E	40	1				WT	TRC+ASHVL	
140	65578	ABIDJAN	5.2N	3.9W	16	1				WT	TRC+ASHVL	
141	72201	KEY WEST	24.6N	81.8W	6	1				WT	TRC+ASHVL	
142	72202	MIAMI	25.8N	80.3W	4	1				WT	TRC TAPES	
143	72206	JACKSONVILLE	30.4N	81.6W	9	1				WT	TRC TAPES	
144	72208	CHARLESTON	32.9N	80.0W	15	1				WT	TRC TAPES	
145	72211	TAMPA	28.0N	82.5W	3	1				WT	TRC TAPES	
146	72221	VALPARISO	30.5N	86.5W	29	1				WT	TRC TAPES	
147	72226	MONTGOMERY	32.3N	86.4W	62	1				WT	TRC TAPES	
148	72232	BURROCCO(BOOTHVILLE)	29.0N	89.4W	5	1				WT	TRC TAPES	
149	72235	JACKSON	32.3N	90.1W	101	1				WT	TRC TAPES	
150	72240	LAKE CHARLES	30.2N	93.2W	10	1				WT	TRC TAPES	
151	72249	SHREVEPORT	32.5N	93.8W	79	1				WT	TRC TAPES	
152	72250	BROWNSVILLE	25.9N	97.4W	6	1				WT	TRC TAPES	
153	72251	CORPUS CHRISTI	27.8N	97.5W	13	1				WT	TRC TAPES	
154	72253	SAN ANTONIO	29.5N	98.5W	242	1				WT	TRC TAPES	
155	72259	FT WORTH	32.8N	97.1W	176	1				WT	TRC TAPES	
156	72261	DEL RIO	29.4N	100.9W	313	1				WT	TRC TAPES	
157	72265	MIDLAND	31.9N	102.2W	872	1				WT	TRC TAPES	
158	72270	EL PASO	31.8N	106.4W	1194	1				WT	TRC TAPES	
159	72274	TUCSON	32.1N	110.9W	779	1				WT	TRC TAPES	
160	72280	YUMA NEVA	32.7N	114.6W	134							
161	72290	SAN DIEGO	32.7N	117.2W	124	1				WT	TRC TAPES	
162	72295	LOS ANGELES	33.9N	118.4W	38	1				WT	TRC TAPES	
163	72308	NORFOLK	36.9N	76.2W	9	1				WT	TRC TAPES	
164	72311	ATHENS	34.0N	83.3W	247	1				WT	TRC TAPES	
165	72327	NASHVILLE	36.1N	86.7W	184	1				WT	TRC TAPES	
166	72340	LITTLE ROCK	34.7N	92.2W	81	1				WT	TRC TAPES	
167	72363	AMARILLO	35.2N	101.7W	1099	1				WT	TRC TAPES	
168	72386	LAS VEGAS	36.1N	115.2W	664	1				WT	TRC TAPES	

STATION LIST FOR TROPICAL STUDY

KN	WMO	STATION NAME	LAT	LONG	HT	00	06	12	18	TYPE	SOURCE	COMMENTS
169	72392	PT ARGUELLO	34.6N	120.6W	22	1				WT	TRC TAPES	
170	7.445	COLUMBIA	39.0N	92.4W	239	1				WT	TRC TAPES	
171	7.476	GRAND JUNCTION	39.1N	108.5W	1475	1				WT	TRC TAPES	
172	72493	OAKLAND	37.7N	122.2W	2	1				WT	TRC TAPES	
173	72518	ALBANY	42.8N	73.8W	89	1				WT	TRC TAPES	
174	7.645	GREEN BAY	44.5N	88.1W	214	1				WT	TRC TAPES	
175	7.662	RAPID CITY	44.1N	103.1W	966	1				WT	TRC TAPES	
176	7.694	SALEM	44.9N	123.0W	61	1				WT	TRC TAPES	
177	74794	CAPE KENNEDY	28.5N	80.6W	3	1				WT	TRC TAPES	
178	76458	MAZATLAN	23.2N	106.4W	78	1				WT	TRC TAPES	
179	76644	MERIDA	21.0N	89.7W	22	1				WT	TRC+ASHVL	
180	76679	TACUBAYA	19.4N	99.2W	2306	1				WT	TRC+ASHVL	NO WINDS UNTIL 1/61
181	76692	VERA CRUZ	19.2N	96.1W	16	1				WT	TRC+ASHVL	NO WINDS UNTIL 5/62
182	74016	KINDLEY FIELD	32.4N	64.7W	6	1				WT	TRC+ASHVL	
183	74063	GOLD ROCK CREEK AFB	26.6N	79.3W	6	1				WT	TRC TAPES	
184	74076	COFFIN HILLS AFB	25.3N	76.3W	9	1				WT	TRC TAPES	
185	74089	ROMEFISH BAY AFB	24.1N	74.5W	9	1				WT	TRC+ASHVL	
186	74118	TURKS ISLAND AFB	21.5N	71.1W	7	1				WT	TRC+ASHVL	
187	74325	HAVANA	23.2N	82.4W	49	1				WT	TRC+ASHVL	
188	74355	CAMAGUEY	21.4N	77.9W	120	1				WT	TRC TAPES	
189	74367	GUANTANAMO	19.9N	75.2W	23	1				WT	TRC+ASHVL	
190	74383	GRAND CAYMAN	19.2N	81.4W	6	1				WT	TRC+ASHVL	
191	74397	KINGSTON/PALISADOES	17.9N	76.8W	12	1				WT	TRC+ASHVL	
192	74467	SABANA DELAMAR	19.1N	69.4W	11	1				WT	TRC TAPES	
193	74486	SAN DOMINGO	18.5N	69.9W	14	1				WT	TRC+ASHVL	STARTS 8/62
194	74501	SWAN ISLAND	17.4N	83.9W	11	1				WT	TRC+ASHVL	
195	78526	SAN JUAN	18.4N	66.0W	19	1				WT	TRC+ASHVL	
196	78806	ALBRCOK FIELD	9.0N	79.6W	66	1				WT	TRC+ASHVL	
197	78861	COOLIDGE AFB ANTIGUA	17.1N	61.8W	10	1				WT	TRC TAPES	STARTS 4/61
198	78862	COOLIDGE FLD ANTIGUA	17.1N	61.8W	10	1				WT	TRC+ASHVL	ENDS 8/60
199	78866	JULIANA AP/STMAARTEN	18.0N	63.1W	0	1				WT	TRC+ASHVL	
200	78897	RAIZET GUADELOUPE	16.3N	61.5W	8	1				WT	TRC+ASHVL	
201	78967	CHAGUARAMAS TRINIDAD	10.7N	61.4W	13	1				WT	TRC+ASHVL	
202	78988	PLESMAN AP,CURACAO	12.2N	69.0W	0	1				WT	TRC+ASHVL	
203	80001	SAN ANDRES	12.8N	81.7W	6	1				WT	TRC+ASHVL	
204	80222	BOGOTA/ELDORADO	4.6N	74.1W	2547	1				WT	TRC+ASHVL	STARTS 8/60
205	91066	MIDWAY ISLAND	28.2N	177.3W	13	1				WT	TRC+ASHVL	
206	91115	IWO JIMA AFB	24.3N	141.3E	106	1				WT	TRC+ASHVL	
207	91131	MARCUS ISLAND	24.3N	154.0E	17	1				WT	TRC+ASHVL	
208	91165	LIHUE	22.0N	159.4W	45	1				WT	TRC+ASHVL	
209	91217	TAGUAC GUAM	15.0N	144.8E	111	1				WT	TRC+ASHVL	
210	91218	ANDERSON APT	13.6N	144.9E	162							
211	91245	WAKE ISLAND	19.3N	166.6E	4	1				WT	TRC+ASHVL	
212	91250	ENIWETOK ATOLL	11.3N	162.3E	6	1				WT	TRC+ASHVL	
213	91275	JOHNSTON ISLAND	16.7N	169.5W	5	1				WT	TRC+ASHVL	
214	91285	HILO	19.7N	155.1W	11	1				WT	TRC+ASHVL	
215	91334	TRUK	7.4N	151.8E	2	1		1		WT	ASHEVILLE	
216	91348	PONAPE	7.0N	158.2E	46	1		1		WT	ASHEVILLE	
217	91366	KWAJALEIN	8.7N	167.7E	8	1				WT	TRC+ASHVL	
218	91376	MAJURO	7.1N	171.4E	3	1		1		WT	ASHEVILLE	
219	91408	KOROR	7.4N	134.5E	33	1		1		WT	ASHEVILLE	
220	91413	YAP	9.5N	138.1E	17	1				WT	TRC+ASHVL	TRAV. DATA PATCHY
221	91700	CANTON IS	2.8S	171.7W	3	1				WT	TRC+ASHVL	
222	98327	CLARK AFB	15.2N	120.6E	196	1				WT	TRC+ASHVL	
223	98645	CEBU	10.3N	123.9E	42	1				T	TRC TAPES	POOR COVERAGE
224	OWS K	WEATHER SHIP K	45.0N	16.0W	12	1				WT	TRC TAPES	

STATION LIST FOR TROPICAL STUDY

KN	WMO	STATION NAME	LAT	LONG	HT	00	06	12	18	TYPE	SOURCE	COMMENTS
225	OWS T	WEATHER SHIP T	29.0N	135.0E	12	1				WT	TRC TAPES	TYPHOON SEASON ONLY
226	OWS D	WEATHER SHIP D	44.0N	41.0W	12	1				WT	TRC TAPES	
227	OWS E	WEATHER SHIP E	35.0N	48.0W	12	1				WT	TRC TAPES	
228	OWS N	WEATHER SHIP N	30.0N	140.0W	12	1				WT	TRC TAPES	
229	OWS V	WEATHER SHIP V	34.0N	164.0E	12	1				WT	TRC TAPES	
230	63032	MAUI	20.0S	23.0E	945		1			WT	FOREIGN	S. AFR. 7/57-12/60
231	69100	SWAKOPMUND	22.7S	14.0E	19		1			WT	FOREIGN	S. AFR. 7/57-12/58
232	63110	WINDHOEK	22.6S	17.1E	1725		1			WT	FOREIGN	S. AFR. 1/59-12/60
233	64262	PRAETORIA	25.9S	28.2E	1374		1			WT	FOREIGN	S. AFR. 7/57-11/60
234	6.290	BAMAKO	12.6N	8.0W	330		1			W	FOREIGN	FR.
235	6+501	PORT GENTIL	0.7S	8.8E	4		1			W	FOREIGN	FR. FEW T OBS ON MCDS
236	6+870	N'GAOUNDERE	7.3N	13.3E	1115		1			W	FOREIGN	FR.
237	67001	MORONI	11.7S	43.2E	12					W	FOREIGN	FR. 1963 ONLY
238	67009	DIEGO SUAREZ	12.4S	49.3E	114	1				W	FOREIGN	FR.
239	67197	FORT DAUPHIN	25.0S	47.0E	8	1				W	FOREIGN	FR.
240	8.405	CAYENNE	4.8N	52.4W	8			1		W	FOREIGN	FR.
241	6+910	DOUALA	4.0N	9.7E	13		1			WT	FOREIGN	FR.
242	67085	TANANARIVE	18.9S	47.0E	1300	1				WT	FOREIGN	FR.
243	9:938	TAHITI	17.6S	149.6W	2	1				WT	FOREIGN	FR.
244	4.350	GAN	0.7S	73.2E	2		1	1	1	WT	FOREIGN	BRT. 10/59- 12Z WINDS INTERP.
245	63741	NAIROBI	1.3S	36.8E	1792	1	1	1		WT	FOREIGN	BRT.
246	63894	DAR ES SALAAM	6.9S	39.3E	58		1	1		WT	FOREIGN	BRT.
247	9:517	HONIARA	9.4S	160.0E	57	1				WT	FOREIGN	AUST.
248	94027	LAE	6.7S	147.0E	8	1				WT	FOREIGN	AUST.
249	94120	DARWIN	12.4S	130.9E	26	1				WT	FOREIGN	AUST.
250	94294	TOWNSVILLE	19.3S	146.8E	4	1				WT	FOREIGN	AUST.
251	94299	WILLIS IS.	16.3S	150.0E	8	1				WT	FOREIGN	AUST.
252	94300	CARNARVON	24.9S	113.7E	5	1				WT	FOREIGN	AUST.
253	94312	PT. HEDLAND	20.4S	119.6E	8	1				WT	FOREIGN	AUST.
254	94326	ALICE SPRINGS	23.8S	133.9E	546	1				WT	FOREIGN	AUST.
255	94335	CLONCURRY	20.7S	140.5E	188	1				WT	FOREIGN	AUST.
256	9+996	COCOS IS.	12.1S	96.9E	3	1				WT	FOREIGN	AUST.
257	9+836	ZAMBOANGA	6.9N	122.1E	6	1				T	ASHEVILLE	1958 MOSTLY
258	6.900	ASCENSION IS.	7.9S	14.4W	6	1				WT	ASHEVILLE	
259	8.400	FERNANDO NORONHA	3.9S	32.4W	45	1				WT	ASHEVILLE	
260	84129	GUAYAQUIL	2.2S	79.9W	4	1				WT	ASHEVILLE	
261	83781	SAO PAULO	23.6S	46.7W	795	1				WT	ASHEVILLE	
262	9.643	FUNAFUTI	8.5S	179.2E	1	1		1		W	FOREIGN	N.Z.
263	9:680	NANDI	17.8S	177.5E	16	1		1		WT	FOREIGN	N.Z. TEMPS 00Z ONLY
264	9:843	RAROTONGA	21.2S	159.9W	3	1		1		W	FOREIGN	N.Z.
265	93997	RAOUL IS.	29.3S	177.9W	48	1				T	FOREIGN	N.Z.
266	8.898	RECIFE	8.0S	34.9W	10	1				WT	ASHEVILLE	
267	84631	LIMA	12.1S	77.0W	155	1				WT	ASHEVILLE	
268	85442	ANTOFAGASTA	23.5S	70.4W	128	1				WT	ASHEVILLE	
269	9.489	CHRISTMAS IS.	2.0N	157.4W	3	1				WT	MCDS+ASHVL	IGY PERIOD
270	9:592	NOUMEA	22.3S	166.5E	75	1				WT	FOREIGN	FR. 1/63-
271	76225	CHIHUAHUA	28.6N	106.1W	1424	1				WT	ASHEVILLE	7/57-11/57 ONLY
272	41756	JIMANI	25.1N	61.8E	55	1				WT	MICROCARDS	3 MONTHS ONLY
273	41917	DACCA	23.8N	90.4E	10	1				WT	MICROCARDS	
274	48097	RANGOON	16.8N	96.2E	22	1				T	MCDS+ASHVL	ENDS 6/61
275	48802	CHAPA	22.4N	103.8E	1570	1				WT	MICROCARDS	FEW WINDS
276	6+005	COQUILHATVILLE	0.1N	18.3E	325		1			WT	MICROCARDS	
277	64210	LEOPOLDVILLE	4.3S	15.3E	309		1			WT	MICROCARDS	
278	6+360	ELISABETHVILLE	11.6S	27.5E	1277		1			WT	MICROCARDS	
279	66160	LUANDA	8.9S	13.2E	70	1				WT	FRN. TAB.	
280	60422	MOCAMEDES	15.2S	12.2E	44	1				WT	FRN. TAB.	

STATION LIST FOR TROPICAL STUDY

KN	WMO	STATION NAME	LAT	LONG	HT	00	06	12	18	TYPE	SOURCE	COMMENTS
281	67241	LUMBO	15.0S	40.7E	11	1				WT	FRN. TAB.	
282	67341	LOURENCO MARQUES	25.9S	32.6E	43	1				WT	FRN. TAB.	
283	67475	KASAMA	10.2S	31.1E	1395		1			WT	MICROCARDS	6 MONTHS ONLY
284	67587	LILONGWE	14.0S	33.7E	1135		1			WT	MICROCARDS	6 MONTHS ONLY
285	67663	BROKEN HILL	14.5S	28.5E	1207		1			WT	MICROCARDS	
286	67774	SALISBURY	17.9S	31.0E	1473		1			WT	MICROCARDS	
287	81401	MARACAY	10.3N	67.7W	432	1				T	MICROCARDS	
288	87157	RESISTENCIA	27.5S	59.0W	52	1				WT	MCDS+ASHVL	
289	96745	DJAKARTA	6.2S	106.8E	8			1		T	MCDS+ASHVL	ENCS 2/61
290	96933	SURABAJA	7.2S	112.7E	3			1		WT	MCDS+ASHVL	
291	41466	COLOMBO	6.9N	79.9E	6	1		1		WT	ASHEVILLE	1960 MOSTLY
292	61967	DIEGO GARCIA	7.2S	72.4E	2	1				WT	FRN. TAB.	7/63-
293	61995	VACOAS	20.3S	57.5E	425	1				WT	FRN. TAB.	1/61-
294	61996	NOUVELLE AMSTERDAM	37.4S	77.6E	28	1				WT	ASHEVILLE	IGY PERIOD (FORMERLY 67198)
295	63450	ADDIS ABABA	9.0N	38.7E	2360			1		WT	ASHEVILLE	1/58-12/62 IRREGULAR
296	64406	ALEXANDER BAY	28.6S	16.5E	27	1				WT	ASHEVILLE	IGY PERIOD
297	64588	DURBAN	30.0S	31.0E	8	1				WT	ASHEVILLE	IGY PERIOD
298	64816	CAPE TOWN	34.0S	18.6E	46	1				WT	ASHEVILLE	IGY PERIOD
299	64906	GOUGH +SLAND	40.4S	9. W	54	1				WT	ASHEVILLE	+GY PERIOD
300	83543	QUILTERO	32.8S	71.5W	2	1				WT	ASHEVILLE	
301	87576	EZEIZA	34.8S	58.5W	24	1				WT	ASHEVILLE	IGY PERIOD
302	94461	GILES	25.0S	128.3E	599	1				WT	FOREIGN	AUST.
303	94510	CHARLEVILLE	26.4S	146.3E	304	1				WT	FOREIGN	AUST.
304	94610	PERTH AP	31.9S	116.0E	18	1				WT	FOREIGN	AUST.
305	94995	LORD HOWE IS.	31.5S	159.1E	46	1				WT	FOREIGN	AUST.
306	94996	NORFOLK IS.	29.1S	167.9E	109	1				WT	FOREIGN	AUST.

APPENDIX B:

SUMMARY TAPE RECORD FORMAT

Total length = 169 7094 words = 1014 characters

7094 Words	Contents	Format
0	Fortran control word	000251000001_8
1	Station serial number (KN)	Fortran Integer (18 high order bits)
2	WMO Index	A5 format
3	month	Fortran Integer
4	year	Fortran Integer
5	Report type	Fortran Integer
6-16	$\overline{u}$ (31 levels)	1
17-27	$\overline{v}$ (31 levels)	1
28-38	$\overline{T}$ (31 levels)	1
39-48	$\overline{Z}$ (20 levels)	2
49-59	σu (31 levels)	1
60-70	σv (31 levels)	1
71-81	σT (31 levels)	1
82-88	σZ (20 levels)	3
89-99	$\overline{u'v'}$ (31 levels)	1
100-106	$\overline{u'T'}$ (20 levels)	1
107-117	$\overline{v'T'}$ (31 levels)	1
118-127	$\overline{u'Z'}$ (20 levels)	2
128-137	$\overline{v'Z'}$ (20 levels)	2
138-168	Numbers of observations (31 levels)	4

DESCRIPTION OF PACKING METHODS

1. Data for 3 levels stored in one word using 12 bits for each. The lowest level is in the high order position. The value in each case is multiplied by 10, converted to an integer and has 4000_8 added to make it positive. ie. 16.9 → 4251_8, -16.9 → 3527_8.

2. Data for 2 levels stored in one word using 18 bits for each. The value is converted to an integer and has 400000_8 added to make it positive. ie. 16463 → 440117_8

3. The same as (1) except that the values are not multiplied by 10.

4. The numbers of observations at each level are stored in one word using 6 bits for each with the 6 high order bits set to zero.

bits 1-6	zero
bits 7-12	no. of wind observations
bits 13-18	no. of temperature observations
bits 19-20	no. of geopotential observations
bits 25-30	no. of wind and temperature observations
bits 31-36	no. of wind and geopotential observations

LEVELS USED

The complete set of 31 levels is: sfc, 1000, 950, 900, 850, 800, 750, 700, 650, 600, 550, 500, 450, 400, 350, 300, 250, 200, 150, 100, 80, 70, 60, 50, 40, 30, 25, 20, 15, 10, 7 mb.

If 20 levels are specified, no data has been included for levels above 100 mb.

UNITS

The units are standardized at m/sec, ^{o}C and g.p.m.

REPORT TYPE

Wind observations are indicated by a bit in position 18, temperature observations by a bit in position 17 and the presence of stratospheric data (above 100 mb) by a bit in position 16.

GENERAL REMARKS

The formats used for packing are such that each item is stored in an integral number of 6 bit characters, and in the form of an integer. With a few exceptions all terms have been computed for the tropospheric levels. For levels above 100 mb most of the data have been obtained from Wallace who did not compute any terms involving Z or the covariance $\overline{u'T'}$ (which may also be missing for some stations at lower levels).

Table 4.1

Zonal Mean Temperatures (^{o}C)

(a) December-February

Lat. p(mb)	41N	33N	24N	15N	5N	5S	15S	24S	33S
100	-57.4	-64.8	-72.4	-77.1	-79.7	-80.6	-79.6	-75.4	-66.6
150	-56.4	-59.8	-63.6	-65.9	-67.1	-67.5	-67.1	-65.1	-61.1
200	-57.9	-55.8	-54.1	-53.5	-53.8	-53.7	-53.3	-53.0	-54.1
300	-50.1	-42.9	-35.8	-32.5	-31.7	-31.3	-31.1	-32.7	-36.8
400	-36.5	-29.1	-21.5	-17.4	-16.2	-15.9	-16.0	-17.8	-21.6
500	-25.0	-17.4	-10.3	- 6.4	- 5.6	- 5.6	- 5.7	- 6.8	- 9.9
700	- 9.1	- 1.8	5.2	9.2	9.9	9.6	9.5	9.1	6.7
850	- 2.3	5.2	12.3	16.6	17.9	17.8	17.8	17.3	14.2
1000	3.6	12.1	19.8	23.8	25.5	25.7	24.6	22.1	18.7

(b) March-May

Lat. p(mb)	41N	33N	24N	15N	5N	5S	15S	24S	33S
100	-56.9	-64.1	-71.4	-76.6	-79.5	-80.5	-78.8	-73.4	-64.0
150	-56.3	-60.0	-63.4	-65.7	-67.0	-67.5	-66.8	-64.2	-60.1
200	-58.0	-56.5	-53.9	-52.9	-53.2	-53.4	-53.3	-53.7	-55.4
300	-46.7	-41.0	-35.2	-31.8	-30.9	-30.8	-31.6	-34.7	-39.7
400	-32.2	-26.2	-20.6	-17.0	-15.9	-15.6	-16.5	-19.7	-24.8
500	-20.3	-14.2	- 9.0	- 6.2	- 5.5	- 5.3	- 5.7	- 8.3	-13.1
700	- 3.8	2.3	7.5	10.0	10.0	9.7	9.2	7.4	3.5
850	4.5	10.4	16.0	19.1	18.8	17.9	17.2	15.2	10.9
1000	10.5	16.2	21.9	25.3	26.2	26.1	23.9	19.6	15.1

(c) June-August

Lat. p(mb)	41N	33N	24N	15N	5N	5S	15S	24S	33S
100	-60.2	-67.5	-71.6	-74.5	-76.3	-77.1	-76.2	-70.7	-60.8
150	-57.6	-61.9	-64.1	-66.2	-67.4	-67.8	-66.9	-63.2	-57.5
200	-52.3	-51.9	-52.0	-53.0	-54.1	-54.5	-54.2	-53.5	-54.1
300	-36.8	-32.3	-30.8	-31.3	-32.3	-32.3	-32.4	-35.7	-42.8
400	-22.2	-17.9	-16.2	-16.4	-17.0	-16.6	-17.1	-21.6	-29.6
500	-10.5	- 6.8	- 5.7	- 6.1	- 6.4	- 6.0	- 6.5	-10.6	-18.0
700	6.4	9.7	10.8	10.3	9.3	8.9	8.1	4.5	- 1.4
850	15.8	18.2	18.9	18.7	17.5	16.3	14.8	11.3	6.6
1000	20.1	23.2	25.9	26.7	25.9	24.0	20.7	16.3	12.2

Table 4.1 (ctd.)

(d) September-November

Lat. / p(mb)	41N	33N	24N	15N	5N	5S	15S	24S	33S
100	-60.7	-67.7	-72.7	-75.8	-77.7	-78.5	-77.2	-71.2	-61.0
150	-59.0	-62.6	-65.0	-66.6	-67.6	-67.9	-67.1	-63.7	-58.0
200	-55.9	-54.4	-53.4	-53.5	-54.0	-54.3	-54.2	-53.9	-54.2
300	-42.5	-36.9	-33.1	-31.8	-31.9	-31.9	-32.4	-35.5	-41.2
400	-27.9	-22.3	-18.2	-16.7	-16.6	-16.4	-17.1	-20.8	-26.9
500	-16.1	-10.4	-07.0	-06.0	-06.1	-06.0	-06.4	-09.5	-15.2
700	00.1	05.4	08.7	09.5	09.2	09.1	08.9	06.8	01.5
850	07.6	13.0	17.2	18.5	17.8	16.9	16.5	14.3	08.7
1000	14.3	19.5	24.3	26.2	25.7	24.5	22.2	18.6	14.3

Table 4.2

Zonal Mean Temperature (^{o}C)

(Values obtained for odd years or even years only shown in parentheses)

Lat.	40N	30N	20N	10N	0	10 S	20 S	30 S
				(a) December-February				
p(mb)								
10	-49.3	-45.7	-43.1	-43.2	-----	-----	-----	-----
20	-53.8	-52.2	-50.5	-51.6	-----	-----	-----	-----
30	-56.3	-55.8	-55.3	-57.4	(-56.8)	(-58.6)	(-54.8)	-----
50	-58.7	-61.6	-64.3	-66.6	-68.1	-66.4	-64.8	-60.9
70	-59.5	-65.4	-74.3	-75.8	-76.2	-74.8	-74.1	-67.6
100	-58.8	-66.4	-74.7	-78.4	-80.4	-80.9	-77.8	-71.1
				(b) March-May				
p(mb)								
10	-45.0	-41.3	-38.8	-39.6	-----	-----	-----	-----
20	-50.6	-49.1	-47.6	-48.8	-----	-----	(-48.8)	-----
30	-53.2	-53.4	-53.4	-55.3	(-56.8)	-54.8	-53.4	-----
50	-56.6	-59.3	-62.9	-65.6	-66.8	-65.7	-63.2	-60.0
70	-58.6	-60.5	-72.0	-75.0	-76.4	-74.9	-71.3	-65.3
100	-58.1	-66.1	-74.1	-78.3	-80.7	-80.3	-76.0	-68.7
				(c) June-August				
p(mb)								
10	(-39.2)	-39.7	-40.0	-41.8	-----	-----	-----	-----
20	-45.3	-46.2	-47.6	-48.6	(-46.4)	-----	-----	-----
30	-49.5	-50.8	-51.9	-53.7	(-55.4)	-55.0	(-54.6)	(-54.8)
50	-54.5	-57.6	-59.9	-61.8	-62.9	-62.4	-60.8	-59.0
70	-58.4	-62.9	-66.8	-68.9	-69.5	-70.1	-68.6	-62.9
100	-61.3	-68.9	-72.8	-75.9	-77.1	-76.9	-73.6	-66.0
				(d) September-November				
p(mb)								
10	(-46.8)	-43.6	-41.5	-41.7	-----	-----	-----	-----
20	-51.1	-49.3	-48.1	-49.3	-----	-----	-----	-----
30	-54.4	-53.4	-53.0	-56.0	-56.8	(-54.0)	(-54.4)	-----
50	-58.1	-59.5	-61.1	-63.0	-64.4	-62.5	-61.3	-58.3
70	-60.7	-64.3	-68.6	-70.0	-71.4	-70.2	-69.1	-63.1
100	-61.7	-69.2	-74.1	-77.0	-78.4	-78.2	-74.3	-65.7

Table 4.3

Mean Zonal Wind in m sec^{-1}

(a) December-February

Lat. p(mb)	41N	33N	24N	15N	5N	5 S	15S	24 S	33 S
100	18.8	26.6	22.2	7.1	-2.6	-4.1	-0.3	5.2	9.3
150	25.1	36.5	31.6	13.6	0.3	-3.4	3.3	15.2	22.0
200	23.6	38.6	34.1	15.0	-1.0	-4.5	3.9	17.4	25.1
300	19.9	31.9	28.5	10.9	-2.3	-4.0	3.2	12.6	18.5
400	15.9	25.0	22.1	5.5	-4.6	-4.0	2.1	7.6	12.3
500	13.0	19.1	16.4	2.4	-5.4	-3.7	1.1	4.3	8.3
700	8.6	10.1	6.5	-1.5	-4.6	-2.4	0.0	0.6	3.8
850	5.1	5.1	0.9	-4.5	-4.7	-1.8	-0.6	-2.0	-0.0
1000	3.0	1.7	-1.2	-3.0	-2.4	-1.4	-1.0	-1.9	-0.9

(b) March-May

Lat. p(mb)	41N	33N	24N	15N	5N	5 S	15S	24 S	33 S
100	13.8	19.7	16.2	5.0	-1.9	-1.6	4.7	11.2	13.9
150	18.0	28.6	26.2	12.1	0.1	-0.8	9.6	21.8	24.2
200	19.0	30.0	27.7	12.7	-1.0	-2.2	10.1	24.3	26.4
300	16.5	23.4	21.4	8.6	-2.4	-3.1	6.8	18.7	21.8
400	13.9	18.4	15.6	4.0	-4.1	-3.9	3.8	12.3	16.6
500	11.1	14.2	11.2	1.0	-4.9	-4.0	1.8	7.7	11.8
700	6.3	7.5	4.7	-2.2	-5.0	-3.6	-0.7	2.2	6.0
850	3.6	3.6	0.6	-3.4	-4.0	-3.2	-2.6	-1.8	1.9
1000	2.6	1.0	-1.6	-2.5	-2.0	-1.5	-1.8	-2.5	-0.3

(c) June-August

Lat. p(mb)	41N	33N	24N	15N	5N	5 S	15S	24 S	33 S
100	12.7	2.2	-9.3	-13.5	-9.2	-2.8	4.7	13.7	21.8
150	16.4	8.2	-2.0	- 8.2	-9.8	-3.4	9.8	25.7	33.2
200	22.0	10.9	-0.3	- 6.0	-9.4	-4.5	10.6	30.7	38.3
300	17.1	8.9	-0.6	- 4.9	-7.5	-4.6	8.5	27.3	34.2
400	12.8	6.5	-0.9	- 4.2	-5.9	-4.7	5.3	20.2	26.9
500	9.6	4.7	-1.3	- 4.7	-5.5	-4.5	2.7	13.1	19.2
700	4.8	2.3	-1.4	- 3.4	-3.1	-3.5	-0.7	4.6	10.4
850	2.7	0.7	-1.7	- 1.6	-1.3	-3.9	-4.7	-1.1	6.3
1000	2.1	0.2	-1.7	- 1.3	-0.8	-1.9	-2.9	-2.6	1.6

Table 4.3 (ctd.)

Mean Zonal Wind in m sec^{-1}

(d) September-November

Lat. / p(mb)	41N	33N	24N	15N	5N	5S	15S	24S	33S
100	15.2	11.4	4.0	-3.5	-4.8	-2.0	4.1	10.6	14.8
150	18.3	18.1	11.0	1.2	-3.6	0.3	11.2	22.5	25.0
200	21.1	20.3	12.5	2.1	-4.5	-1.4	11.9	26.4	29.5
300	17.3	16.4	9.5	0.6	-4.9	-2.8	8.5	21.9	26.5
400	14.0	12.6	6.5	-1.3	-5.2	-3.9	4.4	15.5	21.0
500	11.4	9.1	3.6	-2.7	-5.2	-4.2	1.7	10.1	16.1
700	6.4	4.0	0.1	-3.7	-4.3	-4.1	-1.4	3.9	9.1
850	3.6	1.0	-2.1	-3.5	-2.8	-3.7	-4.0	-1.5	4.4
1000	2.0	-0.4	-2.1	-1.8	-0.9	-1.6	-2.8	-2.8	0.7

Table 4.4

Mean Zonal Wind Component ($m.sec^{-1}$)

(Values obtained for odd years or even years only shown in parentheses)

Lat.	40N	30N	20N	10N	0	10 S	20 S	30 S
				(a) December-February				
p(mb)								
10	13.2	8.1	-1.7	-10.7	-----	-----	-----	-----
20	6.5	4.7	-2.5	- 8.4	-----	-----	-20.6	(-8.6)
30	6.8	3.9	-3.0	- 6.2	-6.9	-12.4	-16.6	(-8.6)
50	8.9	7.3	0.2	- 1.3	-1.9	-9.9	-10.6	-6.0
70	13.6	13.7	4.6	- 0.7	1.2	-7.4	-3.3	-3.9
100	19.1	27.3	15.7	0.2	0.3	-4.5	5.3	7.5
				(b) March-May				
p(mb)								
10	15.3	5.3	-7.3	-17.4	-----	-----	-----	-----
20	3.3	-0.5	-6.8	-12.5	-0.4	(-20.4)	-18.5	-----
30	0.8	-1.8	-7.3	-10.3	-9.1	-11.6	-11.6	-----
50	3.2	2.0	-3.8	-4.6	-2.3	-8.5	-6.4	-1.4
70	8.1	9.4	0.9	-1.6	0.1	-3.3	1.4	0.7
100	14.3	20.6	12.2	0.2	-0.5	-0.4	11.5	12.0
				(c) June-August				
p(mb)								
10	-14.8	-17.3	-24.7	-24.4	-----	-----	-----	-----
20	-10.3	-15.6	-21.2	-19.7	-7.1	(-23.0)	2.0	-----
30	-8.7	-14.5	-20.3	-17.0	-8.1	-7.3	1.9	-----
50	-4.5	-10.3	-16.8	-12.2	-0.1	-1.3	2.0	6.2
70	0.1	-6.2	-12.7	-9.1	-0.8	-0.4	5.1	(9.6)
100	9.8	-1.3	-10.0	-12.3	-4.9	-0.3	14.4	17.3
				(d) September-November				
p(mb)								
10	(9.8)	7.0	-8.5	-16.0	-----	-----	-----	-----
20	3.7	1.3	-11.2	-14.6	(-27.4)	-----	-6.2	-----
30	2.8	-1.1	-10.7	-12.5	-9.9	-10.5	-6.3	-2.7
50	3.8	0.0	-8.5	-5.5	0.7	-3.3	-3.9	0.1
70	6.0	3.0	-5.4	-2.4	2.3	-0.4	1.2	2.4
100	14.9	11.6	-0.2	-4.5	-1.5	-0.3	11.9	11.6

Table 4.5

Mean Meridional Wind and Vertical Averages in m sec^{-1}

(a) December-February

Lat. p(mb)	41N	33N	24N	15N	5N	5S	15S	24S	33S
100	-2.06	-0.61	0.78	0.86	0.29	-0.01	0.49	1.18	0.55
150	-2.75	-1.23	0.92	2.02	2.18	0.86	0.09	0.57	1.00
200	-3.13	-1.20	0.89	2.49	3.18	1.46	-0.08	-0.01	-0.07
300	-2.17	-0.45	0.34	0.09	0.72	0.32	0.15	0.63	-0.30
400	-1.97	-0.28	0.43	-0.18	-0.52	-0.52	-0.01	0.77	0.02
500	-1.53	-0.18	0.48	0.06	-0.13	-0.35	-0.17	0.48	0.08
700	-0.97	-0.04	0.31	-0.04	-0.45	-0.51	-0.21	-0.29	-0.59
850	-0.27	0.26	0.10	-0.91	-1.38	-0.58	-0.11	-0.18	-0.25
1000	0.35	-0.06	-1.27	-2.12	-1.03	0.17	0.62	0.77	0.66
Ave.	-1.39	-0.27	0.28	0.01	-0.01	-0.09	-0.01	0.28	-0.05

(b) March-May

Lat. p(mb)	41N	33N	24N	15N	5N	5S	15S	24S	33S
100	-0.94	-0.67	-0.18	0.02	-0.06	-0.08	0.11	0.48	1.16
150	-1.32	-1.13	-0.30	0.73	0.79	-0.34	-0.92	-0.02	1.71
200	-1.47	-1.11	-0.30	1.01	1.17	-0.32	-1.22	-0.25	1.67
300	-1.72	-0.87	-0.41	-0.32	0.34	0.34	0.29	0.00	0.26
400	-1.14	-0.38	-0.28	-0.38	-0.04	0.16	0.26	0.06	-0.09
500	-1.05	-0.36	-0.19	-0.15	-0.02	0.03	0.04	-0.10	-0.02
700	-0.63	-0.02	0.11	-0.16	-0.40	0.00	0.20	-0.65	-1.00
850	-0.18	0.18	0.26	-0.26	-0.11	0.85	0.97	-0.13	-0.74
1000	-0.52	-0.40	-0.77	-1.55	-0.94	0.71	1.91	1.31	-0.21
Ave.	-0.91	-0.38	-0.15	-0.18	0.00	0.21	0.28	-0.06	-0.05

(c) June-August

Lat. p(mb)	41N	33N	24N	15N	5N	5S	15S	24S	33S
100	0.74	-0.34	-0.43	0.16	0.38	-0.08	-0.50	0.80	1.85
150	0.78	0.37	-0.01	-0.56	-1.84	-2.62	-1.81	0.98	2.95
200	-0.05	-0.27	-0.12	-0.40	-2.21	-3.25	-2.08	1.11	3.60
300	-0.38	0.01	-0.01	-0.07	-0.54	-0.85	-0.56	0.35	1.80
400	-0.66	-0.03	0.19	0.06	0.22	0.16	0.04	-0.18	0.11
500	-0.76	0.27	0.44	0.21	-0.10	-0.51	-0.44	-0.21	0.00
700	-0.78	0.36	0.68	0.02	-0.02	0.48	0.25	-0.97	-1.22
850	-0.50	0.22	0.44	0.56	1.06	2.11	1.79	-0.23	-1.41
1000	-0.88	0.13	0.24	0.07	0.63	2.09	2.56	1.00	-0.91
Ave.	-0.49	0.15	0.30	0.08	-0.10	0.04	0.14	0.01	0.18

Table 4.5 (ctd.)

(b) September-November

Lat. / p(mb)	41N	33N	24N	15N	5N	5S	15S	24S	33S
100	-1.04	-0.28	0.42	0.17	0.01	-0.11	0.14	0.37	0.32
150	-0.56	0.09	0.36	0.22	-0.45	-1.27	-0.90	0.44	1.35
200	-1.91	-0.62	0.20	0.22	-0.78	-1.63	-1.03	0.49	1.21
300	-1.18	-0.22	0.12	0.02	-0.13	-0.31	-0.09	0.18	0.08
400	-0.96	-0.15	0.19	0.06	0.24	0.25	0.20	-0.01	-0.18
500	-0.69	-0.07	0.14	0.07	-0.03	-0.10	-0.03	0.01	-0.51
700	-0.34	-0.06	0.02	-0.30	-0.20	0.29	0.31	-0.49	-0.97
850	0.31	-0.28	-0.54	-0.36	0.29	1.06	0.70	0.04	-0.51
1000	-0.10	-1.03	-1.23	-0.76	0.48	1.52	1.46	0.93	0.00
Ave.	-0.60	-0.25	-0.08	-0.13	-0.03	0.13	0.17	0.08	-0.19

Table 5.1

Momentum Fluxes for December-February in Units of $m^2 sec^{-2}$ and Vertical Integrals in Units of 10^{25} gm $cm^2 sec^{-2}$

Lat.	41N	33N	24N	14N	5N	5S	15S	24S	33S
				(a) Transient Eddies $[\overline{u'v'}]$					
p(mb)									
100	10.9	14.6	10.7	0.3	-4.3	-2.7	-1.3	-6.1	-13.1
150	24.1	29.2	17.3	-4.2	-16.3	-13.4	-8.4	-22.0	-37.5
200	21.1	39.9	26.3	1.0	-13.0	-9.2	-6.5	-25.5	-57.9
300	41.3	43.5	23.4	8.3	1.1	-1.1	-3.7	-16.5	-45.3
400	21.8	25.8	16.7	3.7	0.1	-0.2	-1.2	-8.5	-20.2
500	15.6	19.8	13.8	3.0	-0.2	-1.1	-1.7	-5.1	-10.2
700	7.2	7.9	6.3	2.9	0.2	-2.4	-3.9	-3.6	-4.3
850	0.9	3.5	2.0	1.2	1.0	-1.3	-2.6	-2.1	-2.8
1000	-2.3	0.4	0.7	0.7	0.2	-0.9	-1.0	1.7	2.5
Int.	19.0	31.0	23.0	5.5	-4.1	-6.2	-6.9	-16.0	-29.0
				(b) Standing Eddies $[\overline{u}^*\overline{v}^*]$					
p(mb)									
100	5.5	8.3	7.6	2.7	-2.5	-0.3	2.5	1.1	-0.1
150	7.2	13.8	13.2	-9.0	-18.8	-6.8	3.7	0.6	-0.1
200	9.6	19.2	14.3	-2.2	-8.0	-2.4	2.1	-0.1	-0.6
300	12.3	13.5	10.3	3.0	-1.0	-0.1	0.2	-0.1	0.1
400	8.8	9.0	5.1	3.2	-0.0	-0.1	-0.3	-0.2	-0.1
500	6.2	6.5	1.8	1.3	0.2	-0.1	-0.3	-0.4	-0.2
700	0.8	2.5	-0.1	0.1	-0.1	0.2	-0.4	-0.2	0.1
850	0.2	1.4	-0.5	-0.5	-1.7	-0.3	0.0	0.1	0.1
1000	0.9	0.3	0.2	0.3	0.8	-0.5	-0.7	0.0	0.6
Int.	6.6	11.0	7.9	0.6	-4.9	-1.6	0.6	-0.1	0.0
				(c) Mean Motion $[\overline{u}][\overline{v}]$					
p(mb)									
100	-12.6	-9.2	11.0	6.0	-0.8	-0.3	-0.2	4.7	5.6
150	-34.1	-35.2	20.1	27.5	0.6	-3.2	0.3	4.4	23.2
200	-41.0	-36.1	20.7	37.1	-3.0	-7.1	-0.3	-5.0	-0.4
300	-15.5	-5.9	1.6	0.9	-1.7	-1.6	0.5	4.4	-4.6
400	-9.2	-0.4	3.2	-1.0	2.3	1.7	-0.0	3.8	0.9
500	-1.8	1.6	3.2	0.1	0.7	1.0	-0.2	0.9	1.1
700	3.6	2.3	0.2	0.1	2.0	1.0	-0.0	-0.3	-2.1
850	5.7	2.7	-0.2	4.2	6.4	0.9	0.1	0.9	0.0
1000	5.2	0.4	1.9	6.4	2.5	-0.4	-0.7	-1.0	-0.6
Int.	-8.9	-7.8	8.5	13.0	3.8	-0.7	-0.1	2.0	1.2

Table 5.2

Momentum Fluxes for March-May in Units of $m^2 sec^{-2}$ and Vertical Integrals in Units of 10^{25} gm $cm^2 sec^{-2}$

Lat.	41N	33N	24N	15N	5N	5S	15S	24S	33S
				(a) Transient Eddies $[\overline{u'v'}]$					
p(mb)									
100	3.0	11.8	12.1	1.9	-2.4	-2.5	-2.9	-6.8	-13.2
150	12.1	34.2	34.3	9.5	-4.6	-2.8	-6.3	-25.6	-37.2
200	13.6	37.0	36.8	14.2	-5.0	-5.1	-7.5	-30.9	-52.3
300	14.3	32.0	26.9	11.6	1.9	-1.6	-8.5	-33.0	-56.1
400	10.7	22.0	16.3	5.7	1.5	-1.5	-5.4	-19.5	-34.2
500	5.1	11.6	10.6	3.6	1.2	-0.8	-3.9	-10.7	-17.0
700	4.7	5.3	4.2	3.1	1.8	-1.6	-4.0	-4.4	-6.5
850	-0.1	3.3	1.9	2.2	1.0	-1.0	-2.4	-4.3	-8.0
1000	-2.4	-0.6	1.0	0.6	-0.6	-0.9	-0.5	0.6	-2.3
Int.	8.3	24.0	26.0	12.0	0.7	-3.9	-9.8	-2.6	-37.0
				(b) Standing Eddies $[\bar{u}^*\bar{v}^*]$					
p(mb)									
100	-1.8	-0.2	1.8	0.0	-0.6	0.4	1.5	-0.3	-0.2
150	1.3	4.6	0.2	-3.9	-3.4	0.6	0.0	-1.8	-0.5
200	2.4	5.4	-0.1	-1.1	-1.2	0.2	-1.8	-1.3	-0.0
300	3.1	5.5	1.2	-0.4	-0.3	0.3	-0.1	0.4	0.5
400	1.9	3.8	0.8	-0.2	0.2	0.2	-0.0	0.1	0.4
500	1.1	2.5	0.6	0.1	0.1	0.1	-0.1	-0.2	-0.0
700	0.6	1.8	0.0	-0.1	0.5	0.3	-0.1	-0.3	0.5
850	1.1	1.8	-0.5	-0.9	-0.5	0.1	-0.0	-0.1	0.1
1000	0.8	0.4	-0.1	0.6	1.0	0.0	-0.9	-0.0	0.1
Int.	1.8	4.6	0.6	-1.1	-0.5	0.5	-0.4	-0.5	0.3
				(c) Mean Motion $[\bar{u}][\bar{v}]$					
p(mb)									
100	-0.4	-5.7	-0.4	1.0	0.1	0.5	-0.8	6.0	16.9
150	-7.4	-21.5	-3.8	11.0	0.1	0.4	-11.6	0.8	42.6
200	-10.6	-21.9	-4.0	15.1	-1.1	1.2	-15.1	-4.7	45.6
300	-13.4	-11.5	-5.5	-1.2	-0.8	-0.4	0.1	1.1	6.8
400	-3.2	-0.0	-2.0	-0.8	0.2	0.2	-0.1	1.5	-0.6
500	-1.5	0.3	-0.4	0.0	0.1	0.7	-0.4	-0.3	0.4
700	1.8	2.7	1.2	-0.1	2.0	0.8	0.1	-1.3	-5.6
850	2.6	2.0	0.2	0.3	0.4	-2.0	-1.8	0.1	-1.3
1000	1.0	-0.0	1.0	3.5	1.9	-0.8	-2.9	-3.4	0.1
Int.	-3.4	-5.8	-2.1	4.4	1.1	-0.1	-5.5	-0.9	10.0

Table 5.3

Momentum Fluxes for June-August in Units of $m^2\ sec^{-2}$ and Vertical Integrals in Units of $10^{25}\ gm\ cm^2\ sec^{-2}$

Lat.	41N	33N	24N	15N	5N	5S	15S	24S	33S
				(a) Transient Eddies $[\overline{u'v'}]$					
p(mb)									
100	5.6	2.9	-1.2	-1.5	1.6	2.2	-0.8	-5.0	-10.7
150	20.6	12.9	7.4	4.5	8.4	9.5	-2.2	-19.9	-25.5
200	30.4	23.8	14.2	5.4	6.9	11.1	-3.1	-37.0	-49.1
300	25.5	19.2	8.9	2.4	1.9	3.4	-8.5	-42.1	-58.7
400	9.1	8.6	5.9	1.5	-0.6	-1.5	-8.2	-28.7	-44.4
500	6.0	5.7	4.4	1.7	0.1	-1.4	-6.1	-16.9	-28.8
700	2.1	2.6	2.1	1.4	0.5	-2.1	-4.4	-9.0	-14.2
850	-0.6	1.4	1.3	1.4	0.3	-1.9	-3.0	-3.9	-5.2
1000	2.4	1.5	1.0	0.9	0.3	-0.6	0.1	3.3	1.2
Int.	12.0	13.0	9.1	4.3	3.3	1.7	-10.0	-33.0	-42.0
				(b) Standing Eddies $[\overline{u}^*\overline{v}^*]$					
p(mb)									
100	1.7	9.8	5.3	2.9	2.1	0.4	1.2	1.4	0.2
150	0.7	10.5	4.7	1.6	14.3	22.2	16.2	5.2	1.3
200	0.2	11.1	6.4	2.7	8.8	11.7	11.1	4.6	1.1
300	-0.2	2.5	3.1	1.0	1.0	1.1	1.4	2.1	2.0
400	-0.7	0.0	0.2	0.4	-0.3	0.3	-0.5	1.2	2.7
500	-0.6	-0.1	-0.1	0.4	-0.5	-0.0	-0.5	0.8	1.9
700	-0.3	0.5	0.0	-0.0	-0.9	-0.0	-0.4	0.5	2.0
850	0.5	1.3	-1.8	-0.3	0.1	-0.8	-1.3	-0.0	0.7
1000	0.2	0.4	1.2	3.3	1.2	-0.4	-0.9	0.0	0.3
Int.	-0.1	3.9	2.5	1.8	3.5	5.1	3.3	2.6	2.5
				(c) Mean Motion $[\overline{u}][\overline{v}]$					
p(mb)									
100	15.6	-1.1	6.8	-1.1	-4.4	0.3	-3.0	10.8	36.3
150	20.8	1.8	0.6	5.2	17.1	9.0	-19.2	24.9	91.8
200	9.7	-4.6	0.1	2.9	19.9	14.6	-23.6	33.7	131.1
300	1.9	-1.2	0.2	0.7	3.3	4.1	-6.0	9.3	55.4
400	-2.2	-1.2	0.1	0.1	-1.9	-0.6	-0.5	-3.8	-1.9
500	-2.6	0.6	-0.2	-0.6	-0.0	2.5	-1.6	-2.9	-3.5
700	-1.4	0.5	-0.5	0.2	-0.3	-1.5	-0.1	-4.5	-14.6
850	-0.0	0.0	-0.2	-0.8	-1.5	-8.1	-7.7	0.3	-10.0
1000	-0.8	-0.0	0.1	0.0	-0.6	-3.9	-7.0	-2.6	-1.7
Int.	2.1	-0.6	0.2	0.9	5.3	1.3	-13.0	7.0	29.0

Table 5.4

Momentum Fluxes for September-November in Units of $m^2\ sec^{-2}$ and Vertical Integrals in Units of 10^{25} gm $cm^2\ sec^{-2}$

Lat.	41N	33N	24N	15N	5N	5S	15S	24S	33S
				(a) Transient Eddies $[\overline{u'v'}]$					
p(mb)									
100	6.0	9.3	8.0	3.1	-0.0	-1.0	-1.6	-2.8	-8.2
150	24.1	22.0	16.7	9.8	8.3	5.2	-6.6	-21.5	-27.5
200	38.8	32.5	17.1	8.2	7.7	5.3	-10.1	-31.6	-49.1
300	34.1	28.2	15.5	6.2	3.5	1.0	-9.1	-28.6	-60.4
400	18.2	16.4	10.5	3.6	0.3	-0.8	-5.6	-18.9	-35.0
500	10.5	8.8	6.5	3.2	0.9	-1.4	-4.7	-11.2	-24.4
700	2.8	2.6	2.9	2.7	2.0	-0.4	-3.7	-7.2	-7.8
850	-0.4	1.8	1.7	2.7	1.9	-1.2	-3.0	-3.7	-2.9
1000	0.1	1.7	1.9	1.7	0.1	-1.1	-1.1	2.3	2.3
Int.	17.0	19.0	15.0	8.9	5.5	0.3	-11.0	-25.0	-37.0
				(b) Standing Eddies $[\overline{u}^*\overline{v}^*]$					
p(mb)									
100	5.4	5.8	6.6	0.9	0.4	0.9	1.6	0.8	-0.7
150	5.2	11.0	12.0	-0.4	1.0	8.7	9.2	3.5	0.6
200	7.9	12.7	9.9	0.3	0.0	5.9	7.3	3.0	1.1
300	7.3	6.9	4.6	0.8	-0.2	0.6	0.5	1.3	1.0
400	3.7	2.6	1.2	0.1	0.2	0.3	-0.8	0.1	0.5
500	1.7	1.7	-0.0	-0.1	0.1	-0.1	-1.0	-0.4	0.4
700	0.0	0.9	-0.3	-0.7	0.2	0.5	-0.6	0.1	1.2
850	0.2	0.4	-1.5	-1.3	-1.8	-0.7	-0.6	0.0	-0.1
1000	-0.1	-0.3	-0.4	-0.1	0.1	-0.8	-1.5	-0.3	0.1
Int.	3.5	5.5	3.8	-0.6	-0.4	2.3	1.4	1.1	0.9
				(c) Mean Motion $[\overline{u}][\overline{v}]$					
p(mb)									
100	-6.8	-0.3	2.0	-1.0	-0.2	0.5	-0.1	3.0	7.5
150	0.6	6.2	4.9	0.4	1.5	-0.4	-12.1	8.0	38.3
200	-27.8	-7.5	3.5	0.7	3.3	2.4	-14.4	10.7	41.1
300	-10.1	0.5	1.9	0.1	0.5	1.2	-2.2	2.1	7.0
400	-5.1	1.3	1.8	-0.2	-1.4	-0.5	0.1	-1.5	0.1
500	-1.1	1.7	0.8	-0.5	-0.0	1.0	-0.4	-0.8	-5.3
700	1.6	0.8	0.0	0.6	0.7	-0.7	-0.2	-2.3	-7.2
850	3.3	-0.0	1.0	0.8	-0.9	-3.4	-2.1	0.1	-1.4
1000	1.0	0.3	2.4	1.1	-0.5	-2.3	-3.6	-2.4	0.1
Int.	-4.5	0.6	3.0	0.7	0.5	-1.1	-6.3	1.4	6.7

Table 5.5

Momentum Flux by Transient Eddies, $[\overline{u'v'}]$, for Stratospheric Levels. Values for Odd Years or Even Years Only Shown in Parentheses

(a) December-February

Lat. p(mb)	40N	30N	20N	10N	00	10S	20S	30S
10	21.7	24.0	10.0	1.0	----	----	----	----
20	10.1	10.0	3.2	1.0	----	----	1.9	(-4.6)
30	6.4	6.3	1.8	0.2	-3.7	2.6	0.8	(-1.2)
50	6.0	4.8	2.8	-0.1	0.1	0.6	-0.3	2.3
70	9.8	8.5	1.3	-0.3	-1.2	-0.2	-1.4	1.3
100	10.6	14.1	1.1	-2.0	-2.4	1.1	-4.8	-3.3

(b) March-May

Lat. p(mb)	40N	30N	20N	10N	00	10S	20S	30S
10	11.6	7.3	-0.2	0.5	----	----	----	----
20	8.4	2.7	0.8	1.1	-2.3	(-0.4)	0.1	----
30	4.7	2.1	1.0	-0.4	-2.3	2.9	0.9	----
50	2.2	2.2	0.7	0.2	-1.1	-0.0	-0.4	1.6
70	1.3	3.1	1.1	-0.6	-1.5	0.5	-1.9	-3.3
100	2.2	8.5	5.4	-0.5	-0.4	0.0	-5.8	-3.8

(c) June-August

Lat. p(mb)	40N	30N	20N	10N	00	10S	20S	30S
10	(3.0)	-0.4	-1.4	9.7	----	----	----	----
20	-0.3	-0.8	-0.6	0.1	-1.7	0.3	-6.6	----
30	0.0	-0.3	0.4	-0.3	-1.0	-3.9	-2.0	----
50	0.3	0.4	-0.4	0.1	-4.0	-0.0	-2.4	3.5
70	1.8	0.2	0.0	-1.5	-3.6	-0.2	-1.7	(-2.6)
100	3.0	2.4	0.3	1.8	2.7	0.4	-4.8	-5.2

(d) September-November

Lat. p(mb)	40N	30N	20N	10N	00	10S	20S	30S
10	(13.2)	-0.3	-0.6	3.5	----	----	----	----
20	4.3	2.1	1.7	0.1	(-4.2)	----	----	----
30	4.0	1.3	1.2	0.0	-0.4	1.1	-1.1	-12.9
50	2.3	1.8	0.0	-0.5	-2.5	0.5	-1.0	-10.0
70	2.2	3.3	-0.2	0.2	-1.6	-2.0	-2.8	-3.4
100	4.7	6.3	3.6	1.0	-0.4	0.5	-6.5	-3.2

Table 6.1

Transient Eddy Flux of Sensible Heat [$\overline{v'T'}$] in Units of m sec^{-1} ^{o}K

(a) December-February

Lat. / p(mb)	41N	33N	24N	15N	5N	5S	15S	24S	33S
100	3.79	1.98	-0.32	-1.35	-1.46	-1.45	-0.66	-0.29	-1.28
150	9.53	3.71	0.22	-1.01	-0.85	-0.13	0.34	-0.03	-3.27
200	9.99	4.33	0.11	-0.67	0.03	0.64	-0.31	-2.34	-4.19
300	5.58	6.87	1.11	-0.67	-0.31	0.36	-0.50	-1.96	-2.97
400	4.45	5.72	0.37	-1.15	-0.55	0.27	-0.01	-0.85	-0.96
500	5.72	4.42	-0.25	-1.28	-0.57	0.24	0.50	0.44	0.41
700	10.95	7.00	2.15	0.03	-0.36	-0.11	0.29	0.23	-1.98
850	12.02	10.92	6.59	1.22	-0.60	0.02	0.65	-2.77	-7.71
1000	8.29	7.31	4.98	1.66	-0.47	-1.03	-0.85	-1.55	-2.67

(b) March-May

Lat. / p(mb)	41N	33N	24N	15N	5N	5S	15S	24S	33S
100	6.52	3.44	-0.12	-0.87	-0.43	0.02	-0.27	-0.44	-1.51
150	1.34	8.69	1.03	-1.49	-0.77	0.34	0.49	-1.12	-4.47
200	1.45	6.98	-0.82	-1.83	-0.57	0.51	0.03	-2.03	-6.22
300	6.95	4.44	0.38	-0.98	-0.51	0.23	-0.01	-1.22	-3.41
400	8.42	4.58	0.44	-0.81	-0.35	0.37	0.60	-0.03	-1.80
500	7.55	3.61	-0.27	-1.19	-0.49	0.39	1.13	0.40	-1.78
700	10.59	6.22	1.21	-0.75	-0.60	0.12	0.72	-0.55	-4.67
850	11.66	9.06	4.69	0.44	-0.63	-0.16	-0.77	-5.03	-9.02
1000	7.33	6.72	2.83	0.75	-0.12	-0.80	-1.22	-0.97	-2.17

(c) June-August

Lat. / p(mb)	41N	33N	24N	15N	5N	5S	15S	24S	33S
100	1.46	0.43	0.74	1.39	1.17	0.32	0.08	-0.24	-3.49
150	3.28	2.55	1.39	-0.28	-0.09	1.12	1.84	-0.71	-8.98
200	8.48	3.01	-0.17	-0.32	0.44	0.85	0.65	-0.69	-10.25
300	3.65	1.03	-0.21	-0.22	0.22	0.26	0.12	-0.78	-5.55
400	1.63	0.07	-0.57	-0.07	0.20	0.40	0.54	-0.40	-3.40
500	0.13	-0.34	-0.49	-0.02	0.26	0.58	1.15	0.26	-3.65
700	1.77	0.63	-0.39	-0.51	-0.20	0.29	1.15	-0.33	-7.02
850	3.48	1.55	-0.11	-0.99	-0.43	0.27	-1.10	-6.05	-10.40
1000	2.11	1.43	0.14	-0.01	0.06	-0.23	-1.60	-3.77	-5.27

Table 6.1 (ctd.)

(d) September-November

Lat. / p(mb)	41N	33N	24N	15N	5N	5 S	15 S	24 S	33 S
100	4.95	2.30	0.20	0.67	0.44	-0.06	-0.27	0.32	-0.99
150	6.84	3.41	0.63	-0.18	0.19	0.16	-0.09	-0.44	-4.86
200	8.98	4.92	1.25	-0.64	-0.19	0.18	0.20	-0.47	-7.95
300	6.10	5.08	1.20	0.04	-0.03	0.14	-0.45	-1.19	-1.02
400	4.11	2.99	0.20	-0.40	-0.32	0.15	0.37	-0.33	-1.47
500	2.84	1.14	-0.75	-0.43	-0.14	0.15	0.63	0.81	-1.01
700	5.93	2.42	0.18	-0.30	-0.16	0.11	0.45	-0.96	-5.40
850	9.40	5.34	1.94	0.09	-0.39	-0.35	-1.04	-5.43	-8.65
1000	6.12	4.53	1.75	0.64	0.11	-0.56	-1.49	-2.67	-3.62

Table 6.2

Standing Eddy Flux of Sensible Heat [$\overline{v}^*\overline{T}^*$] in units of m sec^{-1} ^oK

(a) December-February

Lat. p(mb)	41N	33N	24N	15N	5N	5S	15S	24S	33S
100	2.85	1.13	1.90	2.90	0.62	-0.28	1.39	0.85	0.33
150	1.22	1.82	0.72	0.05	-0.55	0.19	1.61	-0.22	-0.13
200	3.40	3.03	0.20	-0.53	-0.05	0.81	0.96	-0.36	-0.10
300	1.75	2.02	0.46	-0.56	-0.27	0.29	0.05	-0.07	0.16
400	1.72	1.68	0.23	-0.39	-0.36	-0.10	-0.14	0.00	0.07
500	2.14	1.76	0.17	-0.14	-0.15	-0.06	-0.08	-0.08	0.07
700	4.84	2.21	0.63	-0.02	-0.04	-0.08	0.04	-0.14	-0.30
850	6.58	2.76	0.30	-0.54	-0.33	-0.24	-0.01	0.40	0.32
1000	3.01	1.82	0.03	0.43	-0.35	-1.20	-0.96	-0.14	-0.36

(b) March-May

Lat. p(mb)	41N	33N	24N	15N	5N	5S	15S	24S	33S
100	1.10	0.36	1.89	2.15	0.64	-0.51	0.47	0.46	0.05
150	0.56	1.64	2.60	2.13	0.05	0.02	1.19	0.10	-0.13
200	1.62	1.69	2.40	1.31	-0.01	0.38	1.21	0.37	-0.10
300	0.52	0.58	0.70	0.29	0.10	0.21	0.08	-0.32	-0.32
400	0.32	0.18	0.09	0.00	-0.03	0.01	-0.13	-0.24	-0.31
500	0.39	0.16	0.12	0.05	0.05	0.00	-0.10	-0.21	-0.18
700	0.96	0.23	-0.12	-0.54	-0.17	-0.06	-0.26	-0.78	-0.79
850	0.10	0.37	-2.03	-1.65	0.57	-0.05	-0.24	0.06	-0.28
1000	-0.30	0.74	0.66	0.47	-0.27	-0.74	-1.16	-0.82	-0.23

(c) June-August

Lat. p(mb)	41N	33N	24N	15N	5N	5S	15S	24S	33S
100	0.38	0.33	-0.20	1.50	0.23	-0.38	-0.36	-0.37	-0.18
150	2.32	5.03	4.46	2.17	1.14	0.00	-0.18	-1.09	-0.66
200	-0.79	0.41	1.32	0.12	-0.06	0.05	-0.08	-1.25	-0.99
300	-1.19	-2.16	-1.24	-0.52	0.11	0.31	-0.10	-0.02	0.09
400	-0.52	-1.04	-0.49	-0.27	0.04	-0.08	-0.16	0.13	-0.27
500	0.03	-0.07	0.10	0.24	0.10	-0.05	0.03	-0.15	-0.47
700	0.76	0.35	-0.41	-0.65	-0.24	-0.29	-0.55	-1.42	-1.09
850	1.01	1.20	-1.03	0.30	0.28	-1.08	-1.46	-1.02	-0.73
1000	0.59	2.43	1.77	0.23	-0.37	-0.99	-0.81	-0.35	0.02

Table 6.2 (ctd.)

(d) September-November

Lat. p(mb)	41N	33N	24N	15N	5N	5S	15S	24S	33S
100	1.47	1.01	1.34	1.44	0.60	-0.19	0.02	-0.08	0.31
150	2.15	3.36	3.99	2.07	0.68	0.45	0.62	-0.27	0.19
200	3.10	1.97	2.20	0.98	0.32	0.34	0.27	-0.03	0.27
300	1.74	0.63	0.24	0.05	0.14	0.40	0.11	0.02	-0.45
400	0.66	0.46	0.24	0.01	0.02	-0.03	-0.16	-0.12	-0.50
500	0.00	0.20	0.25	0.10	0.01	-0.10	-0.19	-0.26	-0.37
700	0.41	0.10	0.14	-0.14	-0.04	-0.24	-0.45	-0.79	-0.60
850	0.50	0.32	-0.73	-0.89	-0.17	-0.42	-0.59	0.17	-0.05
1000	0.08	0.92	0.28	-0.02	-0.23	-1.26	-1.27	-0.36	-0.23

Table 6.3

Sensible Heat Flux by Transient Eddies, $[\overline{v'T'}]$, for Stratospheric Levels. Values for Odd Years or Even Years Only Shown in Parentheses.

(a) December-February

Lat. p(mb)	40N	30N	20N	10N	00	10S	20S	30S
10	5.6	0.7	-2.3	-0.3	----	----	----	----
20	3.2	1.3	-0.2	0.3	----	----	----	----
30	3.4	1.1	0.3	0.7	(-0.4)	(0.0)	----	----
50	2.8	1.4	0.5	0.2	0.0	-0.6	-1.2	----
70	2.2	0.9	-0.3	0.7	-0.3	-0.7	-0.4	-1.0
100	3.6	1.1	-0.9	-1.0	-1.1	-1.2	-0.1	-1.1

(b) March-May

Lat. p(mb)	40N	30N	20N	10N	00	10S	20S	30S
10	1.7	-0.1	0.4	1.0	----	----	----	----
20	1.1	0.4	0.4	0.6	----	----	----	----
30	1.4	0.5	0.3	0.5	(-0.8)	----	0.1	----
50	1.4	0.7	0.5	0.5	-0.4	-0.5	-0.1	----
70	2.4	1.2	0.1	0.6	0.5	-0.6	-1.0	-1.5
100	3.8	2.3	-0.9	-0.1	-0.4	-0.1	1.0	-1.7

(c) June-August

Lat. p(mb)	40N	30N	20N	10N	00	10S	20S	30S
10	(-0.0)	1.1	2.2	2.1	----	----	----	----
20	0.6	0.4	0.3	0.5	(0.2)	----	----	----
30	0.5	0.4	0.4	0.3	(0.2)	0.3	(0.2)	----
50	0.5	0.1	0.4	0.8	-0.3	-0.9	0.1	----
70	0.5	0.3	0.3	1.8	-0.2	-0.4	0.2	----
100	0.9	0.6	1.2	0.6	1.2	-0.3	-0.4	-2.1

(d) September-November

Lat. p(mb)	40N	30N	20N	10N	00	10S	20S	30S
10	0.0	0.3	0.5	1.0	----	----	----	----
20	0.4	0.4	0.4	0.4	----	----	----	----
30	0.9	0.7	0.8	0.1	-0.3	(-0.2)	(-1.2)	----
50	1.9	1.1	0.6	0.9	-0.7	-0.4	-0.4	-1.6
70	3.0	1.7	0.6	0.8	-0.5	-0.4	-0.9	-0.5
100	2.7	1.6	0.3	0.6	-0.8	-0.5	-0.2	-1.3

Table 6.4

Transient Eddy Flux of Geopotential, $[\overline{v'z'}]$, in Units of $m^2 \cdot sec^{-1}$

(a) December-February

Lat. p(mb)	41N	33N	24N	15N	5N	5S	15S	24S	33S
100	- 70	-29	- 3	6	2	- 7	- 7	3	18
150	-182	-73	-25	5	10	8	2	17	42
200	-185	-72	-53	- 6	2	6	10	14	119
300	-104	-25	-16	-15	- 7	6	8	4	92
400	- 59	-15	-17	- 9	- 9	- 2	6	10	26
500	- 38	-14	- 4	- 3	- 3	- 1	3	8	14
700	- 9	- 8	- 9	- 3	- 3	1	7	12	- 6
850	- 7	-19	-13	- 8	- 6	- 2	3	12	3
1000	-20	-42	-37	-12	2	3	1	11	14

(b) March-May

Lat. p(mb)	41N	33N	24N	15N	5N	5S	15S	24S	33S
100	1	-52	-48	-26	0	16	5	- 0	67
150	-60	-82	-55	-41	-20	3	15	12	57
200	-56	-97	-85	-49	-18	19	20	-39	- 1
300	-12	-43	-32	-13	- 4	- 4	6	67	83
400	-12	-13	- 2	1	- 0	- 3	6	47	67
500	5	4	5	-00	- 5	- 4	6	19	23
700	11	0	- 1	- 6	- 5	1	8	9	1
850	- 3	- 9	- 5	- 1	2	3	5	17	37
1000	-21	-21	-27	-12	3	5	5	15	15

(c) June-August

Lat. p(mb)	41N	33N	24N	15N	5N	5S	15S	24S	33S
100	-36	7	13	-11	-16	- 1	0	-37	44
150	- 3	6	-19	-20	1	7	2	23	164
200	-69	-41	-16	- 9	13	13	13	65	232
300	-29	-34	-14	3	8	- 8	- 2	88	180
400	-32	-22	- 8	2	4	- 2	4	48	110
500	-12	- 9	- 4	- 0	- 0	- 3	5	34	40
700	- 7	1	2	- 3	- 3	- 0	9	18	23
850	- 1	- 0	5	0	- 1	- 1	6	22	17
1000	-11	- 6	- 5	- 1	- 0	0	14	38	37

Table 6.4 (ctd.)

(d) September-November

Lat. p(mb)	41N	33N	24N	15N	5N	5S	15S	24S	33S
100	- 1	22	18	8	- 5	- 8	- 6	11	32
150	-54	-19	-12	- 1	9	11	10	43	132
200	-26	6	-14	- 2	11	9	9	70	168
300	-70	2	1	- 0	- 7	- 3	7	66	285
400	-50	-18	- 5	2	- 3	- 5	6	39	102
500	-23	3	4	- 0	- 3	- 0	7	17	61
700	- 2	0	- 2	- 6	- 3	1	6	7	4
850	5	- 2	- 4	- 5	1	1	2	25	29
1000	-24	-25	-21	-12	- 1	5	12	23	25

Table 6.5

Standing Eddy Flux of Geopotential, $[\bar{v}^*\bar{z}^*]$,

(a) December-February

Lat. p(mb)	41N	33N	24N	15N	5N	5S	15S	24S	33S
100	-37	-22	7	31	- 2	13	35	20	7
150	-51	-73	10	20	15	41	40	- 5	4
200	-118	-117	-51	-10	0	25	18	- 7	0
300	-42	-26	-23	-14	- 8	4	2	0	2
400	5	4	- 4	-12	- 4	- 1	1	3	2
500	22	10	9	- 1	- 1	0	2	2	0
700	44	11	9	1	0	- 1	2	2	- 1
850	26	0	9	2	1	2	3	- 1	- 0
1000	- 1	- 0	- 0	- 2	4	15	12	2	2

(b) March-May

Lat. p(mb)	41N	33N	24N	15N	5N	5S	15S	24S	33S
100	9	- 9	5	44	17	5	16	-15	- 9
150	6	- 3	15	41	4	13	36	3	- 7
200	3	- 6	5	19	6	13	22	- 2	- 4
300	16	8	1	1	- 1	2	1	- 5	- 5
400	- 1	3	- 2	- 3	- 1	1	- 0	- 1	- 4
500	10	- 1	2	- 1	- 1	0	- 1	- 1	- 3
700	10	0	5	1	0	1	2	1	- 3
850	4	- 2	5	3	3	6	6	- 1	0
1000	0	1	-12	- 4	1	8	9	- 1	- 0

(c) June-August

Lat. p(mb)	41N	33N	24N	15N	5N	5S	15S	24S	33S
100	-50	-77	-27	13	24	- 0	-10	-21	- 4
150	0	16	44	10	22	15	- 5	-35	-11
200	-35	-59	-12	3	19	23	5	-27	3
300	- 0	-14	- 9	2	4	9	2	- 5	1
400	10	21	2	4	4	3	0	- 3	-14
500	3	9	3	1	1	1	- 1	- 6	-13
700	- 7	3	- 7	- 2	3	4	1	- 4	- 9
850	-20	- 5	- 3	3	6	15	13	- 2	- 3
1000	- 6	-24	-46	-25	1	10	7	- 0	0

Table 6.5 (ctd.)

(d) September-November

Lat. p(mb)	41N	33N	24N	15N	5N	5S	15S	24S	33S
100	48	-17	-17	28	7	7	5	-12	- 9
150	-21	-25	-21	8	- 1	19	10	-19	-13
200	10	-51	-43	- 6	- 0	15	- 1	-18	-18
300	23	- 9	-17	- 5	- 0	5	- 2	-10	-23
400	- 4	12	0	- 1	1	0	- 1	- 5	-14
500	- 5	- 5	2	1	- 0	- 0	1	- 3	- 9
700	4	2	8	4	0	0	4	0	- 5
850	4	1	8	7	5	7	5	- 3	- 1
1000	- 1	1	- 4	- 1	3	9	7	2	1

Table 6.6

Integrals of the Transport of Latent Heat, Lq, Potential Energy, gZ, and Sensible Heat, c_pT, by Mean Motions, Standing and Transient Eddies in 10^{21} erg sec^{-1}

(a) December-February

Lat.	41N	33N	24N	15N	5N	5S	15S	24S	33S
				Mean Motion					
Lq	6.9	3.4	-8.8	-28.6	-37.1	-10.7	1.7	----	----
gZ	-104.2	-50.6	54.9	147.9	171.7	66.7	3.5	29.1	19.6
c_pT	56.7	29.2	-33.1	-96.7	-116.8	-47.2	-3.3	-18.8	-12.6
sum	----	----	13.1	22.5	17.8	8.8	1.8	----	----
				Standing Eddies					
Lq	4.2	3.4	2.9	1.6	0.5	-0.7	-0.2	----	----
gZ	-0.0	-0.4	-0.1	-0.1	-0.0	0.2	0.3	0.0	0.0
c_pT	9.7	6.6	1.3	-0.5	-0.8	-0.3	0.4	-0.0	-0.0
sum	13.8	9.6	4.1	1.0	-0.3	-0.7	0.5	----	----
				Transient Eddies					
Lq	11.4	15.5	13.6	7.0	5.2	-0.1	-7.9	----	----
gZ	-1.5	-0.8	-0.6	-0.2	-0.1	0.0	0.2	0.3	0.9
c_pT	23.3	20.3	7.0	-0.8	-1.8	0.0	0.3	-3.3	-8.8
sum	33.2	35.0	20.0	6.0	3.3	-0.0	-7.4	----	----
Total	47.0	44.6	37.2	29.5	20.8	8.1	-5.1	----	----

(b) March-May

				Mean Motion					
Lq	4.0	4.1	1.3	-14.2	-16.8	13.4	22.2	----	----
gZ	-45.4	-47.8	-14.1	60.7	67.3	-42.5	-92.9	-5.6	98.1
c_pT	28.5	30.2	9.9	-40.2	-45.3	27.6	59.9	1.4	-60.2
sum	----	----	----	6.4	5.2	-1.4	-10.8	----	----
				Standing Eddies					
Lq	0.9	1.9	4.3	3.7	-0.2	-0.3	-0.4	----	----
gZ	0.2	-0.0	0.1	0.2	0.1	0.1	0.2	-0.0	-0.1
c_pT	1.5	1.6	0.7	-0.0	0.3	0.1	-0.1	-0.9	-1.0
sum	2.6	3.5	5.1	3.9	0.1	-0.3	-0.3	----	----
				Transient Eddies					
Lq	12.3	14.1	10.3	4.1	1.6	-2.4	-6.0	----	----
gZ	-0.4	-0.7	-0.6	-0.4	-0.2	0.1	0.3	0.6	1.0
c_pT	27.1	18.7	4.3	-2.4	-1.9	0.5	0.7	-4.5	-13.3
sum	39.0	32.1	14.1	1.4	-0.5	-1.9	-5.1	----	----
Total	41.6	35.7	19.1	11.6	4.9	-3.6	-16.1	----	----

Table 6.6 (ctd.)

(c) June-August

Lat.	41N	33N	24N	15N	5N	5S	15S	24S	33S
				Mean Motion					
Lq	-3.9	2.2	5.0	7.5	28.6	55.1	33.9	----	----
gZ	42.1	-15.7	-33.6	-31.9	-114.0	-220.2	-174.9	52.4	196.3
c_pT	-24.1	10.1	22.2	21.6	77.5	144.3	108.5	-34.9	-113.1
sum	----	----	-6.4	-2.8	-7.9	-20.8	-32.4	----	----
				Standing Eddies					
Lq	1.3	8.1	12.0	3.5	0.4	0.5	-0.6	----	----
gZ	-0.2	-0.2	-0.2	-0.0	0.2	0.3	0.1	-0.3	-0.2
c_pT	0.7	1.3	0.2	0.2	0.2	-1.1	-1.7	-2.2	-1.7
sum	1.8	9.2	12.1	3.8	0.9	-0.3	-2.1	----	----
				Transient Eddies					
Lq	9.6	5.8	2.1	2.6	0.8	-2.7	-7.1	----	----
gZ	-0.5	-0.3	-0.1	-0.1	0.0	-0.0	0.2	1.2	2.4
c_pT	7.4	3.0	-0.6	-1.1	0.2	1.5	1.2	-5.3	-20.4
sum	16.5	8.5	1.4	1.4	1.0	-1.2	-5.7	-4.1	-18.0
Total	18.3	17.7	7.1	2.4	-6.0	-22.4	-40.3	----	----

(d) September-November

				Mean Motion					
Lq	6.3	-2.6	-12.5	-11.0	9.6	30.5	16.5	----	----
gZ	-57.2	8.2	48.5	38.4	-34.8	-117.4	-81.4	13.8	67.5
c_pT	35.3	-4.0	-30.0	-24.7	23.7	77.5	52.5	-10.9	-40.3
sum	----	----	6.0	2.7	-1.6	-9.4	-12.4	----	----
				Standing Eddies					
Lq	0.6	1.8	3.6	2.4	-0.2	0.1	0.1	----	----
gZ	0.1	-0.2	-0.1	0.1	0.1	0.2	0.1	-0.2	-0.3
c_pT	2.4	2.1	1.6	0.3	0.2	-0.5	-1.0	-0.8	-0.8
sum	3.1	3.8	5.0	2.8	0.0	-0.3	-0.8	----	----
				Transient Eddies					
Lq	14.4	14.5	10.3	5.3	-0.2	-1.6	-6.0	----	----
gZ	-0.7	-0.1	-0.1	-0.1	-0.0	0.0	0.2	1.0	2.5
c_pT	17.0	10.8	2.3	-0.5	-0.5	-0.0	-0.4	-4.7	-13.0
sum	30.8	25.2	12.5	4.6	-0.8	-1.6	-6.2	----	----
Total	33.9	29.0	23.5	10.1	-2.3	-11.3	-19.4	----	----

Table 7.1

Zonal Temperature Variance, $[\overline{T}^{*2}]$,

in units of $(^{o}C)^{2}$

(a) December-February

Lat. p(mb)	41N	33N	24N	15N	5N	5S	15S	24S	33S
100	5.5	2.5	7.5	8.7	5.0	2.8	3.0	1.4	0.8
150	5.3	2.0	2.4	1.7	0.8	0.5	1.1	0.8	0.3
200	7.6	6.2	2.4	1.1	0.8	0.7	0.9	0.5	0.3
300	2.4	3.9	4.3	1.6	1.1	1.0	0.8	0.6	0.9
400	5.9	3.3	3.0	1.2	0.7	0.5	0.4	0.4	0.6
500	9.4	4.0	2.1	0.9	0.4	0.2	0.2	0.3	0.5
700	15.6	7.5	2.2	0.7	0.5	0.2	0.3	0.8	0.7
850	23.6	11.0	4.0	2.2	0.8	0.4	0.8	2.7	2.3
1000	23.8	16.3	7.6	3.0	1.7	1.2	2.7	3.1	0.7

(b) March-May

Lat. p(mb)	41N	33N	24N	15N	5N	5S	15S	24S	33S
100	1.8	1.7	5.7	4.8	2.3	1.4	2.3	1.3	0.7
150	1.4	1.5	3.2	2.4	0.8	0.7	1.1	0.8	0.5
200	2.2	3.1	3.6	1.7	0.7	0.6	0.9	0.8	0.4
300	1.2	3.0	3.1	1.1	0.4	0.4	0.7	0.6	0.5
400	0.8	2.3	2.2	0.8	0.3	0.2	0.4	0.3	0.4
500	1.2	1.7	1.3	0.6	0.2	0.1	0.1	0.2	0.5
700	3.5	2.3	1.1	1.2	0.2	0.2	0.5	0.9	0.8
850	7.9	10.5	11.0	8.8	1.7	0.3	0.9	1.7	1.6
1000	5.2	3.2	2.1	1.5	0.8	0.7	2.5	2.9	0.4

(c) June-August

Lat. p(mb)	41N	33N	24N	15N	5N	5S	15S	24S	33S
100	2.3	6.5	6.5	3.1	2.0	1.2	1.6	1.2	0.7
150	5.3	5.4	5.3	2.8	1.6	1.0	1.3	1.4	0.7
200	13.4	14.1	9.1	2.7	0.5	0.6	1.4	1.5	1.3
300	7.7	12.5	7.1	1.6	0.4	0.6	1.5	1.3	0.5
400	3.9	6.7	4.3	0.8	0.3	0.4	0.7	0.5	1.0
500	1.7	3.6	2.2	0.5	0.3	0.2	0.2	0.3	1.6
700	3.9	4.4	3.8	1.6	0.4	0.6	1.3	1.5	1.9
850	11.4	11.9	8.5	3.7	0.5	1.0	2.7	3.6	2.9
1000	3.5	5.9	4.4	2.2	1.5	3.3	6.1	2.2	0.3

Table 7.1 (ctd.)

(d) September-November

Lat. p(mb)	41N	33N	24N	15N	5N	5S	15S	24S	33S
100	1.8	2.8	4.6	4.1	2.7	1.6	2.2	1.4	1.0
150	3.5	2.9	2.7	1.7	1.0	0.7	1.6	1.2	0.6
200	3.8	4.9	3.2	1.1	0.5	0.5	1.1	1.0	0.6
300	1.7	4.0	3.8	0.7	0.4	0.6	0.9	0.3	0.6
400	1.9	2.8	2.7	0.6	0.3	0.3	0.4	0.2	1.1
500	2.0	1.9	1.9	0.4	0.2	0.2	0.2	0.4	1.2
700	2.9	1.4	0.6	0.4	0.3	0.3	0.9	1.7	1.4
850	4.7	4.5	4.5	3.6	0.7	0.8	1.9	3.1	2.3
1000	1.9	3.1	3.0	1.2	1.1	2.3	5.0	3.3	0.5

Table 7.2

Eddy Kinetic Energy, $[\bar{u}^{*2} + \bar{v}^{*2}] / 2$

in Units of $m^2 \cdot sec^{-2}$

(a) December-February

Lat. p(mb)	41N	33N	24N	15N	5N	5S	15S	24S	33S
100	20.1	29.6	16.2	17.3	19.3	11.6	6.6	3.9	2.4
150	36.5	56.0	27.9	33.0	42.6	28.3	15.0	8.4	3.6
200	35.8	80.2	34.1	30.0	32.1	19.8	12.6	7.0	3.3
300	33.3	64.4	32.8	17.1	14.9	6.3	3.5	3.0	3.2
400	25.5	39.8	25.6	9.1	7.5	2.5	1.5	2.1	3.2
500	17.8	27.2	16.2	5.6	2.9	1.0	0.9	1.7	2.7
700	9.3	10.9	5.2	2.8	2.1	2.4	1.0	1.0	1.8
850	6.4	5.2	2.0	2.3	3.7	3.0	1.3	1.5	1.3
1000	2.0	1.3	1.1	2.9	3.3	2.9	2.0	1.6	1.3

(b) March-May

Lat. p(mb)	41N	33N	24N	15N	5N	5S	15S	24S	33S
100	10.4	9.0	8.2	10.9	11.4	7.7	3.5	3.0	2.1
150	12.6	19.5	11.9	19.9	21.5	15.4	8.2	5.0	1.7
200	13.5	21.3	11.3	15.6	13.2	8.4	6.0	4.1	2.3
300	12.9	15.0	7.6	6.6	4.6	1.7	1.3	2.2	2.5
400	10.1	10.9	5.6	2.2	1.4	0.5	0.4	1.6	1.6
500	7.4	8.2	4.2	1.2	1.0	0.5	0.6	1.1	1.3
700	5.0	5.1	3.7	0.9	2.6	2.5	1.3	1.4	1.6
850	3.8	3.7	3.5	3.3	4.6	3.8	2.2	1.3	0.9
1000	1.3	2.3	3.5	5.1	3.3	2.3	2.0	1.1	0.5

(c) June-August

Lat. p(mb)	41N	33N	24N	15N	5N	5S	15S	24S	33S
100	8.8	13.3	20.2	36.9	20.9	8.0	7.3	4.9	3.0
150	6.4	21.9	34.2	62.8	61.2	46.9	25.5	7.9	5.8
200	15.0	18.1	23.8	35.9	29.5	22.7	15.7	9.7	13.3
300	6.5	7.9	7.2	4.3	2.4	4.1	4.3	11.4	17.1
400	2.4	3.6	2.5	2.5	1.6	1.3	2.7	12.9	12.0
500	2.1	3.2	1.4	3.7	4.3	1.5	2.3	8.6	6.3
700	2.8	3.3	2.8	10.9	10.8	3.1	1.1	3.7	3.9
850	3.3	3.4	6.1	12.9	11.5	3.9	3.1	1.8	1.9
1000	1.7	3.0	5.4	7.6	4.0	2.6	2.5	1.0	0.3

Table 7.2 (ctd.)

(d) Septermber-November

Lat. / p(mb)	41N	33N	24N	15N	5N	5S	15S	24S	33S
100	15.8	10.2	9.8	12.6	11.6	7.3	6.3	3.3	2.3
150	11.6	15.5	18.0	20.9	31.8	28.0	14.9	7.4	2.4
200	23.7	20.7	15.7	13.7	19.2	17.2	11.6	8.7	3.9
300	14.7	15.4	10.1	4.9	3.9	3.9	4.7	8.2	5.3
400	8.2	7.8	5.5	1.7	0.6	1.0	3.6	6.0	3.5
500	5.2	4.5	4.4	1.3	0.6	0.5	2.7	4.5	2.8
700	2.6	2.2	2.4	2.0	3.9	1.8	1.4	2.2	2.7
850	2.1	1.4	2.5	2.5	5.0	2.8	2.3	1.3	1.4
1000	1.6	1.7	2.2	2.5	2.4	3.3	3.2	1.9	0.8

Table 7.3 a

Conversions From Zonal Available Potential Energy to Eddy Available Potential Energy (erg sec^{-1} gm^{-1}) for December-February

(a) Transient Eddies

Lat. p(mb)	37N	29N	20N	10N	0	10S	20S	29S
100	-5.768	-1.569	0.900	0.803	0.313	-0.235	-0.460	-1.714
150	-4.833	-1.464	0.163	0.207	0.033	0.007	0.057	-1.307
200	2.689	0.655	-0.023	0.011	0.002	0.011	-0.053	0.561
300	6.494	3.761	0.089	-0.047	0.001	-0.001	0.238	1.336
400	4.651	2.598	-0.165	-0.102	-0.005	-0.002	0.077	0.392
500	4.142	1.471	-0.275	-0.063	-0.000	-0.004	-0.050	-0.130
700	5.799	2.619	0.331	-0.008	0.005	-0.000	-0.009	0.170
850	6.862	4.542	1.155	0.026	0.003	0.000	0.033	1.191
1000	4.850	3.146	0.821	0.057	-0.012	0.061	0.185	0.486

(b) Transient Eddies and Standing Eddies

Lat. p(mb)	37N	29N	20N	10N	0	10S	20S	29S
100	-9.747	-4.434	-1.687	-0.203	0.277	-0.111	0.625	-0.426
150	-5.943	-2.409	0.004	0.262	0.045	0.069	0.313	-1.445
200	3.897	1.132	-0.037	0.022	0.004	0.070	-0.041	0.600
300	8.461	4.929	0.069	-0.087	0.002	0.002	0.240	1.312
400	6.205	3.413	-0.199	-0.147	-0.012	-0.000	0.090	0.377
500	5.735	2.152	-0.270	-0.073	-0.001	-0.003	-0.041	-0.128
700	8.077	3.431	0.423	-0.009	0.006	-0.000	-0.008	0.213
850	9.656	5.335	1.120	-0.010	0.005	0.000	0.027	1.109
1000	6.351	3.619	0.878	0.061	-0.024	0.131	0.271	0.544

Table 7.3 b

Conversions From Zonal Available Potential Energy To Eddy Available Potential Energy (erg $sec^{-1} gm^{-1}$) for June-August

(a) Transient Eddies

Lat. p(mb)	37N	29N	20N	10N	0	10S	20S	29S
100	-1.861	-0.594	-0.728	-0.504	-0.132	0.043	-0.102	-4.553
150	-2.725	-0.869	-0.211	0.037	-0.036	0.227	0.384	-5.412
200	0.409	-0.024	0.038	-0.010	-0.040	0.033	-0.002	0.573
300	1.509	0.082	0.013	0.000	-0.000	-0.003	0.131	2.958
400	0.449	-0.049	0.009	-0.003	0.010	-0.024	-0.032	1.706
500	-0.042	-0.046	0.009	-0.004	0.014	-0.032	-0.267	1.239
700	0.350	0.011	0.017	0.026	-0.001	-0.041	-0.113	1.748
850	0.490	0.036	0.009	0.055	0.006	0.040	0.847	2.820
1000	0.394	0.139	0.003	-0.001	0.009	0.178	0.725	1.230

(b) Transient Eddies and Standing Eddies

Lat. p(mb)	37N	29N	20N	10N	0	10S	20S	29S
100	-9.364	-3.072	-1.322	-0.658	-0.071	-0.075	-0.007	-0.565
150	-6.221	-2.776	-0.935	-0.240	-0.045	0.079	-0.058	-3.050
200	2.586	0.864	-0.006	-0.020	-0.012	0.007	-0.001	0.255
300	5.531	1.842	0.126	-0.002	0.000	-0.006	0.288	1.014
400	2.908	0.896	0.004	-0.003	-0.002	-0.013	0.046	0.849
500	1.297	0.145	-0.039	0.003	-0.000	-0.010	-0.140	0.237
700	2.135	0.387	-0.004	0.008	0.002	0.001	0.143	1.677
850	3.431	1.041	0.018	0.031	0.037	0.029	0.535	2.883
1000	2.264	1.202	0.156	-0.008	0.066	0.311	0.669	0.987

Table 7.4 a

Conversions From Eddy Kinetic Energy to Zonal Kinetic Energy
(erg sec^{-1} gm^{-1}) for December-February

(a) Transient Eddies

Lat. p(mb)	37N	29N	20N	10N	0	10 S	20 S	29 S
100	-0.782	0.842	0.844	-0.174	-0.049	0.068	0.201	0.468
150	-2.482	1.869	1.214	-1.276	-0.486	0.670	1.803	2.569
200	-4.061	2.558	2.694	-0.892	-0.361	0.605	2.161	4.100
300	-4.467	2.069	2.845	0.570	0.000	0.158	0.950	2.308
400	-1.865	1.072	1.700	0.177	0.000	0.040	0.272	0.821
500	-0.882	0.713	1.168	0.099	0.009	0.061	0.108	0.363
700	-0.043	0.308	0.359	0.043	0.021	0.070	0.020	0.139
850	0.013	0.128	0.081	0.000	0.004	0.021	-0.034	0.049
1000	-0.017	0.015	0.011	-0.003	0.003	0.002	0.003	-0.021

(b) Transient Eddies and Standing Eddies

Lat. p(mb)	37N	29N	20N	10N	0	10 S	20 S	29 S
100	-1.206	1.372	1.634	-0.164	-0.068	0.031	0.104	0.444
150	-3.458	2.951	1.602	-3.011	-0.906	0.765	1.544	2.544
200	-5.979	3.852	3.889	-1.643	-0.530	0.616	2.023	4.133
300	-5.823	2.804	4.039	0.692	-0.008	0.155	0.945	2.307
400	-2.560	1.428	2.392	0.322	0.000	0.049	0.285	0.829
500	-1.197	0.889	1.381	0.151	0.009	0.070	0.119	0.377
700	-0.053	0.361	0.362	0.044	0.021	0.072	0.022	0.141
850	0.017	0.149	0.057	0.000	0.029	0.022	-0.033	0.047
1000	-0.007	0.022	0.015	-0.006	0.002	0.004	-0.000	-0.024

Table 7.4 b

Conversions From Eddy Kinetic Energy to Zonal Kinetic Energy
(erg sec^{-1} gm^{-1}) for June-August

(a) Transient Eddies

Lat. p(mb)	37N	29N	20N	10N	0	10S	20S	29S
100	0.545	0.096	-0.045	-0.002	-0.010	-0.049	0.266	0.774
150	1.797	1.099	0.340	0.077	-0.523	-0.447	1.788	2.326
200	3.923	2.286	0.514	0.181	-0.404	-0.559	4.088	4.694
300	2.403	1.422	0.224	0.048	-0.070	0.308	4.815	4.900
400	0.731	0.571	0.115	0.007	0.011	0.440	2.776	3.266
500	0.373	0.322	0.095	0.005	0.006	0.247	1.197	1.758
700	0.076	0.089	0.032	-0.004	-0.003	0.080	0.345	0.772
850	0.010	0.033	-0.003	-0.003	-0.020	-0.021	0.113	0.357
1000	0.043	0.023	-0.005	-0.003	-0.002	-0.002	-0.002	-0.094

(b) Transient Eddies and Standing Eddies

Lat. p(mb)	37N	29N	20N	10N	0	10S	20S	29S
100	1.277	0.970	0.092	-0.108	-0.183	-0.105	0.145	0.692
150	2.397	1.917	0.520	0.173	-1.589	-2.787	0.060	1.994
200	4.735	3.334	0.751	0.350	-0.864	-2.139	2.496	4.384
300	2.525	1.703	0.304	0.069	-0.098	0.156	4.483	4.700
400	0.701	0.579	0.123	0.007	0.012	0.453	2.723	3.089
500	0.353	0.319	0.100	0.005	0.008	0.265	1.181	1.652
700	0.079	0.098	0.032	-0.002	-0.005	0.085	0.341	0.687
850	0.033	0.038	-0.002	-0.002	-0.029	-0.029	0.134	0.331
1000	0.050	0.038	-0.016	-0.013	0.003	-0.009	-0.002	-0.100

BIOGRAPHICAL NOTE

John Winton Kidson was born at Christchurch, New Zealand on November 20th, 1940. He attended the Christchurch Boys' High School and in 1958 entered the University of Canterbury on a University National Scholarship. He gained his B. Sc. Degree in 1961 and in 1963 was awarded an M. Sc. with second class honours in Physics. After graduation he joined the New Zealand Meteorological Service in Wellington where he worked in the Research Section until 1965 when he was awarded a fellowship for study at M. I. T.